Active Mitigation of Induced Voltage on Buried Pipelines

by

Hyunjung Yong

A thesis submitted in partial fulfillment of the requirements for the degree of

Master of Science

in

Energy Systems

Department of Electrical and Computer Engineering
University of Alberta

Abstract

Buried pipelines that share a common corridor with nearby overhead AC power lines experience voltage induction. The induced voltages can cause personnel safety and pipeline corrosion problems. Industry has a requirement to reduce the induced voltages below an acceptable level. In view of the limitations of existing methods to reduce the induced voltages and contributions of power line harmonic currents to the voltage induction, this thesis proposes an active method that can neutralize the induced 60Hz and harmonic voltages in buried pipelines.

The idea of the proposed mitigation method is to apply proper neutralizing voltage to the two terminals of the buried pipeline which is parallel to overhead AC power lines. A feedback control system is embedded in the active mitigation device to automatically adjust the generation of the neutralizing voltage. This thesis shows that, by applying two proper neutralizing voltage sources at the two terminals, the whole induced voltage along the parallel zone of the buried pipeline can be mitigated. Methods to estimate the voltage and power ratings of active sources are proposed. Solutions for dealing with some practical issues are also recommended.

Simulation studies are conducted in this thesis to verify the proposed method and to determine the main factors affecting the active mitigation device and its design parameters. The method of the probe-wire-based field measurement is also investigated to help the design of the mitigation device.

Preface

This thesis is an original work by Hyunjung Yong. No part of this thesis has been previously published.

Acknowledgement

First of all, I would like to express my sincere gratitude to my supervisor, Dr. Wilsun Xu for supervising this thesis work and for giving me the chance to work with outstanding researchers. Through research works under his supervision, I have learned how to think creatively and how to do research work.

I would like to show my special appreciation to Dr. Jing Yong who helps me with patient guidance and insightful suggestions to this thesis work. I also thank all my colleagues at the PDS-Lab for their help.

Lastly, I'd like to extend special thanks to my parents Hwangon Yong and Hyunja Kim and my brother Hyojung Yong for their love and support.

Contents

List of Table

List of Figure

List of Abbreviations

EMF	Electromotive Force
CP	Cathodic Protection
AMS	Active Mitigation System
IDD	Individual Demand Distortion
TDD	Total Demand Distortion
AC	Alternating Current
DC	Direct Current
FFT	Fast Fourier Transform

Chapter 1

Introduction

These days, many overhead AC power lines and buried oil and gas pipelines share a common corridor. Although overhead AC power lines are physically disconnected from buried pipelines, they are electromagnetically coupled. Due to a magnetic field generated by overhead AC power lines, pipelines buried nearby may have induced voltage, which sometimes causes personnel safety problems and pipeline corrosion. Such induced voltage on buried pipelines has been an issue for a long time.

This introduction chapter presents background information about inductive coupling on buried pipelines, and mitigation methods for induced voltage on buried pipelines. It also presents the main objectives and outline of this thesis.

1.1 Background

1.1.1 Induced Voltage on Buried Pipelines

Overhead AC power lines basically cause three kinds of coupling effects on nearby metallic structures: (1) capacitive coupling, (2) inductive coupling, and (3) conductive coupling [1]. Capacitive coupling only affects aerial pipelines, but inductive coupling even influences buried pipelines. Conductive coupling only appears when fault currents flow through an earthing electrode of a power line tower [1]. Therefore, the main coupling effect on buried pipelines in a steady state is the inductive coupling effect from nearby overhead AC power lines.

The inductive coupling effect between overhead AC power lines and a buried pipeline can be explained by Faraday's law. As we know, overhead AC power lines generate a magnetic field. Since the pipeline makes one big equivalent loop to the remote earth, the magnetic field induces a certain Electromotive Force

(EMF) on the pipeline according to Faraday's law. The total EMF in the pipeline is the phasor summation of individual EMF, EMF_i induced by each conductor current, I_i, of AC power lines.

$$EMF_{Total} = \sum_i EMF_i = \sum_i Z_{m.i} I_i \qquad (1\text{-}1\text{-}1\text{-}1)$$

where,

i indicates the *i*-th conductors.

$z_{m.i}$ is the mutual impedance between power conductor i and the pipeline.

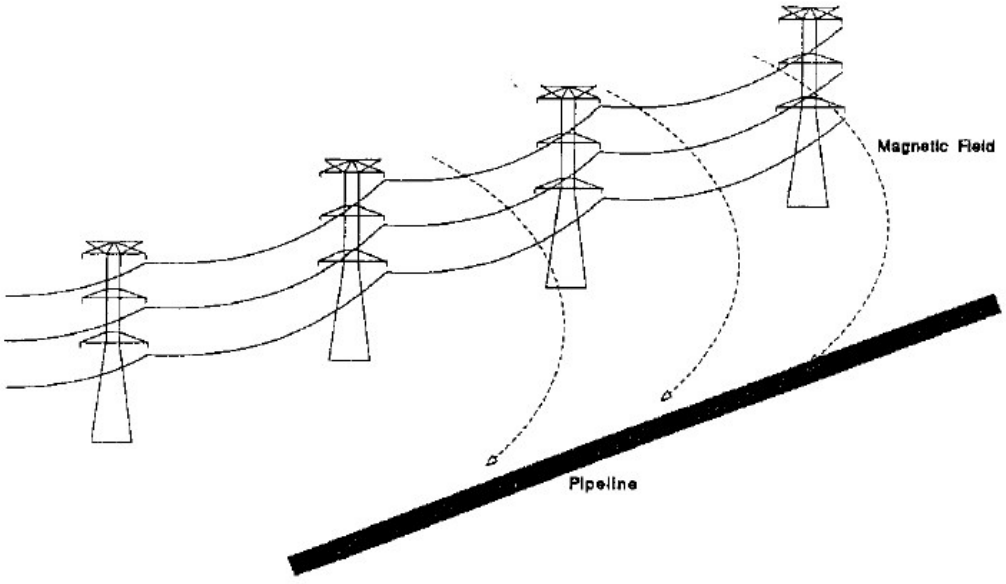

Figure 1-1-1-1: Inductive coupling between a buried pipeline and nearby overhead AC power lines, from Reference [1]

The EMFs embedded in the pipeline manifest themselves through building the different induced voltage V, between the pipeline and the remote earth, along the pipeline, as shown in the following Figure 1-1-1-2.

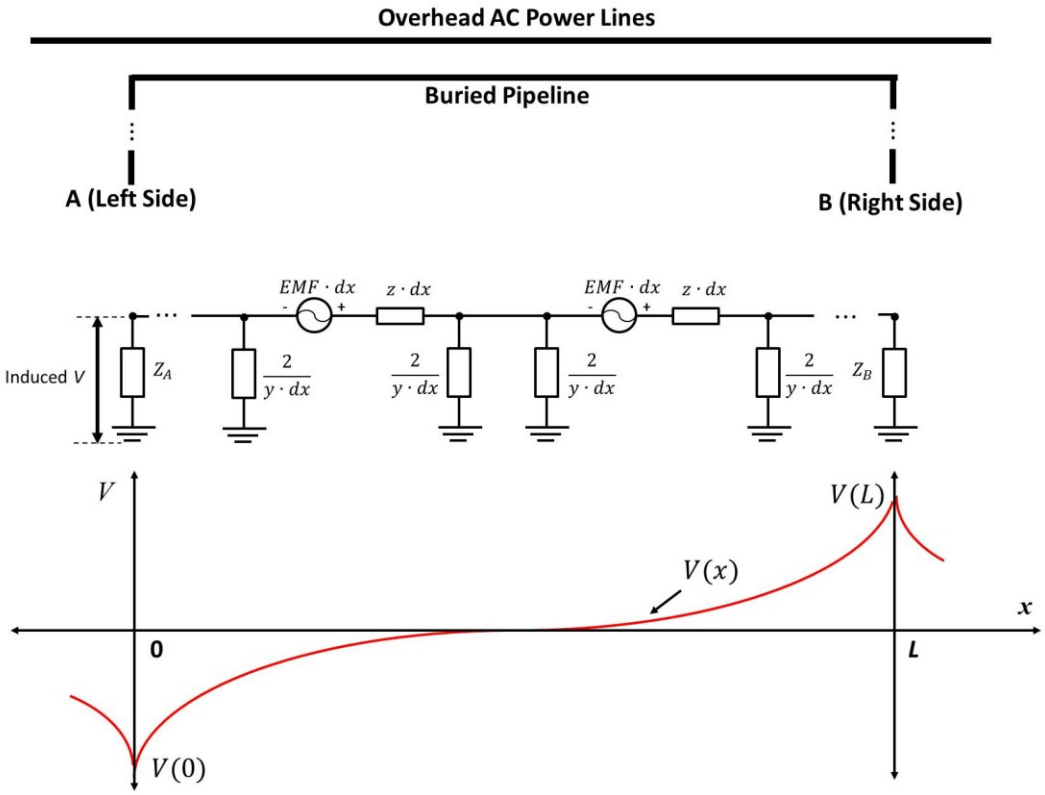

Figure 1-1-1-2 Circuit of the pipeline and induced voltage profile along the pipeline

The induced voltage on the pipeline may produce unacceptable touch voltage to the personnel working near the pipeline and cause corrosion problems to the pipeline coating, or even destroy the pipeline coating. Therefore, some criteria, as shown in Figure 1-1-1-3, have been established to limit those effects.

Issue	Criteria			Standard
	Index	Condition	Limit	
Personnel safety	Touch voltage V_{touch}	normal	15 V	CSA C22.3 No.6-13 NACE SP0177-2014
		Fault	See IEEE std. 80-2000	CSA C22.3 No.6-13 NACE SP0177-2014
Pipeline AC corrosion	AC current density $J_{corrosion}$	Low risk	<20 A/m^2	CSA C22.3 No.6-13
			<30 A/m^2	NACE SP0177-2014 CEN/TS 15280-2006 ISO 15589-1-2003
		Medium risk	20~100 A/m^2	CSA C22.3 No.6-13
			30~100 A/m^2	NACE SP0177-2014 CEN/TS 15280-2006
		High risk	>100 A/m^2	CSA C22.3 No.6-13 NACE SP0177-2014 CEN/TS 15280-2006
	AC corrosion voltage $V_{corrossion}$	Soil resistivity >25Ωm	10V	CEN/TS 15280-2006
		Soil resistivity <25Ωm	4V	
Pipeline coating breakdown	Coating breakdown voltage $V_{breakdown}$	Bitumen coating	1~1.2 kV	NACE SP0177-2014
		FBE, polyethylene	3~5 kV	

Figure 1-1-1-3: Criteria for assessing pipeline concerns, from Reference [2]

The inductive coupling influence on buried pipelines mainly depends on the following impact factors [1].

(1) **Currents of nearby overhead AC power lines**: The current magnitude and imbalance rate plays a key role in induced voltage. During a steady state, the pipeline will experience relatively long exposure to induced voltage with a low magnitude, while during a fault, especially a single phase fault, the pipeline will experience a short exposure to induced voltage with a high magnitude.

(2) **Exposure length**: Exposure length basically indicates the length of a common corridor (parallel route) between a buried pipeline and nearby overhead AC power lines. The total maximum induced voltage on the pipeline increases according to the increase of the exposure length.

(3) **Distance between a buried pipeline and nearby overhead AC power lines**: Since the EMF, the driving force of induced voltage, is determined by both the currents of power lines and mutual impedances as shown in

Equation (1-1-1-1), longer separation distance between a pipeline and a power line results in lower mutual impedance and lower induced voltage.

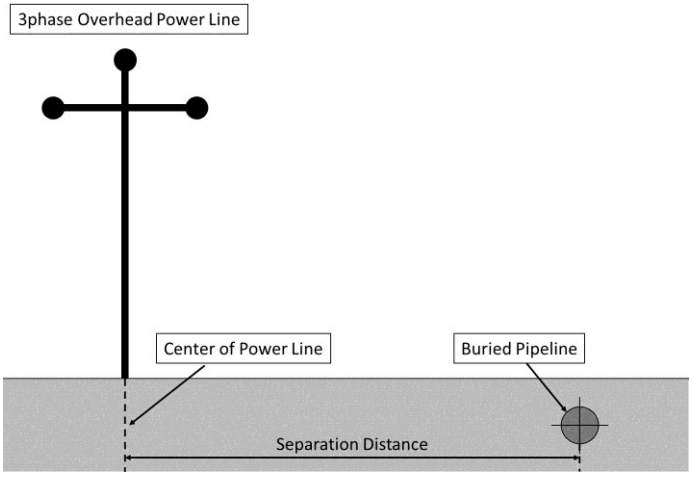

Figure 1-1-1-4: Separation distance between a buried pipeline and power lines

(4) **Conductor configuration of power lines**: If a 3phase AC power line comprises multiple circuits, the induced voltage on the pipeline nearby is different according to the conductor configuration of the power lines.

In the above impact factors, the power line currents and exposure length are very difficult to change for a selected pipeline routine. The most feasible way to limit the induced voltage below those criteria is to increase the separation distance. However, in practice, a wider common corridor may not be available. Those criteria are therefore not easy to meet. The following Figure 1-1-1-5 shows the induced voltage profile on the pipeline, which has 20m separation distance and 4km exposure length under 750A operating phase current of power lines.

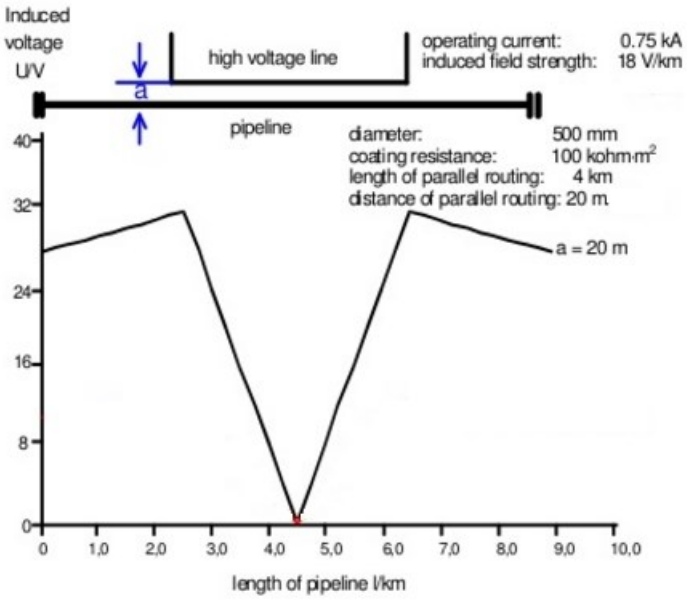

Figure 1-1-1-5: Induced voltage profile on the pipeline exceeding AC corrosion voltage criterion, from Reference [3]

In Figure 1-1-1-5, we can see that the two terminals of the pipeline have the maximum induced voltage of about 32V, which exceeds the AC corrosion voltage criterion of 10V as shown in Figure 1-1-1-3. As shown in Figure 1-1-1-5, some cases of pipelines near overhead AC power lines may not meet the safety and corrosion criteria in practice.

Furthermore, recent research shows the more serious concern of induction issues caused by the triplex harmonics. According to field measurement, the 1^{st}, 3^{rd} and 9^{th} harmonic components of currents in power lines are major contributors to induced EMF as shown in Figure 1-1-1-6.

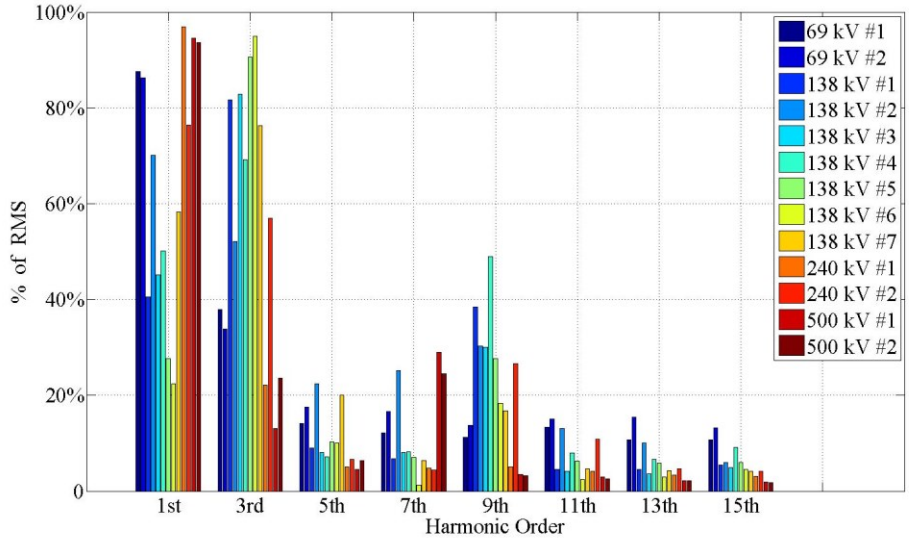

Figure 1-1-1-6: Percent of harmonic components of measured EMF

More information about the field measurement related to harmonics can be referred to in Appendix A.

Therefore, effective mitigation measures are important to maintain the safe induction environment for pipelines.

1.1.2 Existing Solutions for Mitigating Induced Voltage on Buried Pipelines

The commonly used mitigation solutions for pipeline induction are summarized as follows [2][4].

(1) Gradient-control-wire method

The gradient-control-wire method is used to provide an additional grounding effect. The grounding resistance along the pipeline can therefore be reduced so that the induced voltage can be mitigated.

This method is currently considered as the most effective one. Appendix B provides detailed information about the gradient-control-wire method and how it compares to the active mitigation method proposed in this thesis.

The drawbacks of this method are installation and maintenance. In order to obtain an acceptable mitigation effect, gradient-control wires need to be buried in parallel to the buried pipeline. The installation length depends on the case, but it is usually hundreds of meters from the pipeline's terminals. Moreover, the gradient-control wire usually requires the installation of a DC isolator to protect the pipeline from stray currents and prevent leakage of cathodic protection current. Since the gradient-control wires are buried with the pipeline, they are not easy to access for maintenance.

(2) Cancelation-wire method

The cancelation-wire method is to install the wire, of which two ends are grounded, parallel to a buried pipeline. Since the cancelation-wire has induced current from the same power lines, this current also induces the other EMF on the pipeline with an opposite phase angle to the EMF induced directly from the power lines. Therefore, part of the induced EMF on the pipeline from the power lines can be canceled. The cancelation effect can be controlled by the distance between the cancelation wire and the pipeline.

The drawback of this cancelation-wire method is installation. In order to obtain an acceptable mitigation effect, the cancelation-wire needs to be installed along the buried pipeline in parallel.

(3) Insulating flange method

Insulating flanges can be installed to subdivide a pipeline into several sections to reduce induced voltage on the pipeline. However, a long pipeline requires many insulating flanges in order to mitigate induced voltage. Therefore this method is cost and labor intensive for already installed pipelines.

The other methods, such as change of pipeline/power line location, use of nonmetallic pipeline, change of conductor configuration of power line, and use of gradient-control mats, are not valid for existing installations, or only for solving local personnel safety issues.

To address the AC induction issue, this thesis proposes an active mitigation method that has a better mitigation effect and requires less installation.

1.1.3 Proposed Mitigation Method for Induced Voltage on Buried Pipelines

The key idea of the proposed active mitigation method is to apply proper neutralizing voltage to buried pipelines. The applied proper neutralizing voltage plays a role in canceling induced voltage on the buried pipelines.

To achieve this goal, the following issues should be dealt with.

a. Where to apply the voltage source
b. How to adjust the voltage source in order to respond to the variation in induced voltage on pipelines
c. How to estimate the required voltage and capacity of the active device

1.2 Thesis Scope and Outline

The objective of this thesis is to propose an active method to mitigate induced voltage on buried pipelines. This thesis mainly focuses on one typical case: one buried pipeline is parallel to one three-phase AC overhead power line. The separation distance between the pipeline and the three-phase AC overhead power line is constant. And the soil resistivity along the pipeline can be considered as uniform.

Chapter 2 outlines the details of the active mitigation method and the configuration of the mitigation system. An iterative feedback control method is introduced to realize the automatic adjustment for responding to the parameter variations. The chapter also presents determination methods for the required voltage and capacity of the device, together with a case study. Moreover, some practical issues are raised.

Chapter 3 conducts and presents extensive sensitivity studies. The parameters affecting mitigation system design are thoroughly investigated by means of

simulation. A number of useful contour curves are created to intuitively show the impact of some sensitive parameters on the required voltage, device capacity and so on. They can be directly used to select mitigation system parameters.

Chapter 4 evaluates the accuracy of the probe-wire-based measurement method that is essential to determine the rated voltage and capacity of active mitigation devices. The problems to solve are to assess errors caused by capacitive coupling, and the difference due to the area difference between the buried pipeline's and the probe wire's equivalent earth return loop.

The design flowchart for the active mitigation system and one sample design specification are presented in Chapter 5.

Chapter 6 contains the thesis conclusion and recommendations for future work.

Chapter 2

Active Mitigation Method of Induced Voltage on Buried Pipelines

Since this thesis focuses on pipeline induction mitigation by using an active method, the characteristics of induced voltage on pipelines have to be completely understood. In this chapter, a brief review on the characteristics is first presented, followed by a description and an analysis of the idea of the active mitigation method, and by some practical issues to solve.

2.1 Brief Review on Characteristics of Induced Voltage on Buried Pipelines

2.1.1 General Model for Calculation of Induced Voltage

A buried pipeline can be treated and analyzed as a lossy transmission line [1]. The following Figure 2-1-1-1 shows the equivalent circuit of the buried pipeline that is parallel to a three-phase overhead AC power line.

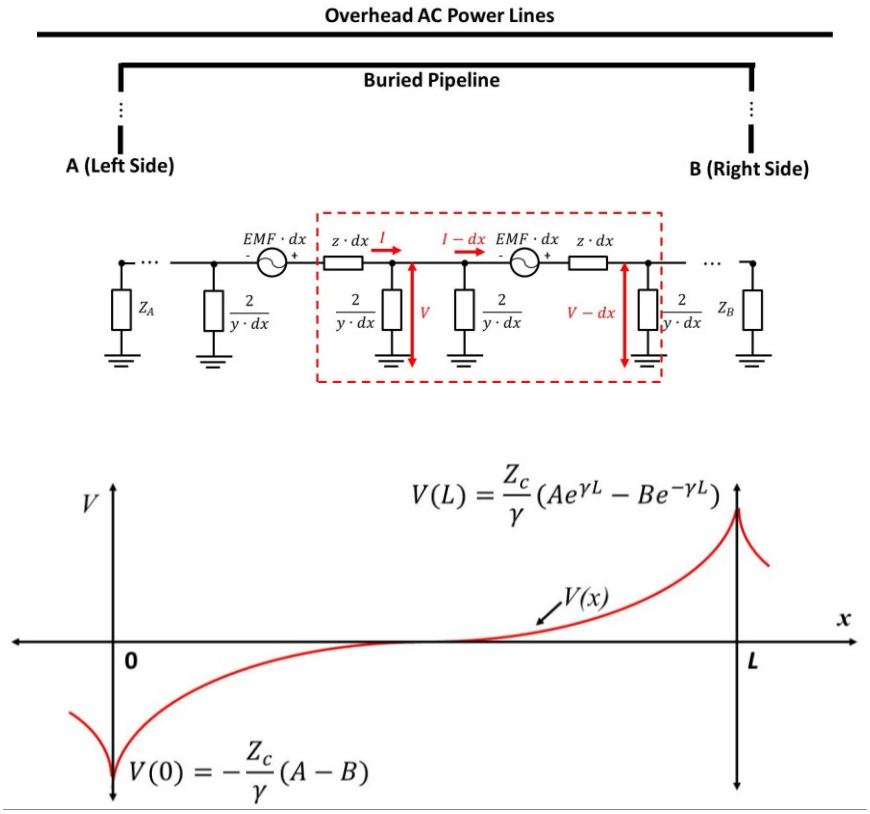

Figure 2-1-1-1: Equivalent circuit of the buried pipeline having induced voltage

where,

EMF : induced EMF, [V/m]

Z_A : the equivalent impedance of the left side of a buried pipeline, [Ω]

Z_B : the equivalent impedance of the right side of a buried pipeline, [Ω]

z : self-impedance of the pipeline [Ω / m]

y : self-admittance of the pipeline [Sm]

EMF can be obtained by either the probe-wire-based measurement that will be introduced in Chapter 4, or calculated by $EMF_{Total} = \sum_i EMF_i = \sum_i Z_{m.i} I_i$, where the mutual impedance is determined by soil resistivity, distance between a power conductor and a pipeline, and ac current frequency. The detailed calculation

equations of EMF for both fundamental and harmonic components are presented in Appendix C.

The calculation of self-impedance and self-admittance of a pipeline can be referred to in Appendix D.

From the equivalent circuit in Figure 2-1-1-1, it is possible to derive the following equations to calculate induced voltage along the buried pipeline [1][2][5].

$$V(x) = -\frac{Z_c}{\gamma}\left(Ae^{\gamma x} - Be^{-\gamma x}\right) \tag{2-1-1-1}$$

$$A = \frac{EMF}{2Z_c}\frac{(1+\nu_1)\nu_2 - (1+\nu_2)e^{\gamma L}}{e^{2\gamma L} - \nu_1\nu_2} \tag{2-1-1-2}$$

$$B = \frac{EMF}{2Z_c}\frac{(1+\nu_2)\nu_1 - (1+\nu_1)e^{\gamma L}}{e^{2\gamma L} - \nu_1\nu_2}e^{\gamma L} \tag{2-1-1-3}$$

where,

x: the distance from the left terminal of the pipeline, [m]

Z_c : characteristic impedance of the buried pipeline, [Ω]

γ : propagation constant of pipeline [m^{-1}], $\gamma = \sqrt{zy}$

ν_1 : reflection coefficient at the left end, $\nu_1 = \frac{Z_A - Z_C}{Z_A + Z_C}$

ν_2 : reflection coefficient at the right end, $\nu_2 = \frac{Z_B - Z_C}{Z_B + Z_C}$

In Equation (2-1-1-1), two terms of $\frac{Z_c}{\gamma}A$ and $\frac{Z_c}{\gamma}B$ are constant regardless of x. The first term is the exponential function and the second term is proportional to the reciprocal of the first term. The two terms can be represented as curves in

Figure 2-1-1-2. It is obvious that the maximum induced voltages, V(0) and V(L), in the parallel pipeline section occur at the two terminals.

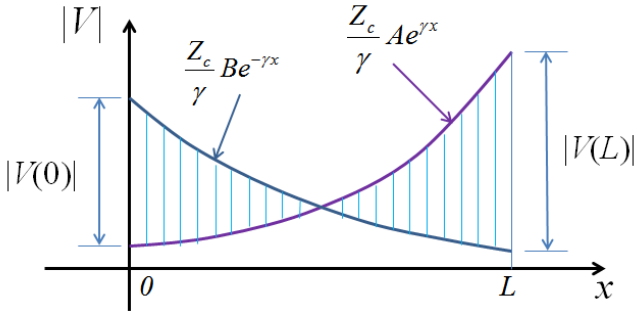

Figure 2-1-1-2: Graph of V(x)

From Equation (2-1-1-1) it can also be seen that both terminal conditions mutually affect induced voltage since this equation contains both terminal impedances. The change of one terminal condition changes all voltages along the pipeline, including voltages at the two terminals. The only exception is the very long pipeline that is presented in the next section.

2.1.2 Equivalent Circuit of Long Pipeline

If parallel route's length of a buried pipeline is long enough, such as [2][6]

$$L > \frac{2}{real(\gamma)} \tag{2-1-2-1}$$

then we have the following condition.

$$\left|e^{-\gamma L}\right| \ll 1 \tag{2-1-2-2}$$

Based on the above condition, the general equation of induced voltage $V(x)$ along the pipeline can be simplified as follows.

$$V(x) = \frac{EMF}{\gamma}\left[-\frac{Z_A}{Z_A + Z_C} e^{-\gamma x} + \frac{Z_B}{Z_B + Z_C} e^{\gamma(L-x)}\right] \tag{2-1-2-3}$$

According to the above Equation (2-1-2-3), the two terminals' voltage of the pipeline will be

Left terminal voltage: $V(0) = -\frac{EMF}{\gamma}\frac{Z_A}{Z_A + Z_C}$ (2-1-2-4)

Right terminal voltage: $V(L) = \frac{EMF}{\gamma}\frac{Z_B}{Z_B + Z_C}$ (2-1-2-5)

Equations (2-1-2-4) and (2-1-2-5) demonstrate that, in the long pipeline case, each terminal voltage is determined only by its terminal impedance and independent of the other terminal's impedance. Therefore, the long pipeline model can be considered as the two terminals decoupled model as shown in Figure 2-1-2-1.

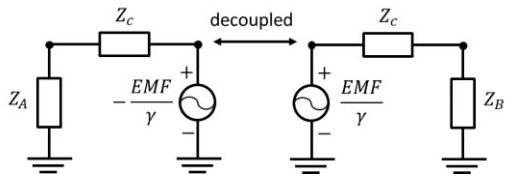

Figure 2-1-2-1: Circuit model of the long line model of a buried pipeline

2.1.3 Characteristic of Induced Voltage on Buried Pipelines

The above analysis suggests the following characteristics of induced voltage on buried pipelines:

(1) The severest induced voltage occurs at the two terminals:

The general induced voltage profile shown in Figure 2-1-1-1 indicates that the induced voltage varies along the pipeline and the extreme voltages occur at both terminals, if the uniform soil resistivity is considered. It intuitively gives us idea that the active mitigation sources should be applied at the terminals. The comprehensive analysis will be conducted in the following chapter.

(2) The change of terminal impedance changes the induced voltage at both terminals:

Expressions of *V(0)* and *V(L)* contain both parameter *A* and *B*, which depend on the terminals' equivalent impedance Z_A and Z_B thus if one of those impedance

values changes, both terminals' induced voltage will change accordingly. This means that the two terminals affect each other.

If the pipeline is long enough, the two terminals' voltage has no mutual effect.

(3) Induced voltage varies according to load currents of overhead AC power lines and soil resistivity.

When the configuration of overhead AC power lines and a buried pipeline is given, all parameters in Equation (2-1-1-1) are fixed except for EMF. The EMF varies only by load currents (unbalanced current and harmonics) of overhead AC power lines and soil resistivity. Consequently, $V(x)$ is only determined by load currents of overhead AC power lines and soil resistivity. In practice, load currents of overhead AC power lines and soil resistivity always vary, so $V(x)$ also varies.

2.2 Proposed Active Mitigation Method

Based on the characteristics of induced voltage on a buried pipeline, the active mitigation method, which applies proper active sources to the buried pipeline, is proposed. The schematic diagram and the equivalent circuit are presented in Figure 2-2-1 and Figure 2-2-2, respectively.

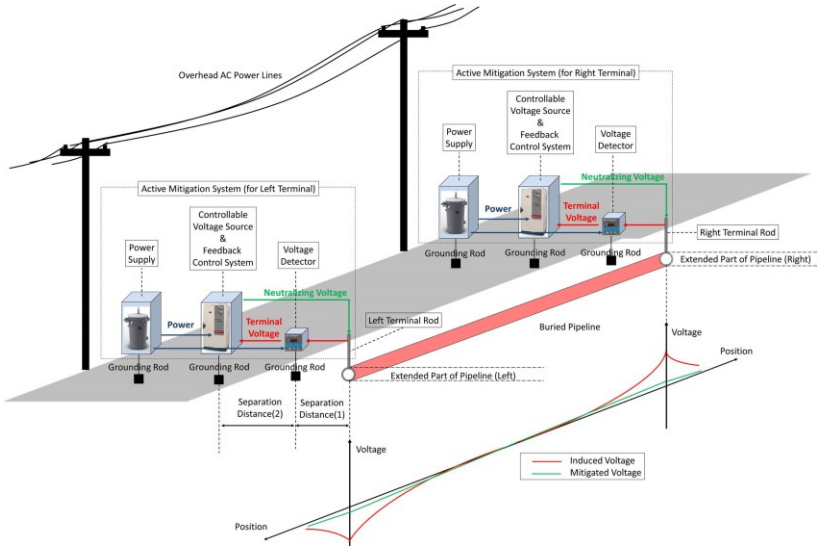

Figure 2-2-1: Scheme of proposed active mitigation method

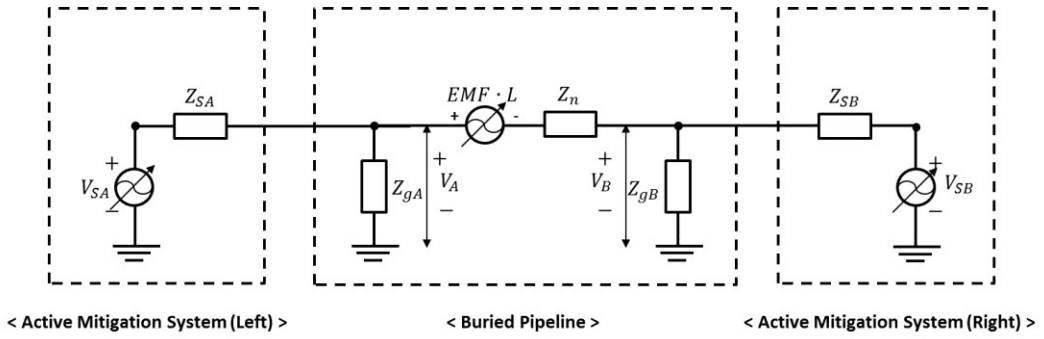

Figure 2-2-2: Equivalent circuit of proposed active mitigation method

This active mitigation system basically comprises two active sources that are applied to the left and right terminal of the buried pipeline parallel to overhead AC power lines. At each terminal there are three major devices: a power supply, a controllable voltage source, and a voltage detector. The power supply provides the required power for the controllable voltage source and the voltage detector. The controllable voltage source has a feedback control system to adjust applied voltage at the terminal for mitigating the entire induced voltage along it. The voltage detector monitors the voltage at the terminal and sends the information to the feedback control system. If the two terminals' devices can work properly to mitigate the induced voltage at the terminals, the active mitigation purpose can be achieved.

This section presents answers to the following questions about the proposed active mitigation method one by one.

- Can two active sources (two active mitigation systems) mitigate the entire induced voltage along the buried pipeline, and is this the optimized scheme?
- How can we determine the voltage and power ratings of two active sources for a given case?
- How can we adjust the applied voltage at two terminals properly to adapt to the variation of induced voltage caused by soil resistivity and power load changes?
- What functions should each device in one active mitigation system perform?

2.2.1 Locations to apply Active Mitigation Sources and Numbers Required

To reduce the installation cost, the minimum number of required active sources should be determined. Intuitively, and based on the above analysis, at least two voltage sources are needed. This subsection seeks to analytically prove that the proper neutralizing voltages at the two terminals are optimized scheme to mitigate the entire induced voltage along the pipeline.

According to the equivalent circuit in Figure 2-2-2, there are three different sources i.e. EMF, V_{SA}, and V_{SB}, if the neutralizing voltage sources are applied at two terminals. In line with the superposition principle, the total voltage on the pipeline will be

$$\begin{aligned} Total\,Voltage = {} & (1)\,Voltage\,caused\,by\,EMF \\ & + (2)\,Voltage\,caused\,by\,V_{SA} + (3)\,Voltage\,caused\,by\,V_{SB} \end{aligned} \qquad (2\text{-}2\text{-}1\text{-}1)$$

In Equation (2-2-1-1), if the total voltage becomes zero regardless of x, we can theoretically conclude that whole voltage caused by EMF is mitigated.

To answer this question, the analytical equation of the voltage caused by V_{SA} and V_{SB} should be derived. The following Figure 2-2-1-1(a) shows the circuit of a buried pipeline with two terminal voltage sources applied. In the circuit, V_{SA} and V_{SB} are the equivalent voltage sources of each active device. Z_{SA} and Z_{SB} represent the equivalent impedances of each active device, the summation of the device's internal impedance Z_{in} and the grounding resistance R_g. To simplify the derivation, V_{SA} and V_{SB} are considered one by one. Figure 2-2-1-1(b) is the equivalent circuit, assuming V_{SB} is zero. Z_c is the characteristic impedance of the pipeline representing the pipeline's part beyond the parallel routine. Z_{in_A} is the impedance seen from the left terminal (A) of the pipeline.

Since a buried pipeline can be considered as a lossy transmission line, the general expression of voltage and current is as follows.

$$V(x) = V_0^+ e^{-\gamma x} + V_0^- e^{\gamma x} \tag{2-2-1-2}$$

$$I(x) = \frac{1}{Z_c}\left(V_0^+ e^{-\gamma x} - V_0^- e^{\gamma x}\right) \tag{2-2-1-3}$$

where V_0^+ and V_0^- are determined by the terminal conditions of the circuit.

From the circuit in Figure 2-2-1-1(b), it is possible to obtain the conditions of the two terminals' voltage i.e. $V(0)$ and $V(L)$. Using Equation (2-2-1-2) and (2-2-1-3), those two conditions can be expressed as follows.

$$V(0) = \frac{Z_c // Z_{in\_A}}{Z_{SA} + Z_c // Z_{in\_A}} V_{SA} = V_0^+ + V_0^- \tag{2-2-1-4}$$

$$V(L) = I(L) \cdot Z_B = \frac{Z_B}{Z_c}(V_0^+ e^{-\gamma L} - V_0^- e^{\gamma L}) = V_0^+ e^{-\gamma L} + V_0^- e^{\gamma L} \tag{2-2-1-5}$$

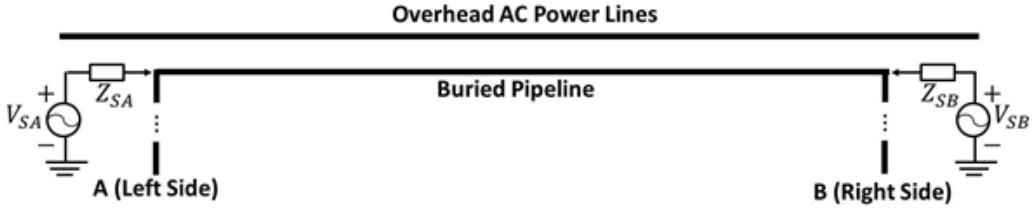

(a) Circuit with two terminal devices applied

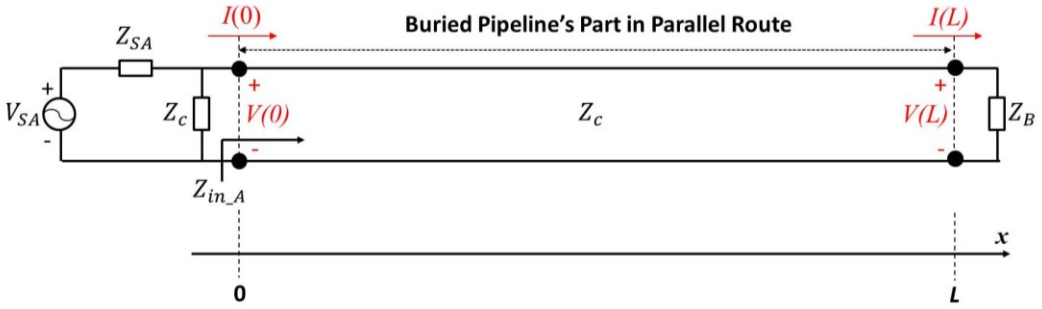

(b) Circuit considering V_{SA} only

Figure 2-2-1-1: Circuit of buried pipeline

By solving Equation (2-2-1-4) and (2-2-1-5), we can obtain the solution of V_0^+ and V_0^- as follows.

$$V_0^+ = \left(\frac{Z_c // Z_{in\_A}}{Z_{SA} + Z_c // Z_{in\_A}} \right) \left(\frac{1}{1 + \nu_2 e^{-2\gamma L}} \right) V_{SA} \tag{2-2-1-6}$$

$$V_0^- = \left(\frac{Z_c // Z_{in\_A}}{Z_{SA} + Z_c // Z_{in\_A}} \right) \left(\frac{\nu_2 e^{-2\gamma L}}{1 + \nu_2 e^{-2\gamma L}} \right) V_{SA} \tag{2-2-1-7}$$

With the above V_0^+ and V_0^-, the equation of $V(x) \, caused \, by \, V_{SA}$ is obtained as follows.

$$V(x) \, caused \, by \, V_{SA} = V_{SA}' e^{-\gamma x} \left(1 + \nu_2 e^{-2\gamma (L-x)} \right) = V_{SA}' e^{-\gamma x} + V_{SA}' \nu_2 e^{-2\gamma L} e^{\gamma x} \tag{2-2-1-8}$$

where,

$$V_{SA}' = \left(\frac{\left(Z_{in\_A} // Z_c \right)}{Z_{SA} + \left(Z_{in\_A} // Z_c \right)} \right) \left(\frac{1}{1 + \nu_2 e^{-2\gamma L}} \right) V_{SA}, \; Z_{in\_A} = Z_c \frac{Z_B + Z_C \tanh\left(\gamma L \right)}{Z_C + Z_B \tanh\left(\gamma L \right)}, \; \nu_2 = \frac{Z_B - Z_C}{Z_B + Z_C}$$

Z_{SA} : equivalent impedance of the active mitigation device at the left terminal.

Z_B : equivalent impedance at the right terminal ($Z_B = Z_{SB} // Z_c$)

Z_{SB} : equivalent internal impedance of active mitigation systems at the right terminal

In Appendix E, simulation results verifying Equation (2-2-1-8) can be found.

The similar equation for the voltage caused by V_{SB} can be obtained as follows.

$$V(x) \, caused \, by \, V_{SB} = V_{SB}' e^{-\gamma (L-x)} \left(1 + \nu_1 e^{-2\gamma x} \right) = V_{SB}' e^{-\gamma L} e^{\gamma x} + V_{SB}' e^{-\gamma L} \nu_1 e^{-\gamma x} \tag{2-2-1-9}$$

where,

$$V_{SB}{}' = \left(\frac{\left(Z_{in\_B} // Z_c \right)}{Z_{SB} + \left(Z_{in\_B} // Z_c \right)} \right) \left(\frac{1}{1 + v_1 e^{-2\gamma L}} \right) V_{SB}, \; Z_{in\_B} = Z_c \frac{Z_A + Z_c \tanh(\gamma L)}{Z_c + Z_A \tanh(\gamma L)}$$

Z_A : equivalent impedance at the left terminal ($Z_A = Z_{SA} // Z_c$)

Therefore, the total voltage caused by EMF, V_{SA} , and V_{SB} is

$$\begin{aligned} Total\,Voltage &= (1)\,Voltage\,caused\,by\,EMF \\ &\quad + (2)\,Voltage\,caused\,by\,V_{SA} + (3)\,Voltage caused\,by\,V_{SB} \end{aligned}$$

$$= -\frac{Z_c}{\gamma} A e^{\gamma x} + \frac{Z_c}{\gamma} B e^{-\gamma x} + V_{SA}{}' e^{-\gamma x} + V_{SA}{}' v_2 e^{-2\gamma L} e^{\gamma x} + V_{SB}{}' e^{-\gamma L} e^{\gamma x} + V_{SB}{}' e^{-\gamma L} v_1 e^{-\gamma x}$$

$$= \left(-\frac{Z_c}{\gamma} A + V_{SA}{}' v_2 e^{-2\gamma L} + V_{SB}{}' e^{-\gamma L} \right) e^{\gamma x} + \left(\frac{Z_c}{\gamma} B + V_{SA}{}' + V_{SB}{}' e^{-\gamma L} v_1 \right) e^{-\gamma x} \qquad (2\text{-}2\text{-}1\text{-}10)$$

$$= Coefficient_1 \cdot e^{\gamma x} + Coefficient_2 \cdot e^{-\gamma x}$$

As shown in Equation (2-2-1-10), the total voltage is the function of $e^{\gamma x}$ and $e^{-\gamma x}$. Theoretically, if two coefficients of $e^{\gamma x}$ and $e^{-\gamma x}$ in Equation (2-2-1-10) become zero then the total voltage become zero regardless of x . Those coefficients are the function of $V_{SA}{}'$ and $V_{SB}{}'$ (corresponding to V_{SA} and V_{SB} respectively). Consequently, we have two conditions in selecting proper V_{SA} and V_{SB} in order to mitigate the entire induced voltage (regardless of x) on the buried pipeline as follows.

$$\begin{bmatrix} V_{SA} \\ V_{SB} \end{bmatrix} = \begin{bmatrix} N_{11} & N_{12} \\ N_{21} & N_{22} \end{bmatrix}^{-1} \begin{bmatrix} \frac{Z_C}{\gamma} A \\ -\frac{Z_C}{\gamma} B \end{bmatrix} \qquad (2\text{-}2\text{-}1\text{-}11)$$

where,

$$N_{11}=\left(\frac{\left(Z_{in\_A}//Z_c\right)}{Z_{SA}+\left(Z_{in\_A}//Z_c\right)}\right)\left(\frac{1}{1+v_2e^{-2\gamma L}}\right)v_2e^{-2\gamma L}$$

$$N_{12}=\left(\frac{\left(Z_{in\_B}//Z_c\right)}{Z_{SB}+\left(Z_{in\_B}//Z_c\right)}\right)\left(\frac{1}{1+v_1e^{-2\gamma L}}\right)e^{-\gamma L}$$

$$N_{21}=\left(\frac{\left(Z_{in\_A}//Z_c\right)}{Z_{SA}+\left(Z_{in\_A}//Z_c\right)}\right)\left(\frac{1}{1+v_2e^{-2\gamma L}}\right)$$

$$N_{22}=\left(\frac{\left(Z_{in\_B}//Z_c\right)}{Z_{SB}+\left(Z_{in\_B}//Z_c\right)}\right)\left(\frac{1}{1+v_1e^{-2\gamma L}}\right)v_1e^{-\gamma L}$$

As long as Equation (2-2-1-11) has a unique solution, the proposed scheme can be proved as optimal to mitigate the entire induced voltage along the pipeline. This is because V_{SA} and V_{SB} are the necessary and sufficient conditions to mitigate the whole pipeline's induced voltage, including the terminals' one. And the application points for the two required neutralizing voltage sources should be the two terminals. Otherwise, we may have some remaining voltage on the pipeline.

In order to investigate whether Equation (2-2-1-11) has a unique solution, we can consider the rank theorem in linear algebra.

$$\begin{bmatrix} N_{11} & N_{12} \\ N_{21} & N_{22} \end{bmatrix}\begin{bmatrix} V_{SA} \\ V_{SB} \end{bmatrix}=\begin{bmatrix} \frac{Z_C}{\gamma}A \\ -\frac{Z_C}{\gamma}B \end{bmatrix} \qquad (2\text{-}2\text{-}1\text{-}12)$$

$$[N][V]=[k]$$

According to Equation (2-2-1-12), the rank of [N] = the rank of [$N|k$] = 2. This was calculated using Gaussian elimination. Since those values of rank are equal to the number of variables (V_{SA} and V_{SB}), in Equation (2-2-1-11) V_{SA} and V_{SB} are unique solutions. This conclusion also implies that the distributed EMFs can be represented equivalently as the two sources applied at the two terminals.

The mitigation effect can also be conceptually explained using the following voltage profiles.

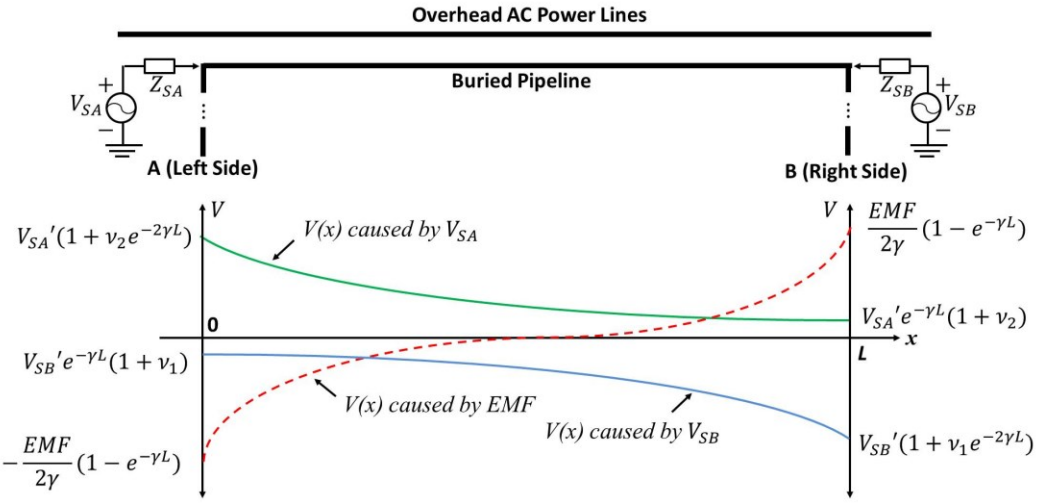

Figure 2-2-1-2: Voltage profiles along the buried pipeline with two applied neutralizing voltage sources

As shown in the above Figure 2-2-1-2, the summation of two voltage profiles caused by V_{SA} and V_{SB} can be the opposite voltage profile to the one caused by EMF. In line with the superposition principle, the three voltage profiles caused by EMF, V_{SA}, and V_{SB} can cancel each other. Based on this condition, the next section will discuss how to determine the required neutralizing voltage and capacity of active mitigation systems.

2.2.2 Determination of Required Neutralizing Voltage and Capacity of Active Mitigation Systems

The determination of devices' ratings is very important for a realistic mitigation system. This section proposes methods for determining the voltage and power ratings of devices.

A. Neutralizing Voltage Rating

Generally, as analyzed in the above, the required neutralizing voltage V_{SA} and V_{SB} can be calculated by Equation (2-2-1-11), with known pipeline parameters and

devices' internal impedance and grounding resistance. After the complicated derivation presented in Appendix F, Equation (2-2-1-11) can be simply expressed as

$$V_{SA} = \frac{-EMF \cdot (1+\nu_1)}{2\gamma \cdot \nu_1} = \frac{EMF \cdot Z_{SA}}{\gamma \cdot Z_c} \tag{2-2-2-1}$$

$$V_{SB} = \frac{EMF \cdot (1+\nu_2)}{2\gamma \cdot \nu_2} = -\frac{EMF \cdot Z_{SB}}{\gamma \cdot Z_c} \tag{2-2-2-2}$$

in which the pipeline length L does not appear.

The above equations (2-2-2-1) and (2-2-2-2) mathematically show that neutralizing voltages V_{SA} and V_{SB} are independent of L. It means that regardless of the pipeline's length, the active source voltage required to mitigate the induced voltage is the same for a given power line and pipeline terminal conditions. It suggests the long pipeline model shown in Figure 2-1-2-1 is valid to determine the required neutralizing voltage. Indeed, when applying two voltage sources calculated by equations (2-2-2-1) and (2-2-2-2) at the long pipeline's terminals, it is found that the terminal voltages become zero.

The above conclusion also implies that the proposed method is more efficient for long pipeline induction mitigation.

In addition, if the measured EMF contains harmonics, the voltage rating should be calculated by taking each harmonic component into consideration as follows.

$$\begin{aligned} V_{SA} &= \sqrt{\sum_h V_{SA}^2(h)} = \sqrt{\sum_h \left(\frac{EMF(h) \cdot Z_{SA}(h)}{\gamma(h) \cdot Z_c(h)} \right)^2} \\ V_{SB} &= \sqrt{\sum_h V_{SB}^2(h)} = \sqrt{\sum_h \left(\frac{EMF(h) \cdot Z_{SB}(h)}{\gamma(h) \cdot Z_c(h)} \right)^2} \end{aligned} \tag{2-2-2-3}$$

B. Power Rating for Active Mitigation System

Taking the left active mitigation system as an example, the equation of the required power S_{SA} can be derived based on the following Figure 2-2-2-1.

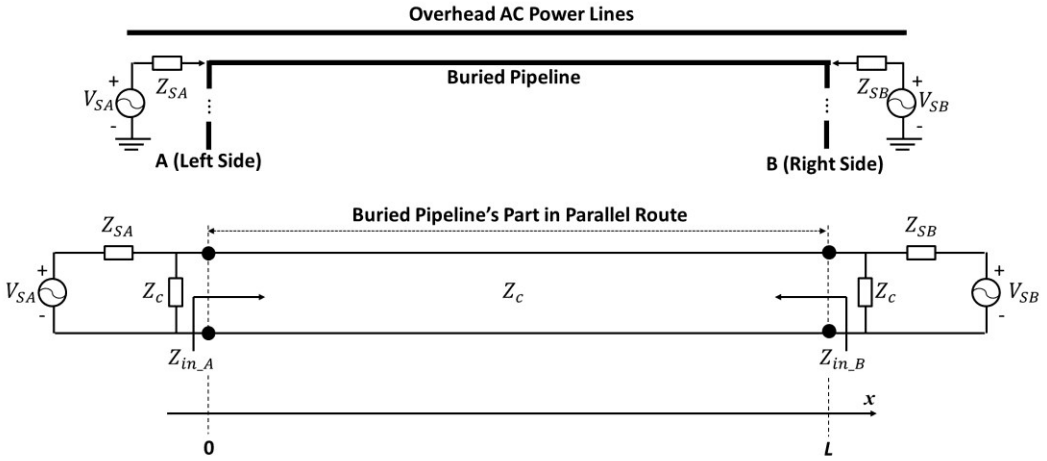

Figure 2-2-2-1: Equivalent circuit of the buried pipeline with active mitigation systems

From the above circuit, it is possible to derive the following equation of the required power S_{SA} for the left active mitigation system.

$$S_{SA} = \frac{(V_{SA})^2}{Z_{Total}} = \frac{(V_{SA})^2}{(Z_{SA} + Z_{eq\_pipe\_A})} \tag{2-2-2-4}$$

where,

$$Z_{eq\_pipe\_A} = Z_c // Z_{in\_A},\ Z_{in\_A} = Z_c \frac{Z_B + Z_C \tanh(\gamma L)}{Z_C + Z_B \tanh(\gamma L)}$$

Similarly, the required power for the active mitigation system at the right terminal will be

$$S_{SB} = \frac{(V_{SB})^2}{(Z_{SB} + Z_{eq\_pipe\_B})} \tag{2-2-2-5}$$

where,

$$Z_{eq\_pipe\_B} = Z_c \,//\, Z_{in\_B},\ Z_{in\_B} = Z_c \frac{Z_A + Z_C \tanh(\gamma L)}{Z_C + Z_A \tanh(\gamma L)}$$

Using Equation (2-2-2-1), equation (2-2-2-4) and (2-2-2-5) can be

$$\begin{aligned} S_{SA} &= \frac{(EMF \cdot Z_{SA})^2 (Z_c + 2Z_{SA})(1 + \tanh(\gamma L))}{\gamma^2 Z_c{}^2 \left[(Z_{SA}{}^2 + 2Z_{SA}Z_c) + (Z_c{}^2 + 2Z_{SA}Z_c + 2Z_{SA}{}^2)\tanh(\gamma L) \right]} \\ S_{SB} &= \frac{(EMF \cdot Z_{SB})^2 (Z_c + 2Z_{SB})(1 + \tanh(\gamma L))}{\gamma^2 Z_c{}^2 \left[(Z_{SA}{}^2 + 2Z_{SB}Z_c) + (Z_c{}^2 + 2Z_{SB}Z_c + 2Z_{SB}{}^2)\tanh(\gamma L) \right]} \end{aligned} \quad (2\text{-}2\text{-}2\text{-}6)$$

As you can see, different from V_{SA} and V_{SB}, the required power S_{SA} and S_{SB} depends on L due to the term of $\tanh(\gamma L)$. If the pipeline is long enough then $\tanh(\gamma L) \cong 1$ so S_{SA} and S_{SB} will be constant regardless of L and Equation (2-2-2-6) can be simplified as follows.

$$\begin{aligned} S_{SA} &= \frac{2(EMF \cdot Z_{SA})^2 (Z_c + 2Z_{SA})}{\gamma^2 Z_c{}^2 (3Z_{SA} + Z_c)(Z_{SA} + Z_c)} \\ S_{SB} &= \frac{2(EMF \cdot Z_{SB})^2 (Z_c + 2Z_{SB})}{\gamma^2 Z_c{}^2 (3Z_{SB} + Z_c)(Z_{SB} + Z_c)} \end{aligned} \quad (2\text{-}2\text{-}2\text{-}7)$$

Similar to V_{SA} and V_{SB}, if harmonics exist, Equation (2-2-2-7) becomes Equation (2-2-2-8).

$$\begin{aligned} S_{SA} &= \sqrt{\sum_h \left[\frac{2(EMF(h) \cdot Z_{SA}(h))^2 (Z_c(h) + 2Z_{SA}(h))}{\gamma(h)^2 Z_c(h)^2 (3Z_{SA}(h) + Z_c(h))(Z_{SA}(h) + Z_c(h))} \right]^2} \\ S_{SB} &= \sqrt{\sum_h \left[\frac{2(EMF(h) \cdot Z_{SB}(h))^2 (Z_c(h) + 2Z_{SB}(h))}{\gamma(h)^2 Z_c(h)^2 (3Z_{SB}(h) + Z_c(h))(Z_{SB}(h) + Z_c(h))} \right]^2} \end{aligned} \quad (2\text{-}2\text{-}2\text{-}8)$$

C. Required neutralizing voltage for feedback control

The above method can be used to determine the voltage and power ratings of devices. However, if the mitigation is not achieved in one step, the required neutralizing voltage needs to be automatically adjusted to a specific value. In this

case, a feedback control system is necessary for the automatic adjustment. For the feedback control, a new equation to calculate the neutralizing voltage in each step is necessary instead of Equation (2-2-1-11). The reason why the mitigation cannot be completed in one step will be explained in the next section.

From Equation (2-2-1-10), we have

$$Total\,V_A = Total\,V(0) = Coefficient_1 + Coefficient_2 \tag{2-2-2-9}$$

$$Total\,V_B = Total\,V(L) = Coefficient_1 \cdot e^{\gamma L} + Coefficient_2 \cdot e^{-\gamma L} \tag{2-2-2-10}$$

Since $Coefficient_1$ and $Coefficient_2$ contain the terms of V_{SA} and V_{SB}, it is possible to organize equations (2-2-2-9) and (2-2-2-10) regarding V_{SA} and V_{SB} as follows.

$$\begin{bmatrix} V_{SA} \\ V_{SB} \end{bmatrix} = \begin{bmatrix} K_{11} & K_{12} \\ K_{21} & K_{22} \end{bmatrix}^{-1} \begin{bmatrix} Total\,V_A - V_A\ caused\ by\ EMF \\ Total\,V_B - V_B\ caused\ by\ EMF \end{bmatrix} \tag{2-2-2-11}$$

where,

$$K_{11} = \frac{\left(Z_{in\_A} // Z_c\right)}{Z_{SA} + \left(Z_{in\_A} // Z_c\right)},\ K_{12} = \left[\left(1+\nu_1\right)e^{-\gamma L}\right]\left[\frac{\left(Z_{in\_B} // Z_c\right)}{Z_{SB} + \left(Z_{in\_B} // Z_c\right)}\right]\left(\frac{1}{1+\nu_1 e^{-2\gamma L}}\right)$$

$$K_{21} = \left[\left(1+\nu_2\right)e^{-\gamma L}\right]\left[\frac{\left(Z_{in\_A} // Z_c\right)}{Z_{SA} + \left(Z_{in\_A} // Z_c\right)}\right]\left(\frac{1}{1+\nu_2 e^{-2\gamma L}}\right),\ K_{22} = \frac{\left(Z_{in\_B} // Z_c\right)}{Z_{SB} + \left(Z_{in\_B} // Z_c\right)}$$

$$V_A\ caused\ by\ EMF = -\frac{Z_C}{\gamma}A + \frac{Z_C}{\gamma}B\ ,\ V_B\ caused\ by\ EMF = -\frac{Z_C}{\gamma}Ae^{\gamma L} + \frac{Z_C}{\gamma}Be^{-\gamma L}$$

Since Equation (2-2-2-11) contains the terms of two terminals' voltage ($Total\,V_A$, $Total\,V_B$), it can be set as the target value for mitigation purposes and directly used for building the feedback control system which monitors and mitigates the voltage of the two terminals of a buried pipeline.

It should be noted that the exact parameters for the above mentioned calculations are not available in practice; the methods in Section A and B are only for estimating ratings of devices by using conservative parameters, and the method in Section C is for determining the reduction rate of each mitigation step, which will be explained in the next section.

2.2.3 Active Mitigation Strategy

Ideally, if the required neutralizing voltages can be calculated exactly and two terminal voltages can be applied simultaneously, the induced voltage on the pipeline will be perfectly mitigated. However, some parameters cannot be exactly known, such as pipeline impedance and admittance, and other parameters vary, such as EMF and soil resistivity. To deal with those issues, feedback control is used to deal with variable induced voltage and unknown parameters by setting a reference voltage.

Feedback control needs a process time to achieve the reference voltage and two terminals of the buried pipeline affect mutually. For these reasons, the two terminal voltages should be adjusted alternatively and gradually. This can be done using a GPS timer.

Additionally, if one terminal voltage is canceled to zero by the one-step feedback control process, the other terminal voltage may increase to an unacceptable value, as shown in Figure 2-2-3-1. In order to avoid this situation, the two neutralizing voltages should be adjusted alternatively and gradually.

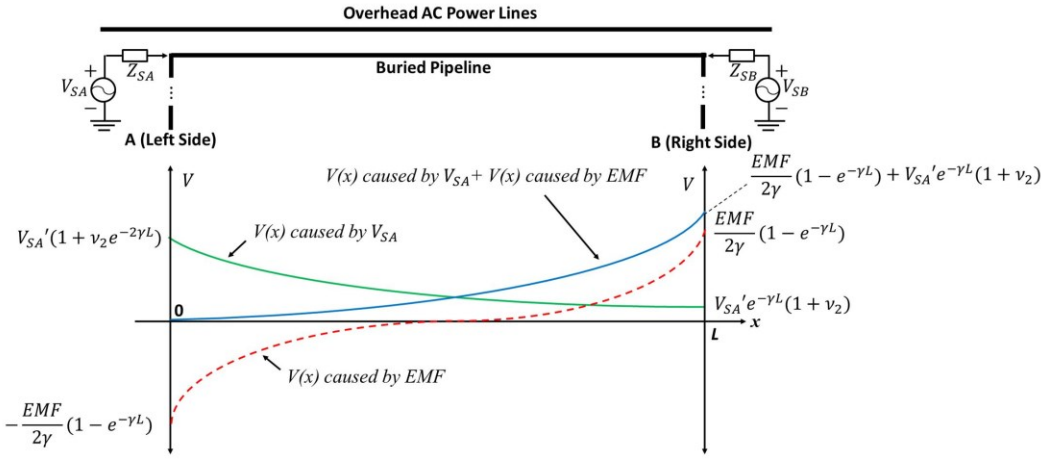

Figure 2-2-3-1: Voltage profile by applying only left terminal voltage

A. Feedback control system

Based on the above analysis, the feedback control system is developed as shown in the following Figure 2-2-3-2. In Figure 2-2-3-2, each active mitigation system is basically supposed to apply proper neutralizing voltage to each terminal in order to make actual voltage at each terminal a respective reference voltage.

Each reference voltage can be considered as the desired terminal voltage to be achieved by the active mitigation systems at each step (state) and obtained by

$$\text{Ref } V_{A(B)}{}^{(n+1)} = \left(1 - \frac{\text{Reduction Rate}}{100}\right) \times \text{Measured Actual } V_{A(B)}{}^{(n)} \qquad (2\text{-}2\text{-}3\text{-}1)$$

where, n+1: future state; n: present state.

With the known reference voltage, each neutralizing voltage at each terminal can be determined by the following equations.

$$V_{SA}{}^{(n+1)} = V_{SA}{}^{(n)} + \frac{\text{Ref } V_A{}^{(n+1)} - \text{Measured Actual } V_A{}^{(n)}}{K_{11}} \qquad (2\text{-}2\text{-}3\text{-}2)$$

$$V_{SB}{}^{(n+1)} = V_{SB}{}^{(n)} + \frac{\text{Ref } V_B{}^{(n+1)} - \text{Measured Actual } V_B{}^{(n)}}{K_{22}} \qquad (2\text{-}2\text{-}3\text{-}3)$$

where,

$$V_{SA}^{(0)} = V_{SB}^{(0)} = 0,\ K_{11} = \frac{\left(Z_{in\_A} // Z_c\right)}{Z_{SA} + \left(Z_{in\_A} // Z_c\right)},\ K_{22} = \frac{\left(Z_{in\_B} // Z_c\right)}{Z_{SB} + \left(Z_{in\_B} // Z_c\right)}.$$

The above equations are derived from Equation (2-2-2-11). According to Equation (2-2-3-2), if we set the reference voltage at the left terminal ($\text{Ref}\,V_A^{(n+1)}$), the required neutralizing voltage ($V_{SA}^{(n+1)}$) can be calculated based on the present state of the left terminal voltage ($\text{Measured Actual}\,V_A^{(n)}$). Through several alternative adjustment cycles, each neutralizing voltage alternatively and gradually converges to each final proper neutralizing voltage.

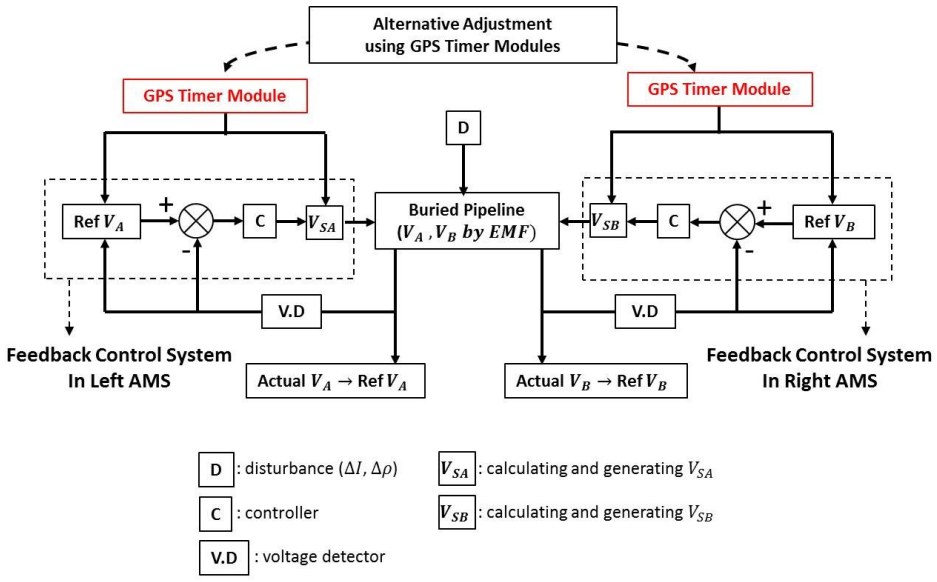

Figure 2-2-3-2: Feedback control diagram in active mitigation system

In Figure 2-2-3-2, each controller adjusts its voltage generator to generate the difference between each reference voltage and each measured terminal voltage. Each GPS timer module is supposed to alternatively provide an operation signal to each feedback control system to achieve the alternative adjustment of neutralizing voltage.

The following Figure 2-2-3-3 describes that two terminals' neutralizing voltages are gradually and alternative adjusted.

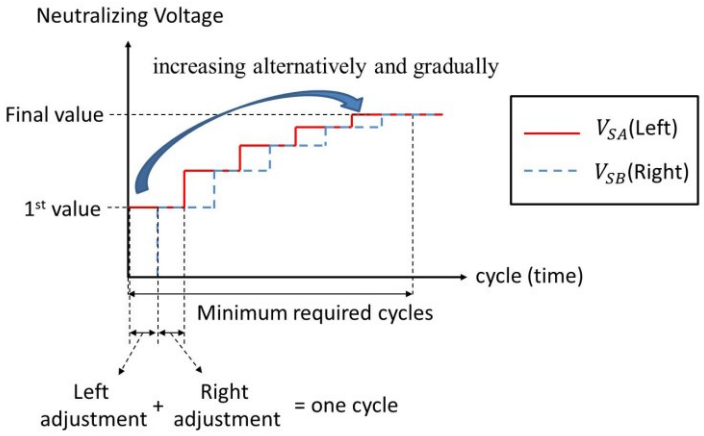

Figure 2-2-3-3: Alternative adjustment for neutralizing voltage

As shown in Figure 2-2-3-3, if we define one cycle as a pair of left and right adjustment, the minimum required number of cycles can be also defined as the first time when the entire voltage on the pipeline is mitigated within a certain criterion. In this thesis, the mitigation criterion is considered as 10V.

B. Determination of reduction rate

The reduction rate in the above equation indicates how much terminal voltage will be reduced by neutralizing voltage in one step. For example, if we set the reduction rate at 50%, each reference voltage is determined as 50% of measured terminal voltage at each adjustment step. Therefore, the terminal voltage converges gradually and alternatively to zero, being reduced to 50% of measured terminal voltage at each adjustment step.

In the case of two coupled terminals, the higher reduction rate causes a higher increase of voltage at the other terminal, but a faster mitigation effect, while the lower reduction rate brings a lower increase of voltage at the other terminal, but slower mitigation. The speed of mitigation and the maximum voltage increase at the other terminal are in a trade-off relation. The proposed value for the reduction rate is 50% in this thesis, but it is not an absolute solution. Depending on a specific case, it can be determined by users (engineers).

Since the maximum voltage increase $dV_{\max}$ (RMS) at the other terminal occurs at the first cycle for a fixed reduction rate, to limit $dV_{\max}$ to an acceptable value, the maximum allowable reduction rate can be calculated by

$$\max K_R = \frac{Criterion\ for\ dV_{\max}}{\left|K_{21} \cdot V_A\right|} = \frac{\left(Criterion\ for\ dV_{\max}\right)}{\left|K_{21} \cdot \frac{Z_c}{\gamma}(A-B)\right|} \tag{2-2-3-4}$$

where,

$Criterion\ for\ dV_{\max}$: the maximum acceptable voltage increase

K_R : reduction rate

$$A = \frac{EMF}{2Z_c}\frac{(1+\nu_1)\nu_2 - (1+\nu_2)e^{\gamma L}}{e^{2\gamma L} - \nu_1\nu_2},\ B = \frac{EMF}{2Z_c}\frac{(1+\nu_2)\nu_1 - (1+\nu_1)e^{\gamma L}}{e^{2\gamma L} - \nu_1\nu_2}e^{\gamma L}$$

$$K_{21} = \left[\left(1+\nu_2\right)e^{-\gamma L}\right]\left[\frac{\left(Z_{in\_A}\,//\,Z_c\right)}{Z_{SA} + \left(Z_{in\_A}\,//\,Z_c\right)}\right]\left(\frac{1}{1+\nu_2 e^{-2\gamma L}}\right)$$

Therefore, if there is a certain limited value for the maximum acceptable voltage increase in practice, engineers can determine the maximum allowable reduction rate using the above Equation (2-2-3-4) for the alternative adjustment.

As mentioned before, in the alternative adjustment, the minimum required number of cycles for mitigation can be considered as the value when both V_A and V_B in RMS become less than the ac corrosion criterion of 10V. In the alternative adjustment, it is hard to express the two terminals' voltage (V_A and V_B) as one simple equation due to its complexity. Therefore, in order to obtain values of V_A and V_B at a certain step (k-th adjustment), it is possible to consider the following sequence for V_{SA}, V_{SB}, V_A, and V_B based on equations (2-2-3-2) and (2-2-3-3).

Table 2-2-3-1: Sequence of V_{SA}, V_{SB}, V_A, V_B in the alternative adjustment

n	$V_{SA}^{(n)}$	$V_{SB}^{(n)}$	$V_A^{(n)}$	$V_B^{(n)}$
0	0	0	$-\frac{Z_c}{\gamma}(A-B)$	$-\frac{Z_c}{\gamma}\left(Ae^{\gamma L}-Be^{-\gamma L}\right)$
1	$-K_R V_A^{(0)}$	0	$V_A^{(0)}+V_{SA}^{(1)}$	$V_B^{(0)}+K_{21}V_{SA}^{(1)}$
2	$-K_R V_A^{(0)}$	$-K_R V_B^{(1)}$	$V_A^{(1)}+K_{12}V_{SB}^{(2)}$	$V_B^{(1)}+V_{SB}^{(2)}$
3	$-K_R V_A^{(2)}$	$-K_R V_B^{(1)}$	$V_A^{(2)}+V_{SA}^{(3)}$	$V_B^{(2)}+K_{21}V_{SA}^{(3)}$
4	$-K_R V_A^{(2)}$	$-K_R V_B^{(3)}$	$V_A^{(3)}+K_{12}V_{SB}^{(4)}$	$V_B^{(3)}+V_{SB}^{(4)}$
⋮	⋮	⋮	⋮	⋮
k-1	$-K_R V_A^{(k-2)}$	$-K_R V_B^{(k-3)}$	$V_A^{(k-2)}+V_{SA}^{(k-1)}$	$V_B^{(k-2)}+K_{21}V_{SA}^{(k-1)}$
k	$-K_R V_A^{(k-2)}$	$-K_R V_B^{(k-1)}$	$V_A^{(k-1)}+K_{12}V_{SB}^{(k)}$	$V_B^{(k-1)}+V_{SB}^{(k)}$

where,

n : adjustment number (step number), n=0 means the initial state, odd numbers = left terminal adjustments (for $V_{SA}^{(n)}$), even numbers = right terminal adjustments (for $V_B^{(n)}$)

Based on the above sequences, it is possible to consider the following condition for the minimum required number of cycles. Using the iteration numerical method from computer programming, we can obtain the minimum value of k, which meets the following condition.

$$\left|V_A^{(k)}\right| \le 10V \text{ and} \left|V_B^{(k)}\right| \le 10V \qquad (2\text{-}2\text{-}3\text{-}5)$$

where,

$$V_{SA}^{(0)} = V_{SB}^{(0)} = 0,\ V_A^{(0)} = \frac{Z_c}{\gamma}(A-B),\ V_B^{(0)} = \frac{Z_c}{\gamma}(Ae^{\gamma L} - Be^{-\gamma L})$$

If k is odd then $V_{SA}^{(k)} = -K_R V_A^{(k-1)},\ V_{SB}^{(k)} = V_{SB}^{(k-1)},\ V_A^{(k)} = V_A^{(k-1)} + V_{SA}^{(k)},\ V_B^{(k)} = V_B^{(k-1)} + K_{21}V_{SA}^{(k)}$

If k is even then $V_{SA}^{(k)} = V_{SA}^{(k-1)},\ V_{SB}^{(k)} = -K_R V_{SB}^{(k-1)},\ V_A^{(k)} = V_A^{(k-1)} + K_{12}V_{SB}^{(k)},\ V_B^{(k)} = V_B^{(k-1)} + V_{SB}^{(k)}$

Since we define that one cycle is a pair of left and right adjustment, the minimum required number of cycles $N_{\min}$ can be

$$\text{minimum required number of cycles } N_{\min} = round\left(\frac{\min k}{2} - 1\right) + 1 \qquad (2\text{-}2\text{-}3\text{-}6)$$

If the current or EMF contains harmonics, each harmonic component should be calculated one by one. The reduction rates for each harmonic are equal.

Figure 2-2-3-4 and 2-2-3-5 show graphs with % of maximum voltage increase at the other terminal, and the minimum required number of cycles for mitigation according to different reduction rates, under the following conditions.

Table 2-2-3-1: Parameters of buried pipeline in case study

Separation distance d_s	20m
Parallel Length L	10km
Soil resistivity ρ	100 Ωm
Phase Current I	500A
Load Imbalance(I_0/I_1) Imb	5%
3rd Harmonic IDD	9%
9th Harmonic IDD	2%

* Other detailed parameters are based on the case study in Section 2.2.6.

Figure 2-2-3-4 and 2-2-3-5 support the above trade-off relation between the speed of mitigation and the % of maximum increased voltage at the other terminal.

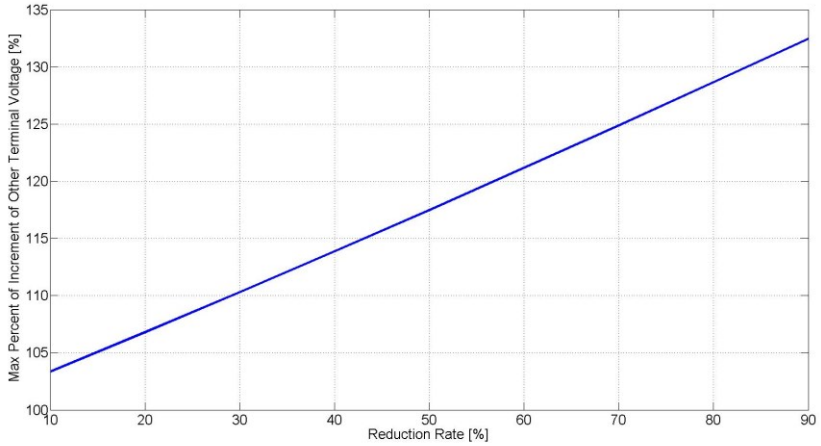

Figure 2-2-3-4: Graph of % of maximum voltage increase at the other terminal acording to different reduction rate in the alternative adjustment

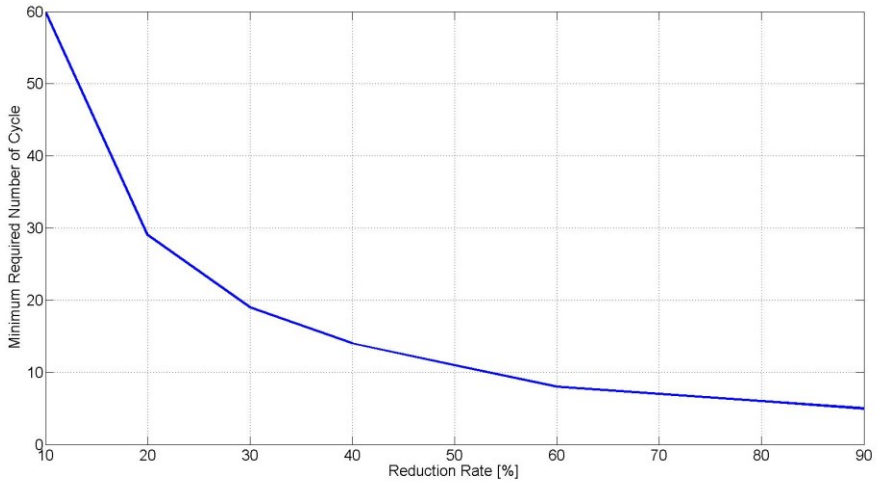

Figure 2-2-3-5: Graph of minimum required number of cycles for mitigation according to different reduction rate in the alternative adjustment

In this section we discussed the active mitigation strategy. Using such an active mitigation strategy, two terminals' voltage can be alternatively and gradually mitigated by two active mitigation sources.

2.2.4 Two Terminals Decoupling Length of Pipelines

As mentioned in Section 2.1.2, the criterion for long line model (two terminals decoupled model) is $L > L_{decoupling} = \frac{2}{real(\gamma)}$ based on the assumption that $\left| e^{-\gamma\left(\frac{2}{real(\gamma)}\right)} \right| = 0.1353 \cong 0$. $L_{decoupling}$ is called decoupling length.

Since the decoupling length $L_{decoupling}$ depends on the propagation constant of the pipeline, it consequently depends on the coating resistance and harmonic orders as the follow Table 2-2-4-1.

Table 2-2-4-1: Parameters of buried pipeline in case study

H	Polyethylene		Bitumen	
	γ	$L_{decoupling}$ [km]	γ	$L_{cecoupling}$ [km]
1	0.0577+j0.0658	34.7	0.6636+j0.5103	3.0
3	0.0743+j0.1527	26.9	1.0423+j0.8355	1.9
9	0.1005+j0.4134	19.9	1.6493+j1.3774	1.2

* H indicates harmonic orders.

The following Figure 2-2-4-1 shows one sample of induced terminal voltage by L based on the conditions described in Table 2-2-3-2.

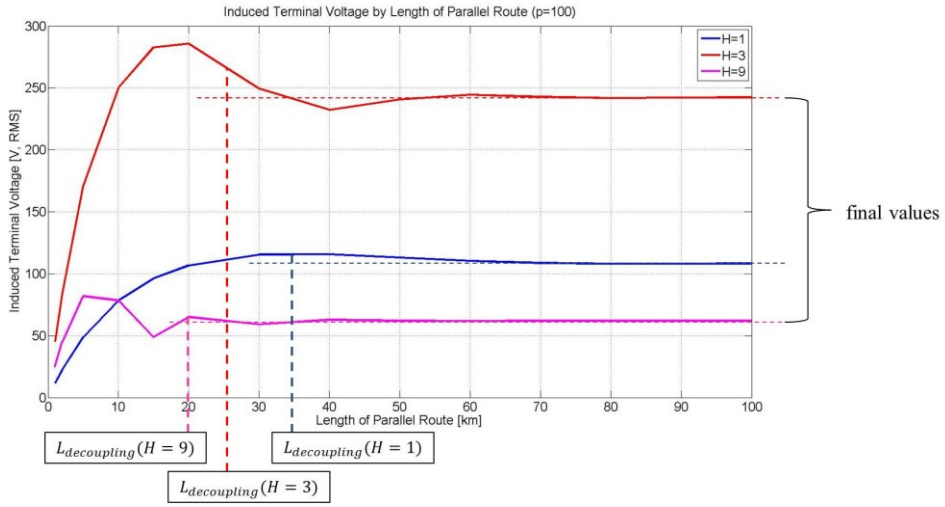

Figure 2-2-4-1: Graph of induced terminal voltage by L

According to Figure 2-2-4-1, induced terminal voltage seems almost constant by L as long as L exceeds $L_{decoupling}$. However, there are some differences between the induced terminal voltage at $L_{decoupling}$ and the final constant value because $\left|e^{-\gamma L_{decoupling}}\right|$ is not exactly zero but small ($\left|e^{-\gamma L_{decoupling}}\right|$=0.1353≠0). The concept of decoupling length used here is to ensure that the voltage applied to one terminal has acceptable impact on the other terminal. Therefore, further analysis is needed.

Considering two applied voltages and assuming zero EMF in Equation (2-2-2-11), the following equation holds.

$$\begin{bmatrix} TotalV_A \\ TotalV_B \end{bmatrix} = \begin{bmatrix} K_{11} & K_{12} \\ K_{21} & K_{22} \end{bmatrix} \begin{bmatrix} V_{SA} \\ V_{SB} \end{bmatrix} \quad \text{(2-2-4-1)}$$

The magnitude of factor K_{12} and K_{21} in Equation (2-2-4-1) indicates the ratio of V_{SB} and V_{SA} which appear on terminal voltage TotalV_A and TotalV_B respectively. Therefore, K_{12} and K_{21} can be the index of the mutual effect between two terminals of the pipeline. They can be used to evaluate the decoupling effect of the pipeline. If K_{12} and K_{21} are zero, the two terminals of the pipeline can be considered as completely decoupled. In this case, the GPS timer is no longer necessary and the two active sources can be operated separately.

The following Figure 2-2-4-2 shows one sample graph of magnitude of K_{12} according to L. The conditions for the following Figure 2-2-4-2 are the same as those for Figure 2-2-4-1.

As shown in Figure 2-2-4-2, $|K_{12}|$ decreases by the increase of L. This means that the mutual effect between the two terminals of the pipeline decreases by the increase of L. In Figure 2-2-4-2 we can see that $|K_{12}|$ at $L_{decoupling}$ is quite small (0.0234 at H=1). However, the voltage increase at the other terminal may not be negligible when we consider that the criterion voltage for AC corrosion is 10V (when $\rho > 25\Omega\text{m}$). Usually the required neutralizing voltage is much higher than the induced voltage. Therefore, the criterion for no interference between two terminals' neutralizing voltage may be considered longer than $L_{decoupling}$ based on Equation (2-1-2-1).

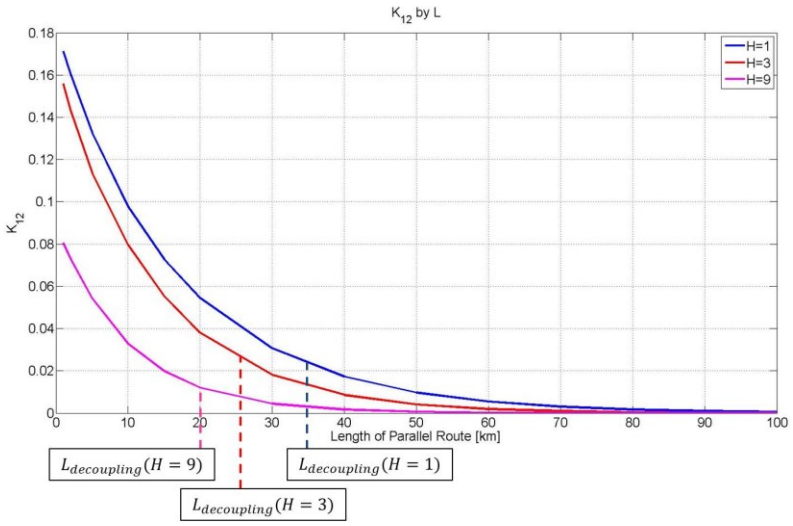

Figure 2-2-4-2: Graph of magnitude of K_{12} according to L

In practice, $L_{decoupling}$ can be determined by the following steps.

- Calculate $|K_{12}|(|K_{21}|)$ by the required voltage V_{SA} (V_{SB}) and the allowable voltage increase at the other terminal (V_A by V_{SA} or V_B by V_{SB}).
- Calculate L by equations for K_{12} (K_{21}).

For example, we can assume the pipeline requires the neutralizing voltage of 500V (at 60Hz) at the right terminal ($V_{SB} = 500V$). In this case, we may consider that the maximum allowable voltage increase at the left terminal can be limited to 10V ($\max \text{allowable} V_A \, by \, V_{SB} = 10\text{V}$).

Based on the maximum allowable voltage increase of 10V at the left terminal, we can consider that the percent of allowable voltage increase is 2% (10V/500V) at 60Hz. This means the minimum acceptable value for $|K_{12}|$ is 0.02.

Since we define the value of L, which causes the acceptable $\min|K_{12}|$, as $L_{decoupling}$, we can obtain the value of $e^{\gamma L_{decoupling}}$ using the equation for K_{12} as follows.

$$K_{12} = f(L) = \left[\left(1+\nu_1\right)e^{-\gamma L}\right]\left[\frac{\left(Z_{in\_B}//Z_c\right)}{Z_{SB}+\left(Z_{in\_B}//Z_c\right)}\right]\left(\frac{1}{1+\nu_1 e^{-2\gamma L}}\right) \qquad (2\text{-}2\text{-}4\text{-}2)$$

Here we should ensure that K_{12} is a complex number. Unfortunately, we only have the condition of $|K_{12}|$ instead of a complex number K_{12}. Therefore, in order to obtain the value of $L_{decoupling}$ which satisfies acceptable $\min|K_{12}| = |f(L_{decoupling})|$, we can use the iteration numerical method from computer programming. By using the iteration numerical method with some range of L, it is possible to obtain the value of $L_{decoupling}$. The value of $L_{decoupling}$ that satisfies $0.02 = |f(L_{decoupling})|$ is 37.251 km.

The above result shows that, in practice, $L_{decoupling}$ with consideration of the absolute value of the allowable voltage increase, may be longer than that calculated by Equation (2-1-2-1).

The above example is based on the following parameters.

ν_1 at $H=1$	-0.2233 + j0.0013
Z_{in_B} at $H=1$	5.1534 + j3.4676 [Ω]
Z_{SB} at $H=1$	10 + j5 [Ω]
Z_c at $H=1$	5.7724 + j2.8306 [Ω]
γ at $H=1$	0.0577 + j0.0658

Because the fundamental component requires longer decoupling length in normal cases, it can be considered as the criterion to identify whether a pipeline can be treated as the pipeline of which two terminals are decoupled.

2.2.5 Other Considerations for Devices in Proposed Active Mitigation System

As mentioned before, each active mitigation system comprises the following three devices.

- a power supply
- a controllable voltage source with a feedback control system
- a voltage detector

There are some other considerations for those devices.

A. Power Supply

The power supply provides sufficient power to all devices in the active mitigation system. The power supply can be either a single phase transformer connected to a nearby distribution power line, or a power panel receiving power from other nearby power sources, such as a low voltage feeder, a solar panel, etc. It depends on the specific site condition of the respective buried pipeline.

B. Controllable Voltage Source with Feedback Control System

In practice, the controllable voltage sources can be realized by Pulse Width Modulation-based power electronic technology. Therefore the neutralizing voltage with a proper waveform can be generated immediately, and the response to the variation of AC currents in overhead power lines and soil resistivity can be completed in several cycles.

C. Voltage Detector

A voltage detector in the active mitigation system measures the one-terminal voltage of the buried pipeline. The PWM-based power electronic device in the controllable voltage source requires terminal voltage data in order to generate proper neutralizing voltage waveforms. Therefore, the voltage detector should be able to provide the correct voltage data (waveform) at a measuring (access) point on the pipeline (usually two terminals). The voltage detector can be the voltage sensor, with one terminal connected to the pipeline's access point and the other one grounded through a reference electrode. To ensure proper operation of this system, the reference electrode must be separated from a grounding point of a

controllable voltage source and a buried pipeline by a certain distance in order to avoid interferences. We will discuss this issue again in Section 2.3.2 and 3.6.2.

2.2.6 Case Study

The case study in this section shows the mitigation availability of the proposed method at both fundamental and harmonic frequencies.

A. Determination of EMF

The required neutralizing voltage is dependent on EMF, which is determined by nearby power lines' current and mutual impedance. EMF can be obtained either by the measurement method to be introduced in Chapter 4, or by calculation based on the Carson-Clem equation [1][6][7] as presented in Appendix C.

B. Description of Case Study

To evaluate the proposed active mitigation system, one simple case study has been conducted. The case study considers one buried pipeline parallel to one three-phase AC power line. The following describes the detailed conditions of the case study.

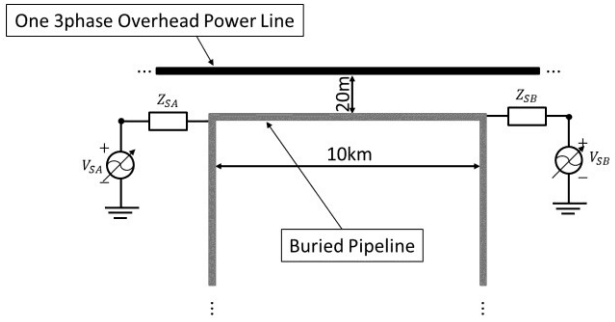

Figure 2-2-6-1: Top view of case study

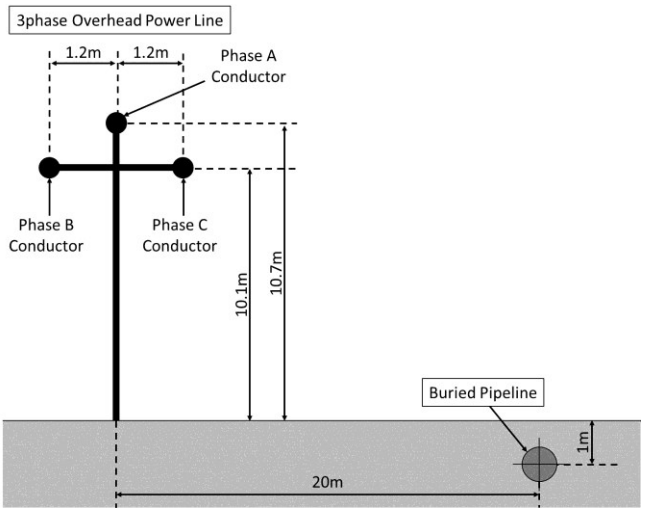

Figure 2-2-6-2: Side view of case study

Major parameter values are as follows.

Table 2-2-6-1: Parameters of overhead power lines in case study

Position of Phase Conductor A [m]	(0, 10.7)
Position of Phase Conductor B [m]	(-1.2, 10.1)
Position of Phase Conductor C [m]	(1.2, 10.1)
Magnitude of Phase Current [A]	500
Load Imbalance [%]*	5

* Load Imbalance is considered in the current of phase conductor C which is the closest to the buried pipeline (magnitude of current of phase conductor C = 500·(1+3·Load Imbalance/100))

Table 2-2-6-2: Parameters of buried pipeline in case study

Position of Buried Pipeline [m]	(20,-1)
Separation Distance from Overhead Power Lines [m]	20
Buried Depth [m]	-1
Length in Parallel [km]	10

Table 2-2-6-3: Other parameters in case study

Soil Resistivity ρ [Ωm]	100
Equivalent Impedance of Active Mitigation System (Left) Z_{SA} [Ω]	10 + j5h
Equivalent Impedance of Active Mitigation System (Right) Z_{SB} [Ω]	10 + j5h

*The other detail parameters can be referred to in Appendix G.

Table 2-2-6-4: Average harmonic sequence characteristics of residential feeder [6]

	Sequence Actual Values [A]		
	Zero	**Positive**	**Negative**
1st	12.68	291.24	13.57
3rd	20.45	1.84	1.68
5th	1.34	1.44	15.28
7th	0.71	6.56	0.84
9th	4.68	0.62	0.49

By comparing voltage profiles of the pipeline in the before and after mitigation cases, it is possible to assess the mitigation effect caused by the proposed active mitigation method. In addition, the analytically calculated voltage profile can be verified by the simulation result.

For the simulation in this case study, the parallel zone (route) of the pipeline is divided into 10 segments; thus a total of 11 measuring points for the voltage profile were considered, as shown in the following Figure 2-2-6-3. The #1 and #11 point correspond to the left and right terminals of the pipeline respectively.

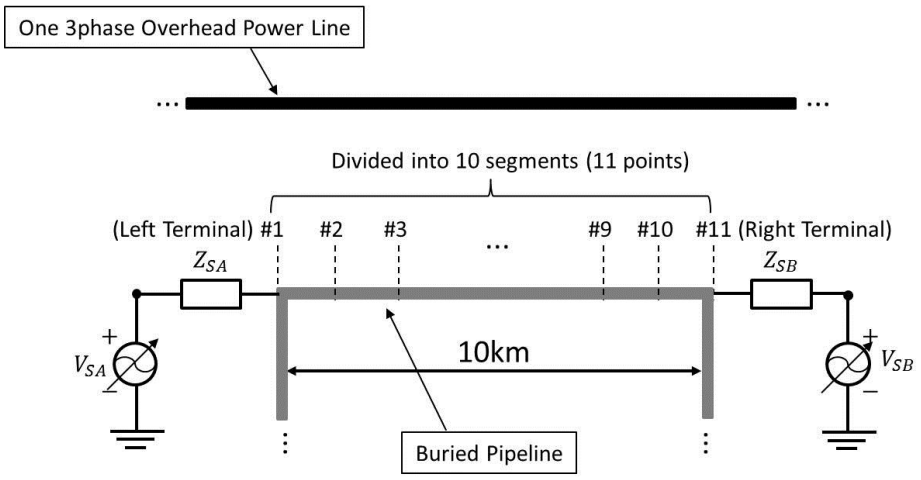

Figure 2-2-6-3: Pipeline divided into 10 Segments

C. Mitigation Effect

Because this case study is based on the known parameters, the alternative mitigation strategy and the feedback control are not necessary to show the final mitigation effect. The calculated neutralizing voltages as shown in Table 2-2-6-5,

including harmonics, are directly applied to the two terminals in order to mitigate the entire induced voltage along the pipeline.

Table 2-2-6-5: Table of neutralizing voltage and K factors by harmonic order

H	1	3	5	7	9
V_{SA}	156.8+j127.6	313.0+j458.7	26.8+j47.6	9.4+j35.8	89.2+j302.3
V_{SB}	-156.8-j127.6	-313.0-j458.7	-26.8-j47.6	-9.4-j35.8	-89.2-j302.3
K_{11}	0.221+j0.011	0.165-j0.122	0.084-j0.120	0.051-j0.103	0.030-j0.088
K_{22}	0.221+j0.011	0.165-j0.122	0.084-j0.120	0.051-j0.103	0.030-j0.088

Following Figure 2-2-6-4 and 2-2-6-5 show the mitigation effect for each component.

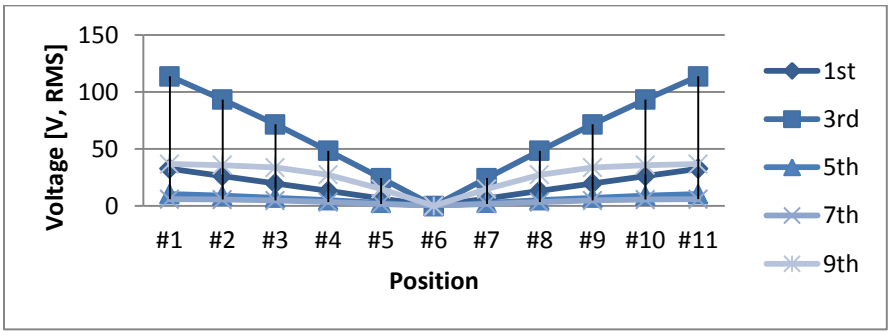

Figure 2-2-6-4: Induced voltage profile (magnitude) before mitigation according to harmonic order

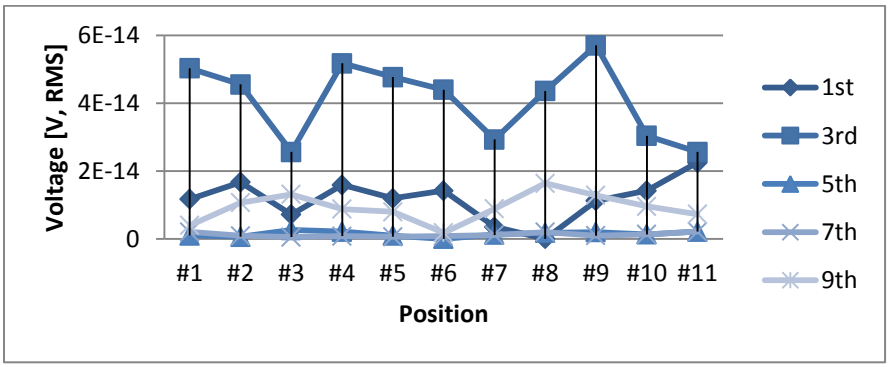

Figure 2-2-6-5: Induced voltage profile (magnitude) after mitigation according to harmonic order

Table 2-2-6-6: Analytical result of voltage profiles at harmonic frequencies (before mitigation)

Before Mitigation (Analytical) [V,RMS]											
	#1	**#2**	**#3**	**#4**	**#5**	**#6**	**#7**	**#8**	**#9**	**#10**	**#11**
1st	32.6	26.1	19.6	13.1	6.5	0.0	6.5	13.1	19.6	26.1	32.6
3rd	113.6	93.3	71.4	48.3	24.4	0.0	24.4	48.3	71.4	93.3	113.6
5th	10.4	9.0	7.2	5.0	2.6	0.0	2.6	5.0	7.2	9.0	10.4
7th	5.9	5.5	4.6	3.4	1.8	0.0	1.8	3.4	4.6	5.5	5.9
9th	36.7	35.7	33.6	27.3	14.8	0.0	14.8	27.3	33.6	35.7	36.7

Table 2-2-6-7: Simulation result of voltage profile at harmonic frequencies (before mitigation)

Before Mitigation (Simulation) [V,RMS]											
	#1	**#2**	**#3**	**#4**	**#5**	**#6**	**#7**	**#8**	**#9**	**#10**	**#11**
1st	32.6	26.1	19.6	13.1	6.5	0.0	6.5	13.1	19.6	26.1	32.6
3rd	113.6	93.3	71.4	48.3	24.4	0.0	24.4	48.3	71.4	93.3	113.6
5th	10.4	9.0	7.2	5.0	2.6	0.0	2.6	5.0	7.2	9.0	10.4
7th	5.8	5.5	4.6	3.4	1.8	0.0	1.8	3.4	4.6	5.5	5.8
9th	36.5	35.6	33.7	27.4	14.9	0.0	14.9	27.4	33.7	35.6	36.5

The calculation and simulation results for the case after mitigation show that all voltages at the measurement points (#1~#11) according to harmonic order are almost zero. The maximum remaining voltage in the simulation result for the case after mitigation is just 0.01V. Therefore, the tables for the calculation and simulation result for the case after mitigation are omitted.

In practice, there would be some discrepancies between the calculation values and the actual values of the parameters. Therefore, we may have some errors in the calculation of neutralizing voltage as well. Due to these errors in practice, a feedback control system is necessary for the proposed active mitigation system.

D. Process of alternative adjustment

Considering the fundamental component only, the following Figure 2-2-6-6 shows the alternative adjustment of neutralizing voltage based on the above case study (500A phase current and 5% load imbalance). It shows the change of voltage profile (real part) during 10 adjustments (5 left and 5 right adjustments).

As you can see, the induced voltage caused by EMF can be mitigated gradually through several cycles of the alternative adjustment. Due to the mutual effect between the two terminals of the pipeline, we may have the maximum voltage increase at the other terminal in the 1st adjustment step. As mentioned earlier, the maximum voltage increase is highly dependent on a reduction rate. Figure 2-2-6-5 is based on the reduction rate of 50%. In the long line model, there is no mutual effect between the two terminals. Therefore, if the pipeline is considered as the long line model, we do not have to consider the alternative adjustment of neutralizing voltages.

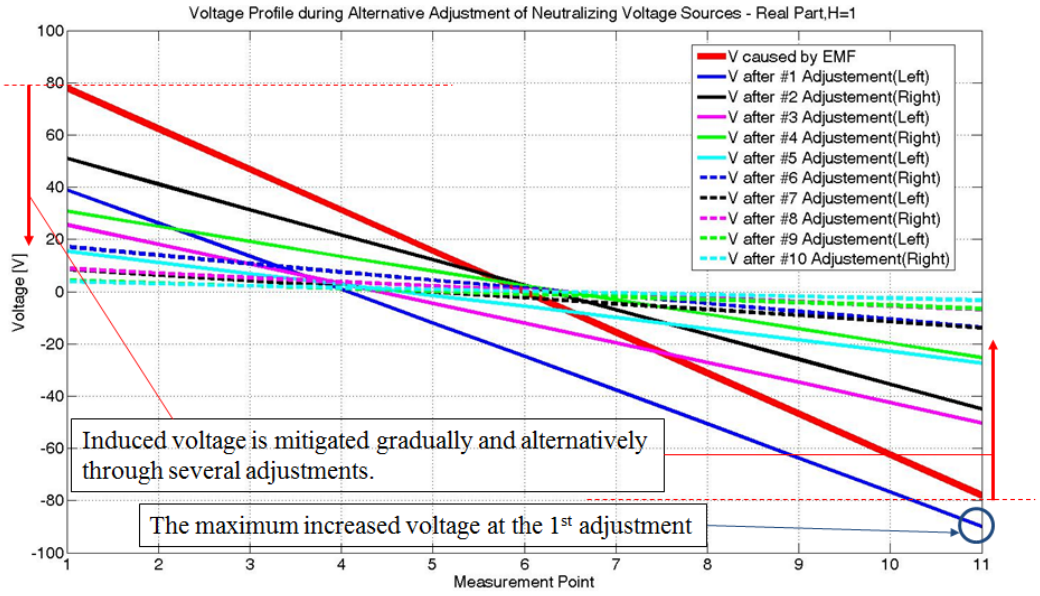

Figure 2-2-6-6: Change of voltage profile duing the alternative adjustment

2.3 Practical Issues to Solve

When we coordinate actual active mitigation systems for buried pipelines, we may encounter several practical issues to solve. In this section, we will discuss those issues.

2.3.1 Grounding Point of Voltage Detector

As mentioned earlier, a voltage detector plays a role in measuring one terminal voltage of a buried pipeline. The voltage data measured at the terminal are essential to calculate and generate the proper neutralizing voltage. Measuring terminal voltage means to measure the potential difference between the pipeline's terminal and the remote earth. In order to measure the correct terminal voltage, the reference potential of the voltage detector should be zero. Therefore, it is important to know where to install the reference electrode of the voltage detector. There are two possible causes of reference potential rise: (1) the buried pipeline, which has induced voltage and increases the ground potential around it and (2) the controllable voltage source, which is returning steady-state current through its grounding point.

Regarding (1) the impact of the pipeline on the ground potential, it would be negligible according to Reference [8]. Through case studies and simulations with the professional software CDEGS, Reference [8] shows that the range of Ground Potential Rise caused by the induced voltage on the pipeline (62~67V) is just a few volts (2.04~2.41V) at the location of the pipeline's terminal. Such GPR caused by the pipeline obviously decreases when the pipeline is mitigated by active mitigation systems. Therefore, the GPR caused by the pipeline would be negligible (close to zero). For this reason, it is acceptable to install a reference electrode of a voltage detector with a few meters (1~2m) away from terminals of the buried pipeline, which is supposed to be mitigated by the active mitigation method. The details supporting the data in Reference [8] can be referred to in Appendix H.

Regarding (2) the impact of a controllable voltage source on the ground potential, it would be a significant disturbance to a voltage detector. This is because the controllable voltage source has a returning steady-state current through its grounding point, and that could cause high GPR. The recommended solution for this issue is to consider the separation distance between the reference electrode of

the voltage detector and the grounding point of the controllable voltage source. In Chapter 3 we explain how to determine that separation distance.

2.3.2 GPR on Grounding Point of Controllable Voltage Source

In the equivalent circuit of the proposed active mitigation method, we have considered two active sources as Thevenin's equivalent voltage source. In reality, a controllable voltage source comprises internal impedance and a grounding resistor as in the following Figure 2-3-2-1.

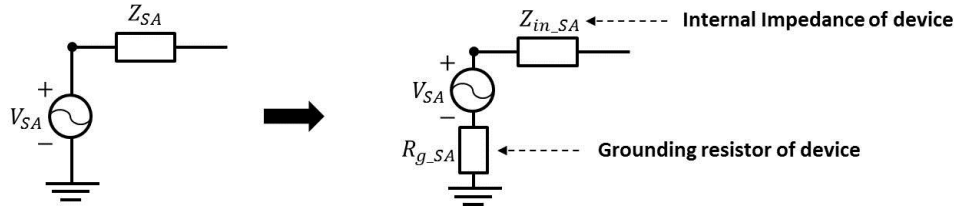

Figure 2-3-2-1: Practical neutralizing voltage source model

Therefore, GPR will be observed at the grounding point when the device is operated as shown in the following Figure 2-3-2-2.

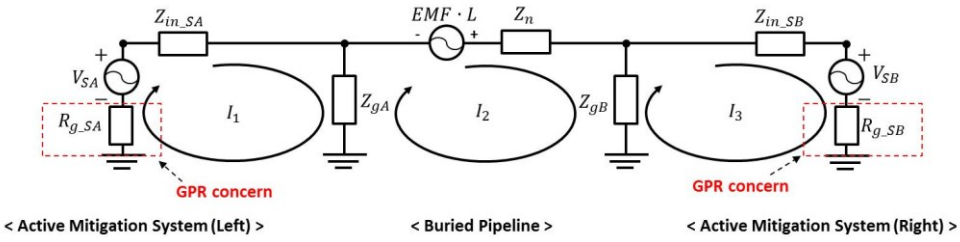

Figure 2-3-2-2: Equivalent circuit of the buried pipeline with practical neutralizing voltage source model

According to Figure 2-3-2-2, mesh current I_1 and I_3 can cancel the voltage drops caused by I_2 at each terminal, which correspond to induced terminal voltage on the pipeline. However, those mesh currents also cause certain voltage drops at R_{g_SA} and R_{g_SB}, which correspond to the equivalent grounding resistors of each controllable voltage source device. Such voltage drops at R_{g_SA} and R_{g_SB} could be GPR concerns. Such GPR may cause a safety issue to the public and utility personnel, and may influence the voltage detection in the active mitigation system.

The recommended solution for such GPR issues is

- to distribute that GPR, using a properly designed grounding grid at the grounding point of the controllable voltage source
- to secure enough separation distance between the reference electrode of the voltage detector and the grounding point of the voltage detector.

A detailed explanation of these solutions is presented in Chapter 3.

2.3.3 Availability of Existing Access Points to Buried Pipelines

In the proposed active mitigation method we consider the two terminals of a buried pipeline as application points for neutralizing voltage. This means that we should install two terminal rods at the locations of the pipeline's two terminals in order to apply the neutralizing voltage.

If there are nearby access points to the buried pipeline, we may consider those existing access points as application points for the neutralizing voltage. In this case, the mitigation effect with those existing access points should be evaluated. Detailed information about the mitigation effect using existing access points is presented in Chapters 3 and 5.

2.4 Summary

Based on the characteristics of induced voltage along a pipeline, an active mitigation method is proposed. The mitigation system requires two active sources, and each source contains three major devices: a voltage detector, a controllable voltage source, and a power supply. The analysis proves that this scheme is optimal. The calculation methods for the determination of voltage and power ratings of the devices are also presented. The voltage rating is independent of the pipeline length, whereas the power rating is slightly affected by the pipeline length when the pipeline is short. This suggests that the proposed method is more suitable for cases with long pipelines.

The feedback control is introduced into this scheme to automatically adjust the applied voltages at two terminals of the pipeline, in responding to the variation in voltage induction. A feedback control strategy, alternative adjustment of active voltage sources step by step, is provided to meet the safety requirement during the mitigation.

The two terminals decoupling length of a pipeline is discussed. Once the decoupling length is met, the active mitigation systems at two terminals can be operated separately.

In addition, some practical issues are raised when we apply the proposed active mitigation method to actual cases. The recommended solutions to those practical issues are presented in the following chapters.

Chapter 3

Sensitivity Studies

The purpose of sensitivity studies in this chapter is to find out major impact factors on major design parameters of the proposed active mitigation system. Through the sensitivity studies with consideration of the practical ranges of the impact factors, it is possible to obtain the practical ranges of the major design parameters. In addition, this chapter presents the estimation charts, which are obtained from sensitivity studies, in order to estimate the rough values of the major design parameters without detail calculation process. The major design parameters and impact factors on the proposed active mitigation system are as follows.

Table 3-1: Major design parameters and impact factors on the proposed active mitigation system

Major Design Parameters	Impact Factors
- Induced Terminal Voltage V_A - Required Neutralizing Voltage V_{SA} - Require Power S_{SA}	- Phase Current (Balanced) I - Load Imbalance Imb - Harmonics (harmonic order H) - Separation Distance d_s - Equivalent Internal Impedance of Controllable Voltage Source Z_{SA} - Length of Parallel Route L - Soil Resistivity ρ

In this chapter, analysis of the impact factors and the sensitivity studies for the major design parameters are presented through Section 3.1 ~ 3.4. A sensitivity study for a reduction rate in the alternative adjustment is presented in Section 3.5.

Sensitivity studies for GPR interference caused by a controllable voltage source and a mitigation effect using existing access points are presented in Section 3.6 and 3.7 respectively.

3.1 Analysis of Impact Factors on Induced Voltage on Buried Pipelines

3.1.1 Impact Factors on Induced Voltage on Buried Pipelines

As discussed earlier, induced voltage on buried pipelines can be calculated using the following analytical equation.

$$V(x) = -\frac{Z_c}{\gamma}\left(Ae^{\gamma x} - Be^{-\gamma x}\right) \tag{3-1-1-1}$$

where,

$$A = \frac{EMF}{2Z_c}\frac{(1+\nu_1)\nu_2 - (1+\nu_2)e^{\gamma L}}{e^{2\gamma L} - \nu_1\nu_2},\ B = \frac{EMF}{2Z_c}\frac{(1+\nu_2)\nu_1 - (1+\nu_1)e^{\gamma L}}{e^{2\gamma L} - \nu_1\nu_2}e^{\gamma L}$$

$$\nu_1 = \frac{Z_A - Z_C}{Z_A + Z_C} \quad \nu_2 = \frac{Z_B - Z_C}{Z_B + Z_C}$$

In order to find out impact factors on induced voltage on buried pipelines, Equation (3-1-1-1) can be expressed as follows.

$$V(x) = -\frac{Z_c}{\gamma}\left(Ae^{\gamma x} - Be^{-\gamma x}\right) = EMF \cdot f\left(\rho, L, x\right) \tag{3-1-1-2}$$

The separation distance d_s between a buried pipeline and overhead AC power lines is normally much longer than the distance between phase conductors in overhead AC power lines. Therefore, the distance between each phase conductor and the buried pipeline can be considered as roughly same. This means that the impact of configuration of power line tower on induced voltage is small [10]. With consideration of normal separation distance d_s ($\geq$15m), it is possible to

consider that the mutual impedance between each phase conductor in the overhead AC power lines and the buried pipeline is the almost same as follows.

$$Z_{ma} \simeq Z_{mb} \simeq Z_{mc} = Z_m$$

Therefore, induced EMF on the buried pipeline can be expressed as follows.

$$EMF \approx Z_m \cdot \left(I_a + I_b + I_c\right) = Z_m \cdot I_{residual} \tag{3-1-1-3}$$

In Equation (3-1-1-3), $I_{residual}$ indicates the residual current with consideration of three-phase current cancelation and corresponds to total zero sequence currents in overhead AC power lines. Based on this, Equation (3-1-1-2) can be as follows.

$$V(x) = EMF \cdot f\left(\rho, L, x\right) = Z_m(d_s, \rho, H) \cdot I_{residual} \cdot f\left(\rho, L, x\right) \tag{3-1-1-4}$$

According to Equation (3-1-1-4), it is obvious that induced voltage $V(x)$ is proportional to $I_{residual}$. However, it is not easy to figure out how $V(x)$ changes according to other impact factors (d_s, ρ, L, H) in Equation (3-1-1-4). In Equation (3-1-1-4), the 1st and 3rd terms are independent of $I_{residual}$. Therefore, induced voltage $V(x)$ can be normalized by $I_{residual}$ as follows.

$$\frac{V(x)}{I_{residual}} = Z_m\left(d_s, \rho, H\right) \cdot f\left(\rho, L, x\right) \tag{3-1-1-5}$$

Since $I_{residual}$ can be calculated according to many combinations of load current, load imbalance, and harmonic current values, it is a much simpler way to consider the normalized $V(x)$ by $I_{residual}$ in order to figure out how $V(x)$ changes according to d_s, L, ρ, H.

We are interested in induced voltage at two terminals ($V(0)$ and $V(L)$) of a buried pipeline because they are the mitigation indicators to be monitored and controlled in the proposed active mitigation system. In the typical case, both the left and right terminal voltage has same magnitude ($|V(0)| = |V(L)|$) but phase angle.

Therefore, it is okay to consider only one terminal voltage for sensitivity studies. In this chapter, we are going to discuss the left terminal voltage's magnitude ($|V_A|$ or $|V(0)|$) for sensitivity studies as follows.

$$V_{A\_per\_A} = \frac{V(0)}{I_{residual}} = Z_m(d_s, \rho, H) \cdot f(\rho, L) \qquad (3\text{-}1\text{-}1\text{-}6)$$

* $V_{A\_per\_A}$ indicates the normalized induced terminal voltage V_A by residual current $I_{residual}$ (voltage per ampere).

Equation (3-1-1-6) suggests that $V_{A\_per\_A}$ is a function of d_s, L for a given H and ρ. With consideration of typical ranges of d_s and L, it is possible to obtain contour curves of $V_{A\_per\_A}$ for a given H, ρ. Those contour curves can be used as estimation charts which provide rough values of $V_{A\_per\_A}$, for a given d_s, L, ρ, and H. Therefore, as long as we have a specific value of $I_{residual}$, we can estimate the magnitude of induced terminal voltage V_A. Similar to $V_{A\_per\_A}$, required neutralizing voltage V_{SA} and required power S_{SA} for one active mitigation system (at left terminal) can be normalized by $I_{residual}$ and we can also consider contour curves of them as estimation charts.

The following Figure 3-1-1-1 shows one example of contour curves of $V_{A\_per\_A}$ according to d_s and L for H=1 and ρ=100 Ωm.

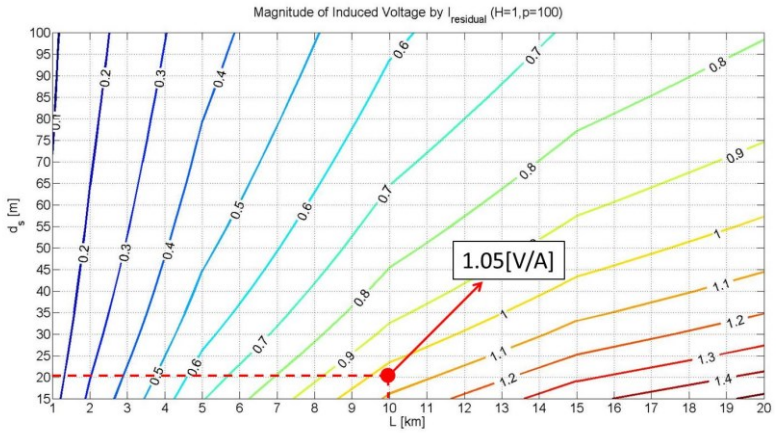

Figure 3-1-1-1: One example contour curves of $V_{A\_per\_A}$ at the fundamental frequency

For example, if we have specific values of the impact factors such as d_s = 20m, L = 10km, ρ =100 Ωm and $I_{residual}$ = 75A at the fundamental frequency, the induced terminal voltage V_A can be easily estimated as follows.

$$V_A = V_{A\_per\_A} \cdot I_{residual} = (1.05) \cdot (75) = 78.75\,\text{V} \quad \text{(correct value: 78.329V)}$$

The above sample is based on the case study in Section 2.2.6.

Based on the above, it is also possible to estimate V_{SA} and S_{SA} for one active mitigation system using contour curves of $V_{SA\_per\_A}$ and $S_{SA\_per\_A}$. In following sections, contour curves (estimation charts) of $V_{A\_per\_A}$, $V_{SA\_per\_A}$, and $S_{SA\_per\_A}$ are presented for a given harmonic order H and soil resistivity ρ in order to estimate the major design parameters (V_A, V_{SA}, S_{SA}).

3.1.2 Determination of Residual Current $I_{residual}$

In the above section, we have discussed the way to estimate the major design parameters using the contour curves of the normalized major design parameters ($V_{A\_per\_A}$, $V_{SA\_per\_A}$, $S_{SA\_per\_A}$). The rest problem is how to determine the residual

current $I_{residual}$. The residual current $I_{residual}$ is essentially caused by the fundamental load imbalance and harmonic currents. We have already checked out that the unbalanced current at the fundamental frequency and the 3rd, 9th harmonic currents are the major contributors to induced voltage on buried pipelines. For a simple case, we will focus on the 1st, 3rd, and 9th harmonic components in the residual current $I_{residual}$ in this chapter.

The load current magnitude ranges from several hundreds of ampere to a thousand ampere in distribution and transmission power lines. However, normally the higher load current has the lower load imbalance and the lower harmonic current ratio based on the field measurement results [9][10].

The fundamental frequency component ($H=1$) of $I_{residual}$ can be calculated using phase current magnitude I and load imbalance Imb as follows.

$$I_{residual(H=1)} = 3 \times \frac{\%Imb}{100} \times I = 3I_{0(H=1)} \tag{3-1-2-1}$$

The residual current $I_{residual}$ at the 3rd and 9th harmonic orders also corresponds to each zero sequence current as follows. We can consider Individual Demand Distortion for the calculation of $I_{residual}$ at the 3rd and 9th harmonic orders as follows.

$$I_{residual(H=3)} = 3I_{0(H=3)} = 3 \cdot IDD_{H=3} \cdot I \tag{3-1-2-2}$$

$$I_{residual(H=9)} = 3I_{0(H=9)} = 3 \cdot IDD_{H=9} \cdot I \tag{3-1-2-3}$$

* $IDD_{H=3}$ and $IDD_{H=9}$ (Individual Demand Distortion) indicate the ratio of harmonic current to phase load current magnitude I at the 3rd and 9th harmonic orders respectively. For sensitivity studies in this chapter, the practical range of $IDD_{H=3}$ and $IDD_{H=9}$ are obtained from the actual field measurement data of distribution and transmission lines in Reference [9][10].

Total residual current in RMS value can be calculated as follows.

$$Total\ I_{residual} = \sqrt{\left(I_{residual(H=1)}\right)^2 + \left(I_{residual(H=3)}\right)^2 + \left(I_{residual(H=9)}\right)^2} \qquad (3\text{-}1\text{-}2\text{-}4)$$

3.1.3 Range of Impact Factors for Sensitivity Study

Based on the case study in Section 2.2.6, the following typical ranges of the impact factors are considered for sensitivity studies in this chapter.

The field measurement data shows that the scale of harmonic currents in distribution system is larger than the one in transmission system [9][10]. Therefore, based on the field measurement data, different ranges of harmonic current ratio are considered for distribution and transmission line cases.

For the load imbalance, there is no different typical range for distribution and transmission line cases. Therefore, the same range of load imbalance is considered for both distribution and transmission line cases.

< Practical Range of Impact Factors for Sensitivity Study >

Separation distance d_s	15 ~ 100m (20)
Parallel Length L	5~100km (10)
Soil resistivity ρ	10~1000 Ωm (100)

( ): considered as a typical value for sensitivity studies

< Practical Range of Current in Overhead Power Lines >

	Distribution	Transmission
Phase Current I	100~500A (500)	500~1000A
Load Imbalance(I_0/I_1) Imb	0 ~ 6.67% (5)	0 ~ 6.67%
3rd Harmonic IDD*	2 ~ 9% (9)	0.3 ~ 1.4%
9th Harmonic IDD*	0.2 ~ 2% (2)	0.04 ~ 0.23%

* based on the field measurement data in Reference [9][10]

( ): considered as a typical value for sensitivity studies

Using the above practical ranges of impact factors, it is possible to obtain the following practical range of total residual current.

	Distribution	Transmission
Total Residual Current $Total\ I_{residual}$ [A, RMS]	6~142	10~182

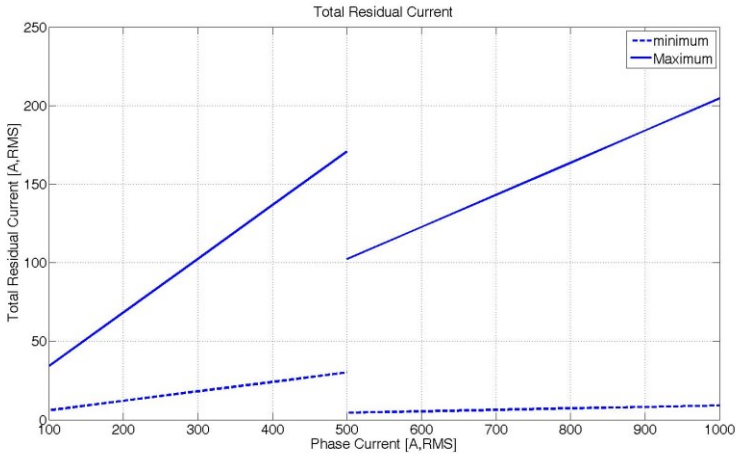

Figure 3-1-3-1: Range of total residual current based on practical ranges of impact factors

As mentioned earlier, the scale of harmonic currents in distribution system is larger than that in transmission system [9]. Therefore, although the range of phase current in the distribution line case is lower than the one in the transmission line case, due to the relatively high scale of harmonic currents in the distribution line case, the induced voltage caused by distribution lines on buried pipelines can be considerable as much as the one caused by transmission lines.

3.2 Sensitivity of Induced Terminal Voltage

In this section, based on sensitivity studies, we are going to discuss how $V_{A\_per\_A}$ (normalized induced voltage) changes according to the impact factors such as d_s and L for a given $\rho = 100\Omega\text{m}$ and $H = 1,3,9$. In addition, contour curves of $V_{A\_per\_A}$ are presented in order to estimate V_A .

Unfortunately, it is not easy to figure out the relation between $V_{A\_per\_A}$ and ρ using the contour curves of $V_{A\_per\_A}$. In addition, the relation between $V_{A\_per\_A}$ and L needs to be explained according to harmonic order H . Therefore, for a better understanding of the contour curves to be presented, we will discuss the sensitivities of $V_{A\_per\_A}$ according to ρ and L firstly.

3.2.1 *Sensitivity of* $V_{A\_per\_A}$ *to* ρ

The mutual impedance Z_m between a buried pipeline and nearby overhead AC power lines increases by the increase of soil resistivity ρ ($Z_m \propto \rho$). Therefore, induced EMF increases by the increase of ρ ($EMF \propto \rho$) and normalized induced voltage $V_{A\_per\_A}$ (corresponding to V_A) eventually increases by the increase of ρ ($V_{A\_per\_A} \propto \rho$) as follows. The following Figure 3-2-1-1 shows that $V_{A\_per\_A}$ is not very sensitive to ρ, especially in the fundamental frequency case. $V_{A\_per\_A}$ becomes more sensitive to ρ at the higher harmonic order.

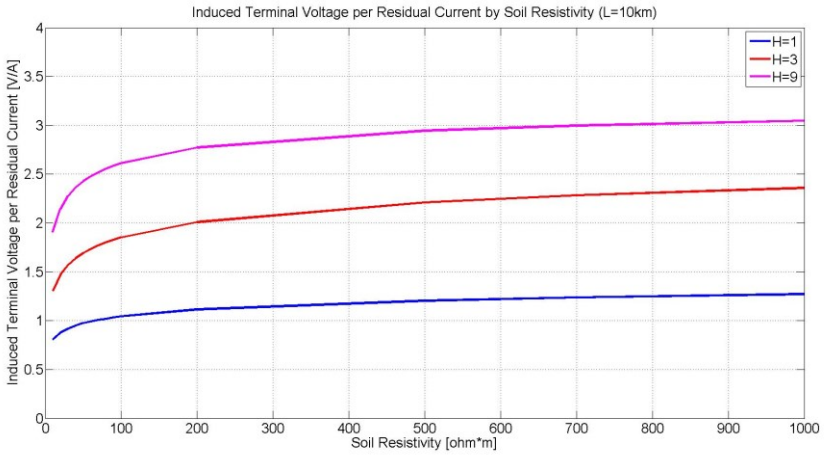

Figure 3-2-1-1: Change of normalized induced terminal voltage according to soil resistivity

3.2.2 *Sensitivity of* $V_{A\_per\_A}$ *to* L

As we know, the equation for induced voltage on a buried pipeline is

$$V(x) = -\frac{Z_c}{\gamma}\left(Ae^{\gamma x} - Be^{-\gamma x}\right) \qquad (3\text{-}2\text{-}2\text{-}1)$$

From Equation (3-2-2-1), it is possible to obtain the following analytical equation for the left terminal voltage $V(0)$.

$$V(0) = -\frac{EMF}{2\gamma}\left(\frac{\frac{(1+\nu_1)\nu_2}{e^{2\gamma L}} - \frac{(1+\nu_2)}{e^{\gamma L}}}{1+\frac{\nu_1\nu_2}{e^{2\gamma L}}} - \frac{\frac{(1+\nu_2)\nu_1}{e^{\gamma L}} - (1+\nu_1)}{1-\frac{\nu_1\nu_2}{e^{2\gamma L}}}\right) \quad \text{(3-2-2-2)}$$

If L is enough long to consider $e^{2\gamma L} \cong e^{\gamma L} \cong \infty$ then $V(0) \cong \frac{EMF}{2\gamma}(1+\nu_1)$.

Therefore, the graph of $V_{A\_per\_A}$ according to L will be the form to converge a certain value by the increase of L. The following Figure 3-2-2-1 shows the graphs of $V_{A\_per\_A}$ according to L and three harmonic orders of 1, 3, 9 respectively.

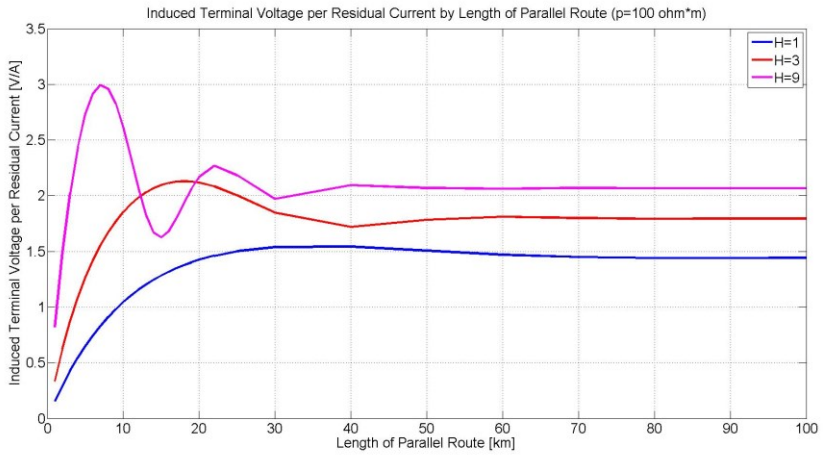

Figure 3-2-2-1: Change of normalized induced terminal voltage according to length of parallel route

According to Figure 3-2-2-1, we can figure out that each induced voltage at each harmonic order converges to certain values by the increase of L. During the convergence, each induced voltage at each harmonic order fluctuates and the degree of the fluctuation depends on the harmonic order. The fluctuation is due to the term of $e^{\gamma L}$ in Equation (3-2-2-1) and the difference of fluctuations' degree at different harmonic orders is caused by different γ according to different harmonic orders.

As shown in Figure 3-2-2-1, we can see that the higher harmonic order brings the higher degree of fluctuation. In the fundamental frequency case, we can normally say that induced voltage increases by the increase of L but in high harmonic

frequency cases, such as the 9th harmonic order case, induced voltage does not always increase by the increase of L.

In this thesis, polyethylene is considered as a typical coating material of pipelines. In the case of polyethylene coating material, we can say that within relatively short length ($\leq$ 7km), induced terminal voltage increases by the increase of L and its sensitivity increases by the higher harmonic order (by the increase of H). If the buried pipeline is longer than 7km, it is hard to generalize the change of induced voltage according to L.

3.2.3 *Sensitivity of $V_{A\_per\_A}$ to d_s and L*

As discussed earlier, the contour curves of the major design parameters according to d_s and L can be utilized to show the sensitivity of $V_{A\_per\_A}$ and as the estimation charts for the major design parameters. From sensitivity studies, following contour curves are obtained at the fundamental frequency.

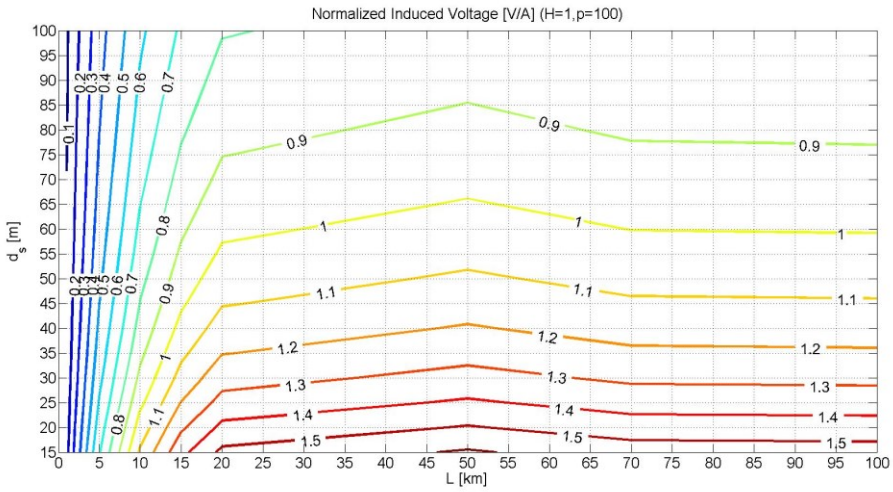

Figure 3-2-3-1: Contour curves of normalized induced terminal voltage at the fundamental frequency according to d_s and L (ρ=100 Ωm)

According to Figure 3-2-3-1, we can see that $V_{A\_per\_A}$ decreases by the increase of d_s. This makes sense because induced voltage decreases by the increase of the separation distance d_s. As discussed earlier, $V_{A\_per\_A}$ converges a certain value

by the increase of L. At the fundamental frequency, due to the relatively small value of γ (by polyethylene coating material), we can obtain the less fluctuating graph during the convergence.

At the 3rd and 9th harmonic orders, $V_{A\_per\_A}$ also decreases by the increase of d_s. However, as discussed earlier, $V_{A\_per\_A}$ fluctuates by the increase of L but converges to a certain value as follows.

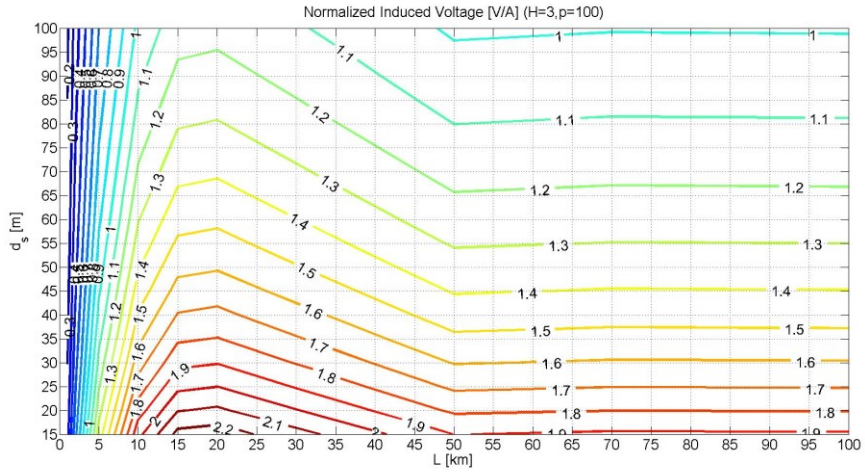

Figure 3-2-3-2: Contour curves of normalized induced terminal voltage at the 3rd harmonic frequency according to d_s and L (ρ=100 Ωm)

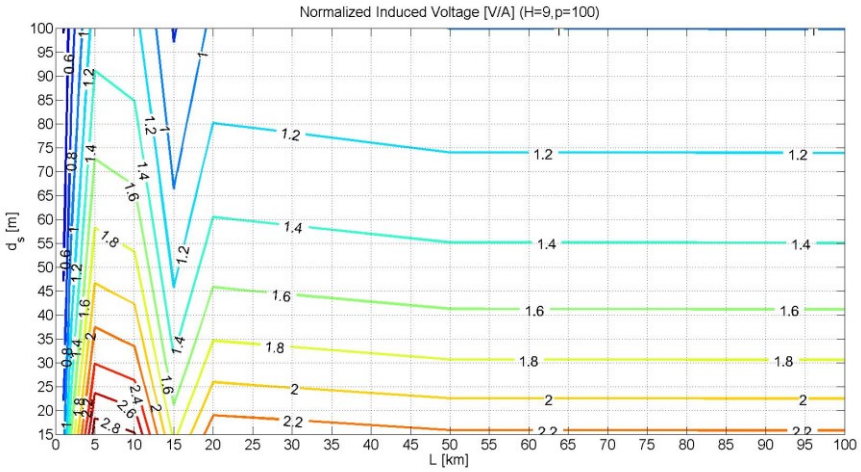

Figure 3-2-3-3: Contour curves of normalized induced terminal voltage at the 9th harmonic frequency according to d_s and L (ρ=100 Ωm)

Using the contour curves, it is possible to estimate a rough value of induced terminal voltage V_A at each harmonic order as long as we have specific values of d_s, L, and $I_{residual}$ at each harmonic order as follows.

$$V_{A(H=1)} = V_{A\_per\_A(H=1)} \cdot I_{residual(H=1)} \quad (3\text{-}2\text{-}3\text{-}1)$$

$$V_{A(H=3)} = V_{A\_per\_A(H=3)} \cdot I_{residual(H=3)} \quad (3\text{-}2\text{-}3\text{-}2)$$

$$V_{A(H=9)} = V_{A\_per\_A(H=9)} \cdot I_{residual(H=9)} \quad (3\text{-}2\text{-}3\text{-}3)$$

In addition, the RMS value of total induced terminal voltage can be calculated using the following equation.

$$Total\,V_A = \sqrt{\left(V_{A(H=1)}\right)^2 + \left(V_{A(H=3)}\right)^2 + \left(V_{A(H=9)}\right)^2} \quad (3\text{-}2\text{-}3\text{-}4)$$

3.2.4 Practical Range of Total Induced Terminal Voltage

Based on the practical ranges of the impact factors as shown in Section 3.1.3, it is possible to obtain the following practical range of total induced terminal voltage V_A from the sensitivity studies.

Total V_A [V, RMS]	0.5 ~ 414.9

With consideration of the criteria for AC corrosion voltage (10V when $\rho \geq 25\Omega\text{m}$) and touch voltage (15V) in Figure 1-1-1-3, the above practical range of total V_A reveals that some cases may not be concerned. However, some cases have high induced voltage (up to approximately 414.9V) so they need to be mitigated to avoid AC corrosion and personnel safety issue.

3.3 Sensitivity of Required Neutralizing Voltage

As mentioned in Section 2.2.2, the equation of neutralizing voltages is as follows.

$$V_{SA} = \frac{EMF \cdot Z_{SA}}{\gamma \cdot Z_c}$$
$$V_{SB} = -\frac{EMF \cdot Z_{SB}}{\gamma \cdot Z_c} \qquad (3\text{-}3\text{-}1)$$

As shown in the above, the required two neutralizing voltages are proportional to the equivalent impedance of the applied devices Z_{SA} and Z_{SB}, respectively. Since Z_{SA} and Z_{SB} are the summation of the two terminal device's internal impedance and their grounding resistance, the required neutralizing voltages are significantly dependent on the internal impedance and their grounding resistance. This means that the equivalent impedance of controllable voltage source needs to have small equivalent internal impedance as possible as can for better efficiency of the system.

In this section, we are going to discuss how neutralizing voltage changes according to ρ, d_s, EMF, and the equivalent internal impedance Z_{SA} of the controllable voltage source at the left terminal of the pipeline.

3.3.1 Sensitivity of $V_{SA\_per\_A}$ to ρ

The following Figure 3-3-1-1 shows the change of the normalized neutralizing voltage $V_{SA\_per\_A}$ according to soil resistivity ρ.

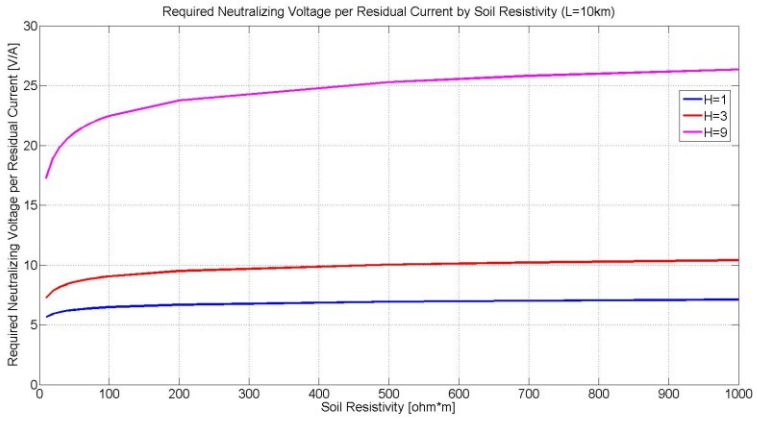

Figure 3-3-1-1: Change of normalized neutralizing voltage according to soil resistivity

According to Figure 3-3-1-1, we can figure out that $V_{SA\_per\_A}$ increases by the increase of ρ and the impact of ρ increases by the higher harmonic order. $V_{SA\_per\_A}$ is not very sensitive to ρ, especially in the fundamental frequency case.

3.3.2 Sensitivity of $V_{SA\_per\_A}$ to d_s and Z_{SA}

As mentioned earlier, since neutralizing voltage is constant regardless of L, we will discuss sensitivity of $V_{SA\_per\_A}$ to d_s and Z_{SA} in this section. The equivalent internal impedance Z_{SA} of the controllable voltage source comprises of the actual internal impedance of the device Z_{in_SA} and the grounding resistor R_{g_SA}.

$$Z_{SA} = Z_{in\_SA} + R_{g\_SA}$$

The default setting of those parameters in this thesis is

Z_{in_SA}	5 + j5 [Ω]
R_{g_SA}	5 [Ω]

Since it is assumed that Z_{in_SA} is the internal impedance value of the designed device, actually the variation of R_{g_SA} will be considered for the variation of Z_{SA} (approximately 5~100 Ω) in this sensitivity study.

The following Figure 3-3-2-1 shows the contour curves of normalized neutralizing voltage $V_{SA\_per\_A}$ at the fundamental frequency according to d_s and Z_{SA}.

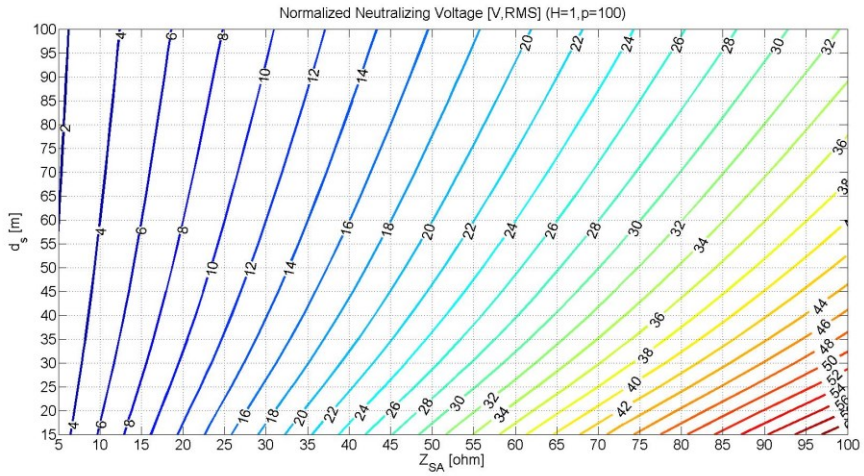

Figure 3-3-2-1: Contour curves of normalized neutralizing voltage at the fundamental frequency according to d_s and Z_{SA} (ρ=100 Ωm)

According to Figure 3-3-2-1, we can figure out that $V_{SA\_per\_A}$ decreases by the increase of d_s but increases by the increase of Z_{SA}. With consideration of fixed d_s (fixed EMF), Z_{SA} needs to be small as possible as it can for better efficiency (lower $V_{SA\_per\_A}$) of the active mitigation system.

The following Figure 3-3-2-2 and 3-3-2-3 show the contour curves of $V_{SA\_per\_A}$ at the 3rd and 9th harmonic frequencies according to d_s and Z_{SA}.

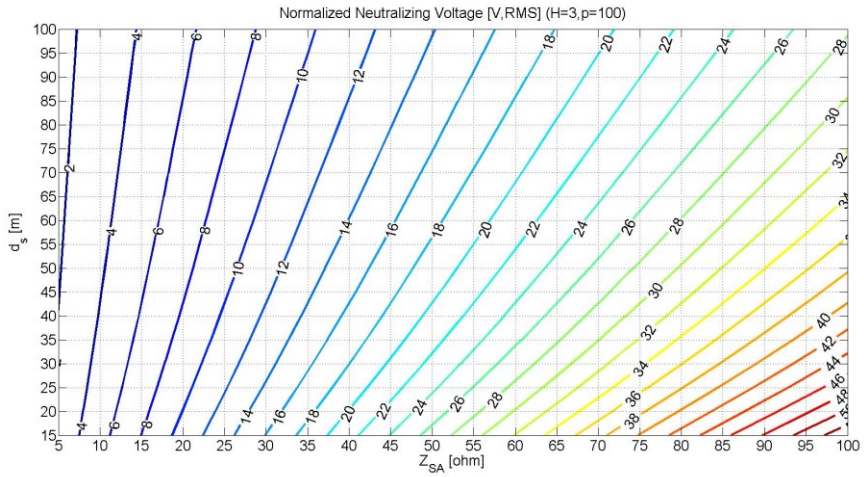

Figure 3-3-2-2: Contour curves of normalized neutralizing voltage at the 3rd harmonic frequency according to d_s and Z_{SA} (ρ=100 Ωm)

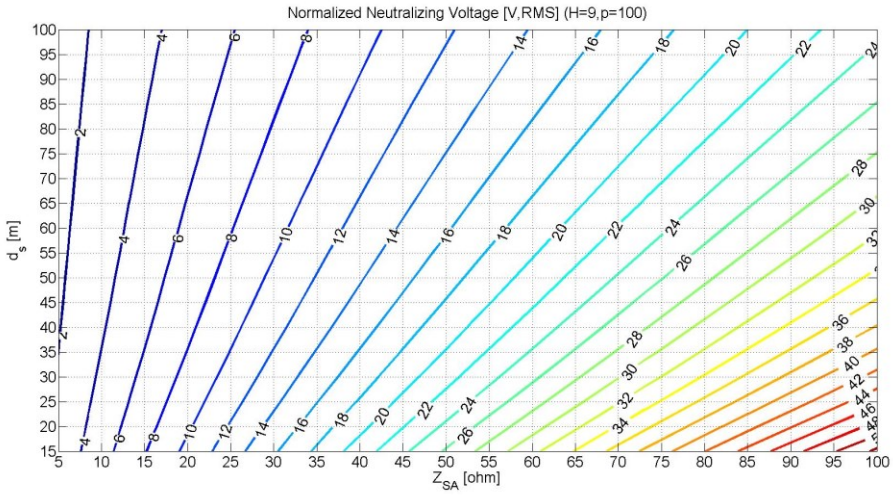

Figure 3-3-2-3: Contour curves of normalized neutralizing voltage at the 9th harmonic frequency according to d_s and Z_{SA} ($\rho = 100\,\Omega\text{m}$)

We need to make sure that the above contour curves are for normalized neutralizing voltage $V_{SA\_per\_A}$. Each neutralizing voltage V_{SA} at each harmonic order can be obtained by multiplying residual current $I_{residual}$ at each harmonic order as follows.

$$V_{SA(H=1)} = V_{SA\_per\_A(H=1)} \cdot I_{residual(H=1)} \tag{3-3-2-1}$$

$$V_{SA(H=3)} = V_{SA\_per\_A(H=3)} \cdot I_{residual(H=3)} \tag{3-3-2-2}$$

$$V_{SA(H=9)} = V_{SA\_per\_A(H=9)} \cdot I_{residual(H=9)} \tag{3-3-2-3}$$

The total required neutralizing voltage in RMS value can be calculated using the following equation.

$$Total\,V_{SA} = \sqrt{\left(V_{SA(H=1)}\right)^2 + \left(V_{SA(H=3)}\right)^2 + \left(V_{SA(H=9)}\right)^2} \tag{3-3-2-4}$$

3.3.3 Sensitivity of V_{SA} to EMF and Z_{SA}

In this section, contour curves of neutralizing voltage V_{SA} according to EMF and Z_{SA} are presented for the sensitivity of V_{SA}. They can be also used to estimate

required neutralizing voltage with the estimated EMF using the probe-wire-based measurement method to be presented in Chapter 4.

The following Figure 3-3-3-1 ~ 3-3-3-3 show contour curves of V_{SA} according to EMF, Z_{SA} and harmonic orders. It is necessary to make sure that following contour curves are not for the normalized one.

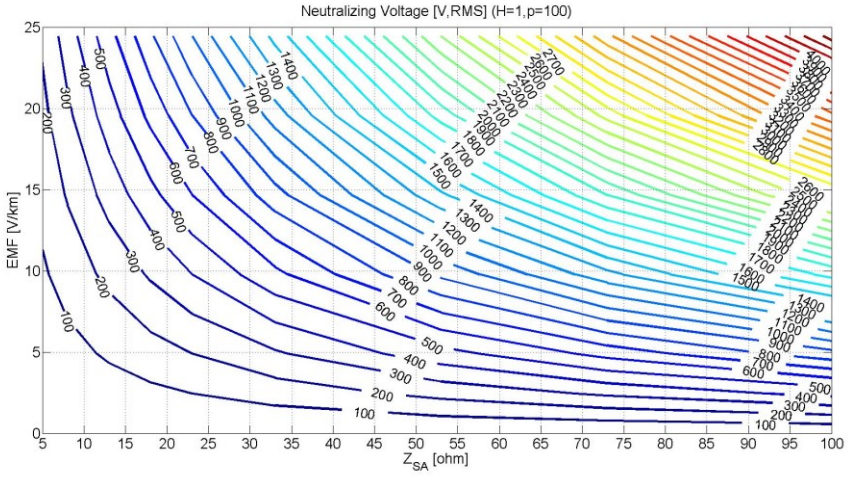

Figure 3-3-3-1: Contour curves of neutralizing voltage at the fundamental frequency according to EMF and Z_{SA} (ρ=100 Ωm)

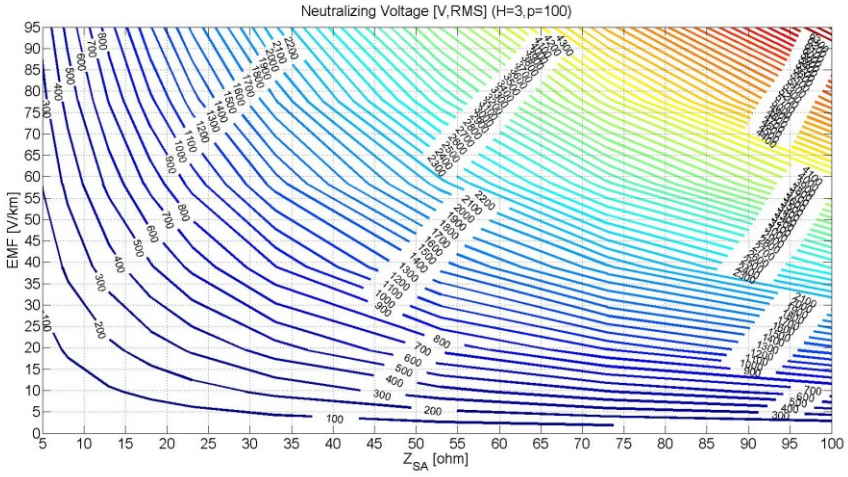

Figure 3-3-3-2: Contour curves of neutralizing voltage at the 3rd harmonic frequency according to EMF and Z_{SA} (ρ=100 Ωm)

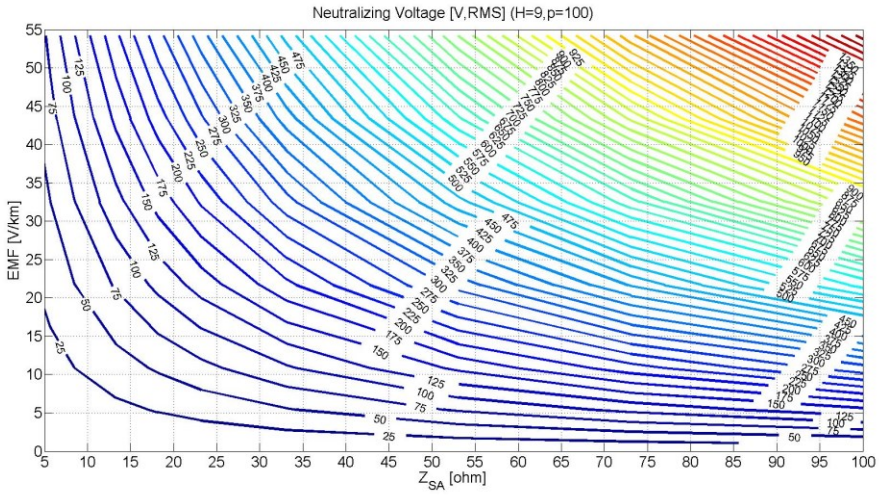

Figure 3-3-3-3: Contour curves of neutralizing voltage at the 9th harmonic frequency according to EMF and Z_{SA} ($\rho = 100\,\Omega\text{m}$)

The above contour curves show that neutralizing voltage increases by the increase of EMF and Z_{SA}. This is matched with Equation (3-3-1).

The above contour curves allow for us to estimate neutralizing voltage at each harmonic order. The total neutralizing voltage in RMS value can be calculated by Equation (3-3-2-4).

3.3.4 Sensitivity of V_A / V_{SA} to Z_{SA} and L

The value of V_A / V_{SA} can be understood as the portion of the required neutralizing voltage which is actually used to cancel the induced voltage V_A. Therefore, V_A / V_{SA} indicates the efficiency of the applied active mitigation source. If we have contour curves of V_A / V_{SA}, we can easily estimate the efficiency of the active source.

As we know, according to Equation (2-1-1-1) and (2-2-2-1), both V_A and V_{SA} are proportional to EMF. Since EMF changes according to d_s, the value of V_A / V_{SA}

is constant regardless of d_s. Therefore, in this section, we will discuss the contour curves of V_A / V_{SA} according to Z_{SA} and L.

Following Figure 3-3-4-1 ~ 3-3-4-3 show the contour curves of V_A / V_{SA} according to Z_{SA} and L. They are based on the conditions: $\rho = 100[\Omega m]$, $d_s = 20[m]$, and other parameters of the case study in Section 2.2.6.

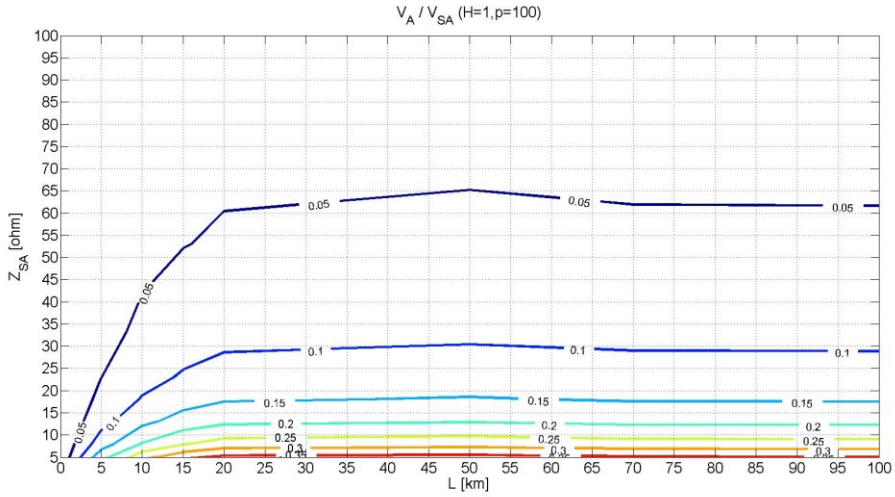

Figure 3-3-4-1: Contour curves of V_A / V_{SA} at the fundamental frequency according to d_s and L ($\rho = 100\,\Omega m$)

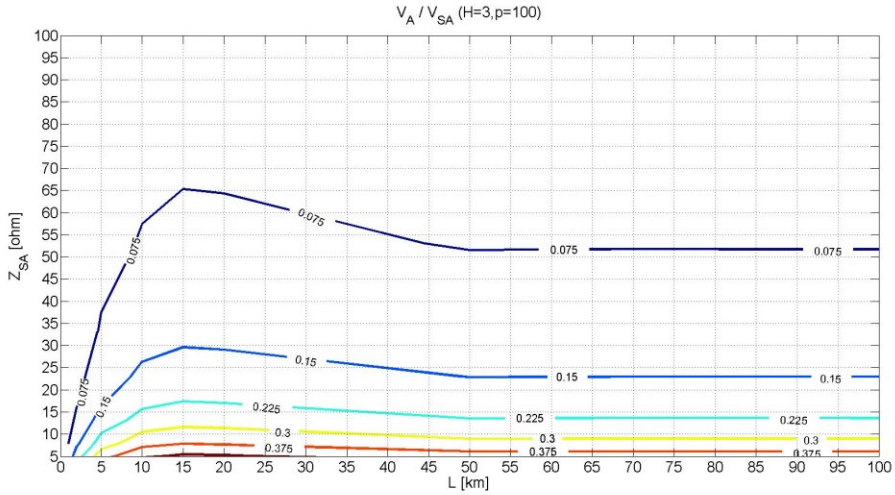

Figure 3-3-4-2: Contour curves of V_A / V_{SA} at the 3rd harmonic frequency according to d_s and L ($\rho = 100\,\Omega m$)

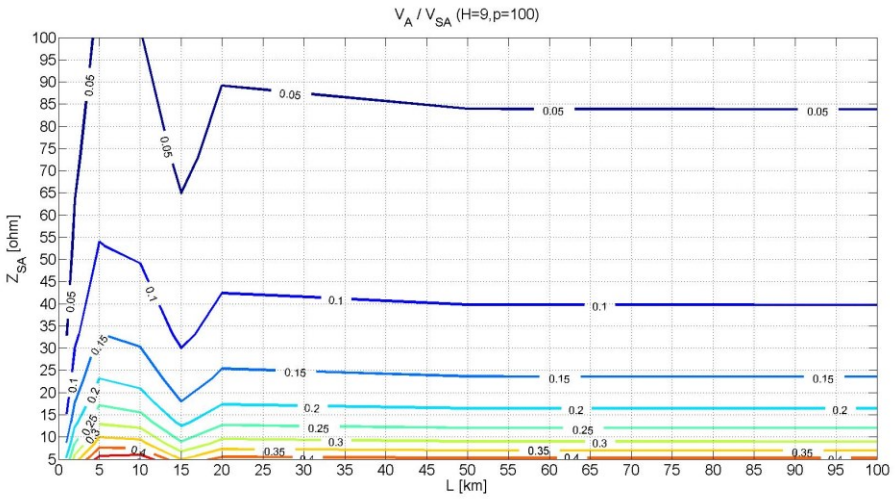

Figure 3-3-4-3: Contour curves of V_A / V_{SA} at the 9th harmonic frequency according to d_s and L (ρ=100Ωm)

As shown in the above Figure 3-3-4-1 ~ 3-3-4-3, the efficiency of the active mitigation source (V_A / V_{SA}) is quite small. Regarding such low efficiency, the most relevant factor is Z_{SA} . When we consider one buried pipeline with active mitigation systems, the actual applied voltage to the pipeline's terminal will follow the simple voltage division by the impedance ratio of the equivalent internal impedance Z_{SA} and the equivalent impedance of the pipeline $Z_{eq\_pipe\_A}$ at the left terminal as follows.

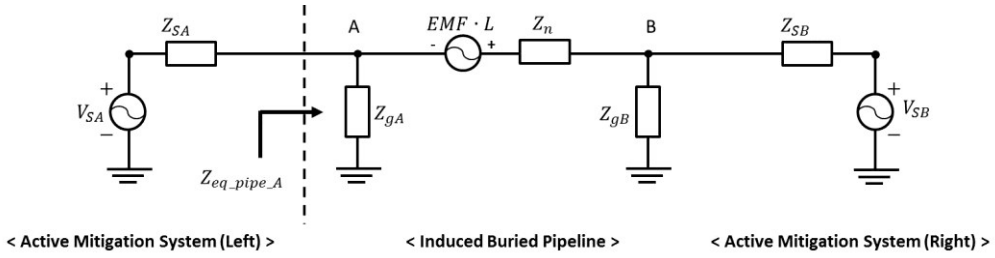

Figure 3-3-4-4: Equivalent circuit of one buried pipeline with active mitigation systems

$$\text{Acutal applied V at the left terminal} = \frac{Z_{eq\_pipe\_A}}{Z_{eq\_pipe\_A} + Z_{SA}} \times V_{SA} \qquad (3\text{-}3\text{-}4\text{-}1)$$

If we assume that the induced voltage on the pipeline is fixed, the actual required voltage to be applied at the left terminal is also fixed. With consideration of the fixed required voltage at the left terminal, the lower Z_{SA} brings the lower V_{SA} according to Equation (3-3-4-1). Usually $Z_{eq\_pipe\_A}$ is quite small (2.8862 + j1.4153 at H=1 in the case study of Section 2.2.6) because the characteristic impedance Z_c itself is quite small (5.7724 + j2.8306 at H=1 in the case study of Section 2.2.6). Z_{SA} is the only factor to be controlled for the efficiency of the controllable voltage source but it is limited to control Z_{SA} smaller than such quite small $Z_{eq\_pipe\_A}$ in practice. Therefore, the efficiency is usually small as shown in the above contour curves.

As long as we know Z_{SA} and L, it is possible to roughly estimate the efficiency of the active source at each harmonic order, using the above contour curves of V_A / V_{SA} according to Z_{SA} and L.

3.3.5 Practical Range of Total Required Neutralizing Voltage

Based on the practical ranges of the impact factors as shown in Section 3.1.3, it is possible to obtain the following practical range of the total required neutralizing voltage for one terminal.

Total V_{SA} [V, RMS]	17.5 ~ 1,843.3

As we can see, the total required neutralizing voltage for one terminal ranges from tens to thousands of volts. Compared to the practical range of the total induced terminal voltage (0.5 ~ 414.9V), the range of total V_{SA} is much higher. This is due to the low efficiency of applied neutralizing voltage as explained in Section 3.3.4.

3.4 Sensitivity of Required Power

In section 2.2.2, we have already discussed how to calculate required power S_{SA} for one active mitigation system as follows.

$$S_{SA} = \frac{(V_{SA})^2}{Z_{Total}} = \frac{(V_{SA})^2}{(Z_{SA} + Z_{eq\_pipe})} = \frac{(EMF \cdot Z_{SA})^2 (Z_c + 2Z_{SA})(1 + \tanh(\gamma L))}{\gamma^2 Z_c^2 \left[(Z_{SA}^2 + 2Z_{SA}Z_c) + (Z_c^2 + 2Z_{SA}Z_c + 2Z_{SA}^2)\tanh(\gamma L) \right]} \quad (3\text{-}4\text{-}1)$$

*based on $Z_{SA} = Z_{SB}$

According to Equation (3-4-1), we can figure out that required power depends on the require neutralizing voltage (V_{SA}) and total equivalent impedance Z_{Total} of the whole system at the terminal (especially depending on L and Z_{SA}).

3.4.1 Sensitivity of $S_{SA\_per\_A}$ to ρ

The following Figure 3-4-1-1 shows the change of the normalized required power $S_{SA\_per\_A}$ according to soil resistivity ρ.

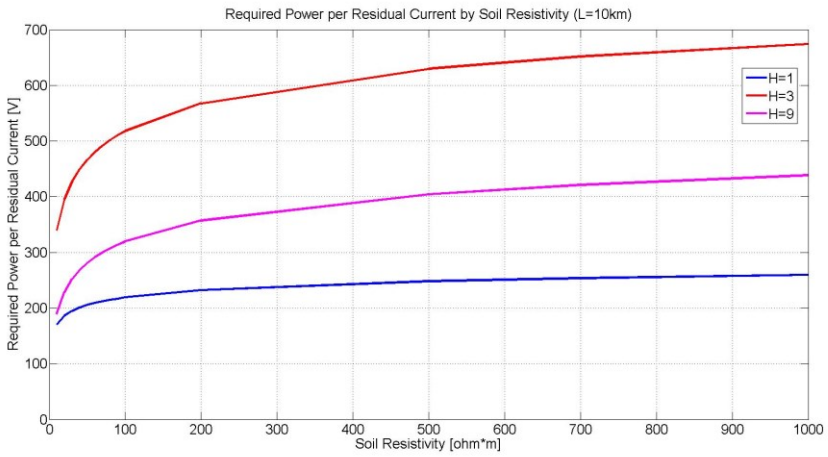

Figure 3-4-1-1: Change of normalized required power according to soil resistivity

According to Figure 3-4-1-1, we can see that $S_{SA\_per\_A}$ increases by the increase of ρ. This is because the larger soil resistivity brings the higher required

neutralizing voltage. Therefore, based on Equation (3-4-1), higher power S_{SA} is required by the increase of ρ. The impact of ρ on $S_{SA\_per\_A}$ increases by the higher harmonic order.

3.4.2 Sensitivity of $S_{SA\_per\_A}$ to L

The following Figure 3-4-2-1 shows the change of the normalized required power $S_{SA\_per\_A}$ according to L.

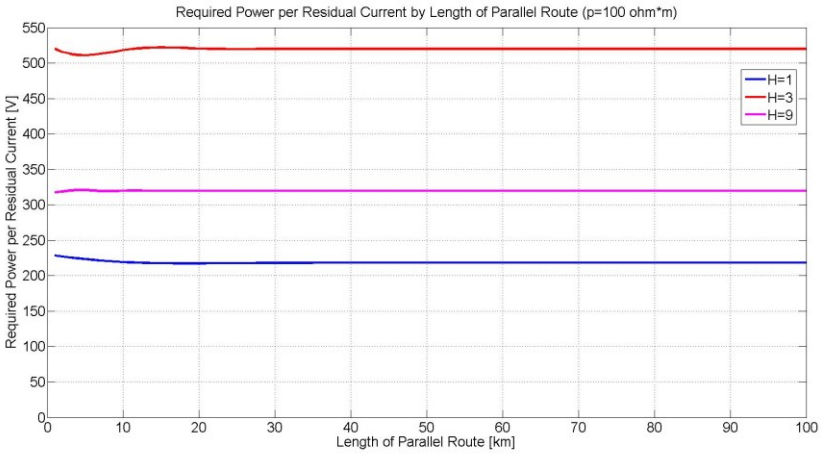

Figure 3-4-2-1: Change of normalized required power according to length of parallel route

According to Figure 3-4-2-1, we can figure out that $S_{SA\_per\_A}$ has less impact of L. As long as L exceeds approximately 10km, it can be considered roughly constant.

Since S_{SA} is not sensitive to L, Equation (2-2-2-7) can be used to roughly estimate the required S_{SA} at design stage.

As shown in Figure 3-4-2-1, $S_{SA\_per\_A}$ converges to a certain value by the increase of L and there are slight fluctuations during the convergence. This is because although V_{SA} is constant regardless of L, $Z_{eq\_pipe\_A}$ in Equation (3-4-1)

slightly varies by the increase of L. This explanation is supported by the following Figure 3-4-2-2 showing the change of $Z_{eq\_pipe\_A}$ according to L.

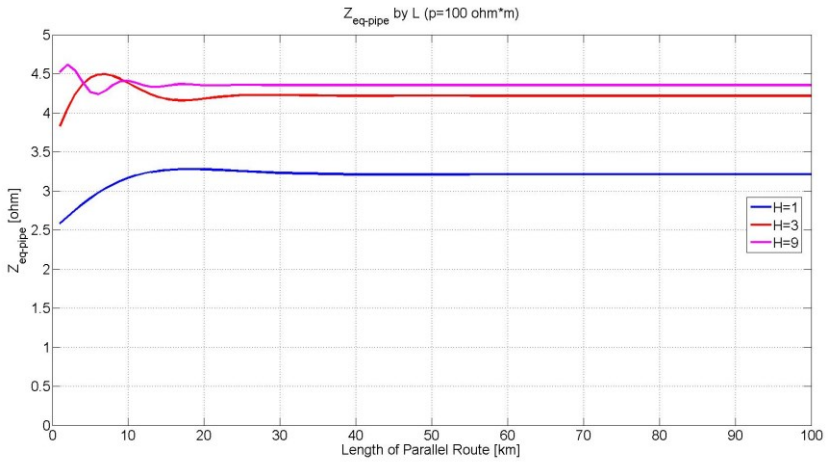

Figure 3-4-2-2: $Z_{eq\_pipe\_A}$ according to length of parallel route

According to Figure 3-4-2-2, $Z_{eq\_pipe\_A}$ fluctuates slightly then converges to a certain value by the increase of L. Based on Equation (3-4-1), such change of $Z_{eq\_pipe\_A}$ is reflected on the required power S_{SA} in Figure 3-4-2-1.

3.4.3 Sensitivity of $S_{SA\_per\_A}$ to d_s and Z_{SA}

The sensitivity of $S_{SA\_per\_A}$ is presented by the contour curves of $S_{SA\_per\_A}$ according to d_s and Z_{SA}. They can be used to estimate a rough value of required power according to specific values of d_s, Z_{SA}, and $I_{residual}$. The default value of L is 10km in this sensitivity study. The following Figure 3-4-3-1 describes the change of the normalized required power $S_{SA\_per\_A}$ at the fundamental frequency according to d_s and Z_{SA}.

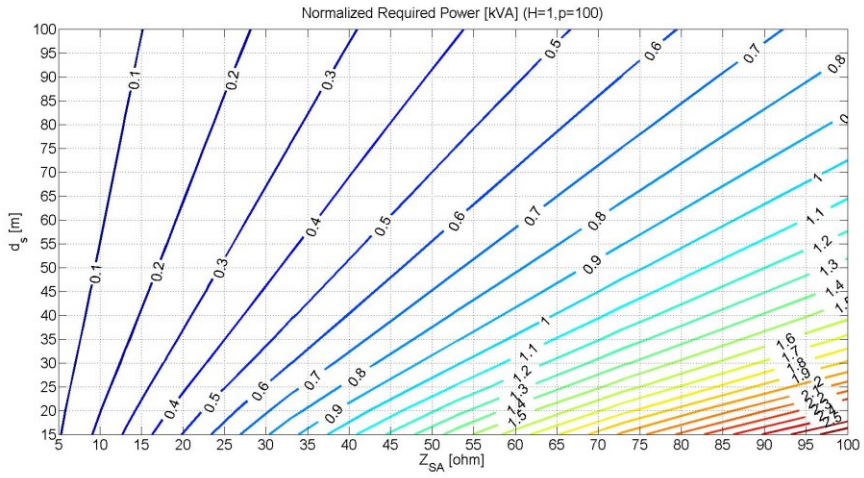

Figure 3-4-3-1: Contour curves of normalized required power at the fundamental frequency according to d_s and Z_{SA} (ρ=100 Ωm)

According to Figure 3-4-3-1, we can figure out that $S_{SA\_per\_A}$ decreases by the increase of d_s but increases by the increase of Z_{SA} . Similar to the case of V_{SA}, for efficient mitigation system, the active mitigation system should be designed to have lower Z_{SA} as possible as it can.

The following Figure 3-4-3-2 and 3-4-3-3 show the contour curves of $S_{SA\_per\_A}$ at the 3rd and 9th harmonic frequencies according to d_s and Z_{SA} .

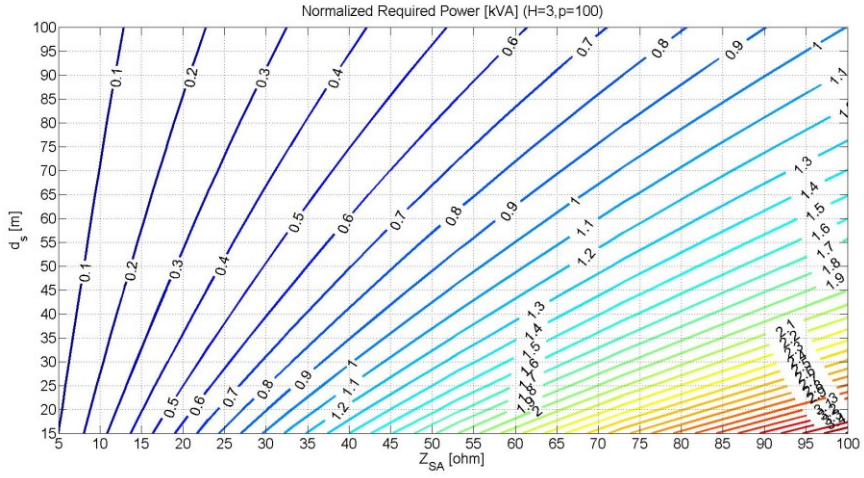

Figure 3-4-3-2: Contour curves of normalized required power at the 3rd harmonic frequency according to d_s and Z_{SA} (ρ=100 Ωm)

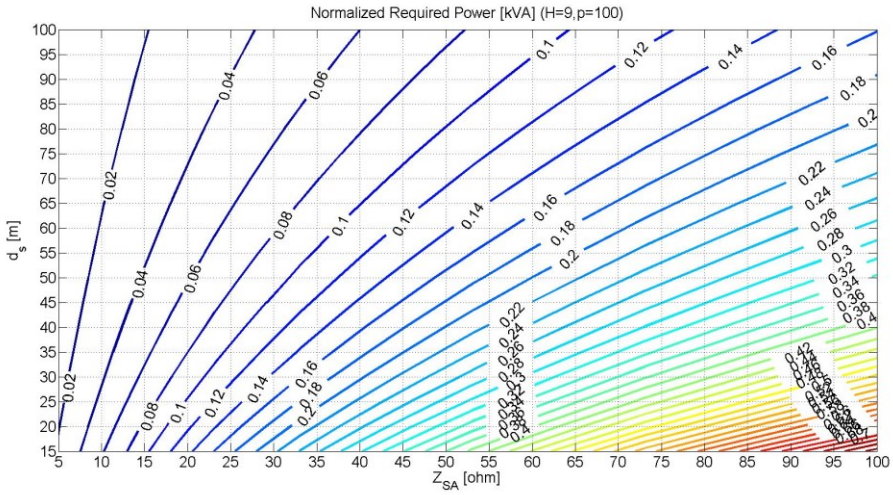

Figure 3-4-3-3: Contour curves of normalized required power at the 9th harmonic frequency according to d_s and Z_{SA} ($\rho = 100\,\Omega\text{m}$)

Each required power S_{SA} at each harmonic order can be calculated as follows.

$$S_{SA(H=1)} = S_{SA\_per\_A(H=1)} \cdot I_{residual(H=1)} \tag{3-4-3-1}$$

$$S_{SA(H=3)} = S_{SA\_per\_A(H=3)} \cdot I_{residual(H=3)} \tag{3-4-3-2}$$

$$S_{SA(H=9)} = S_{SA\_per\_A(H=9)} \cdot I_{residual(H=9)} \tag{3-4-3-3}$$

In addition, the RMS value of the total required power can be calculated using the following equation.

$$\text{Total}\, S_{SA} = \sqrt{\left(S_{SA(H=1)}\right)^2 + \left(S_{SA(H=3)}\right)^2 + \left(S_{SA(H=9)}\right)^2} \tag{3-4-3-4}$$

3.4.4 Sensitivity of S_{SA} to EMF and Z_{SA}

The following contour curves show the sensitivity of required power S_{SA} to EMF and Z_{SA}. As mentioned earlier, those contour curves can be used to estimate required power for one active mitigation system as long as we know the estimated EMF, which can be obtained using the probe-wire-based measurement to be presented in next Chapter 4, and Z_{SA}.

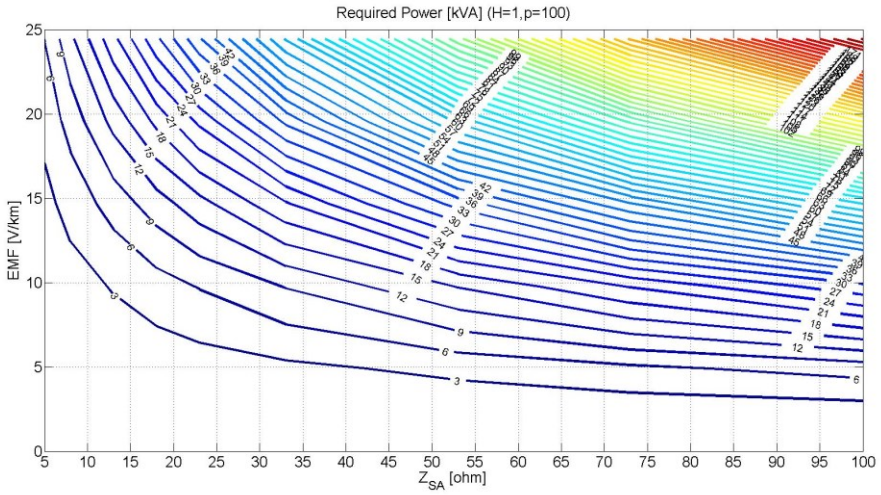

Figure 3-4-4-1: Contour curves of required power at the fundamental frequency according to EMF and Z_{SA} (ρ=100 Ωm)

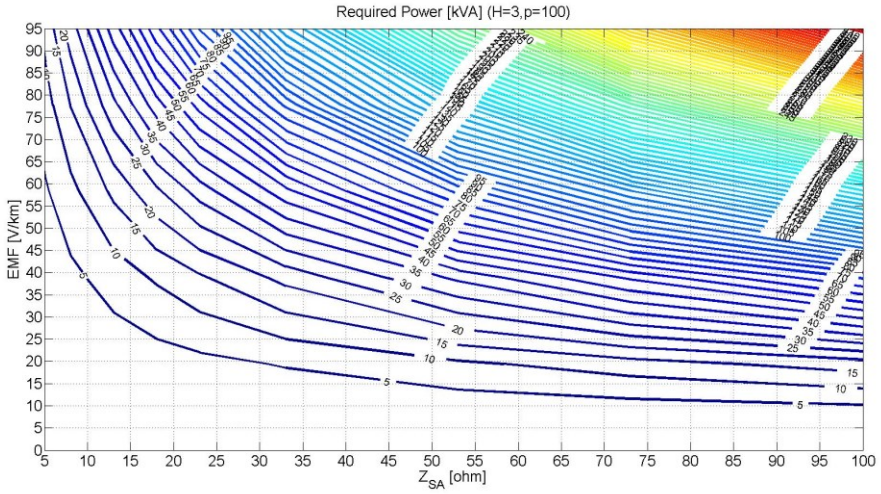

Figure 3-4-4-2: Contour curves of required power at the 3rd harmonic frequency according to EMF and Z_{SA} (ρ=100 Ωm)

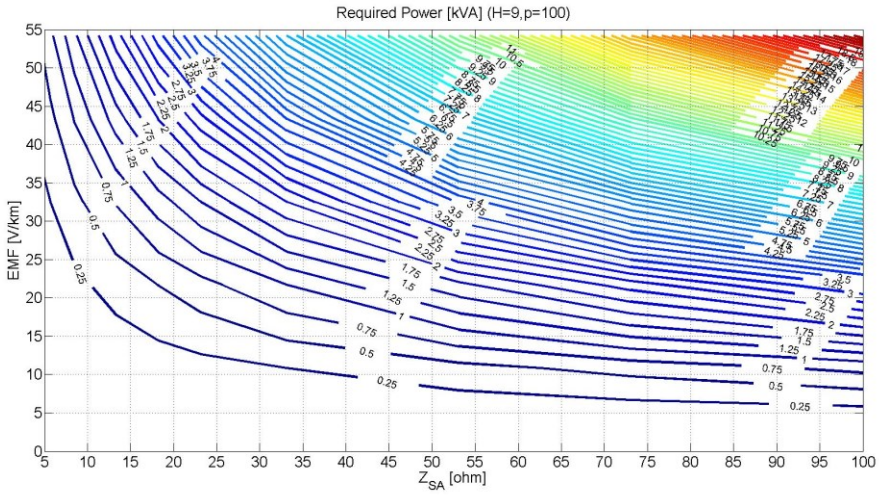

Figure 3-4-4-3: Contour curves of required power at the 9th harmonic frequency according to EMF and Z_{SA} (ρ=100 Ωm)

The above contour curves show the same relationship as shown in Equation (3-4-1). We need to make sure that the above contour curves are not for the normalized value by residual current. Total required power in RMS value can be calculated by Equation (3-4-3-4).

3.4.5 Practical Range of Total Required Power

Based on the practical ranges of the impact factors as shown in Section 3.1.3, it is possible to obtain the following practical range of total required power for one active mitigation system.

Total S_{SA} [kVA]	0.013 ~ 153.3

3.5 Sensitivity Study for the Reduction Rate

As introduced in Section 2.2.3, the reduction rate of each adjusting step has to be setup in the controller to obtain the reference voltage. Once the reduction rate is selected, the required minimum number of cycles can be predicted. Both

reduction rate and the required minimum number of cycles are impacted by some factors as follows.

	Impact factors
Graph of % maximum voltage increase at the other terminal	- Soil resistivity ρ - Parallel route length L - Grounding resistor R_{g_SA} of controllable voltage source
Graph of the minimum required number of cycles for mitigation	- Soil resistivity ρ - Parallel route length L - Separation d_s distance between the pipeline and power lines

The following Figure 3-5-1 ~ 3-5-3 show the graphs of %maximum increased voltage at the other terminal according to different reduction rates and impact factors.

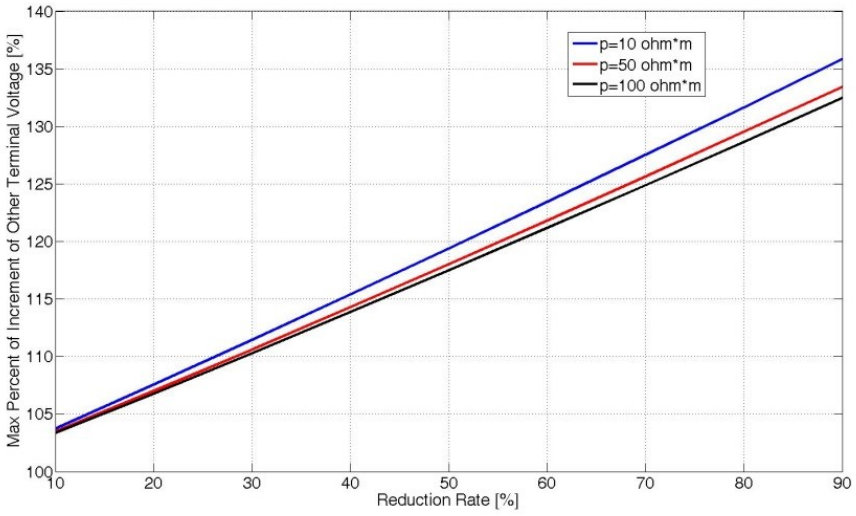

Figure 3-5-1: Graph of % maximum voltage increase at the other terminal according to different reduction rates and soil reisistivity in the alternative adjustment

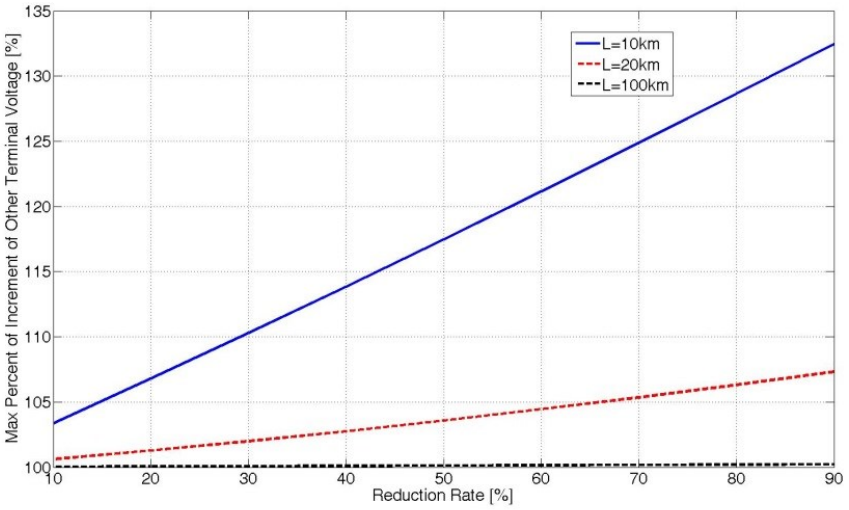

Figure 3-5-2: Graph of % maximum voltage increase at the other terminal according to different reduction rates and parallel route length in the alternative adjustment

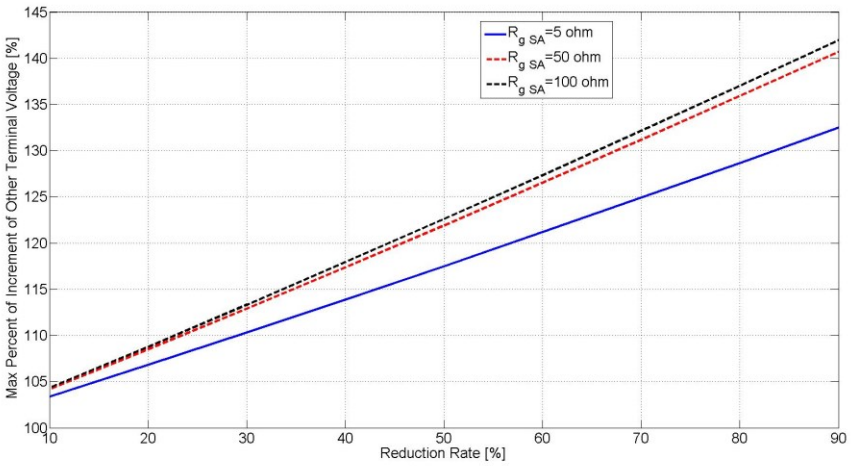

Figure 3-5-3: Graph of % maximum voltage increase at the other terminal according to different reduction rates and a grounding resistor of controllable voltage sources in the alternative adjustment

As you can see, the graph of % maximum voltage increase at the other terminal is affected by the impact factors of ρ, L, R_{g_SA}. According to variation of the impact factors, the graph of %maximum increased voltage at the other terminal changes but its trend, which is proportional to reduction rate, is same.

Except for the case by L, the variation of the graph by the impact factors is not much. In the case by L, we can see that % maximum voltage increase at the other terminal decreases significantly by the increase of L since longer L brings less mutual effect between two terminals as explained above.

Following Figure 3-5-4 ~ 3-5-6 show the graphs of required minimum number of cycles for mitigation by different reduction rate and impact factors.

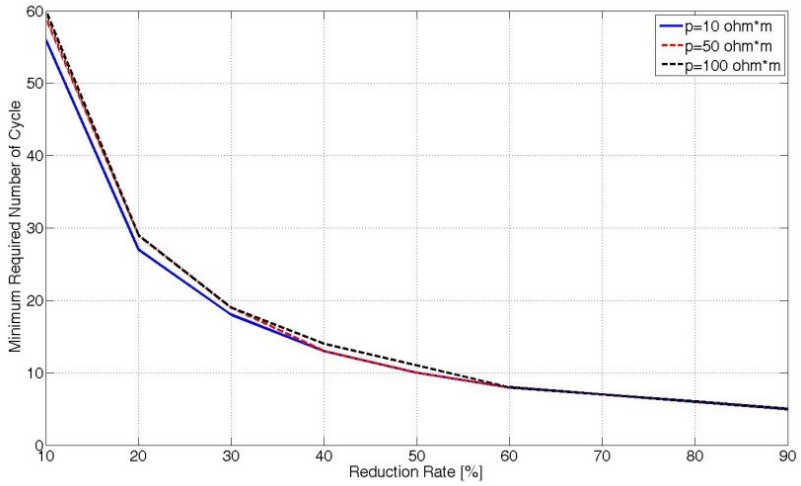

Figure 3-5-4: Graph of minimum required number of cycles for mitigation according to different reduction rates and soil reisistivity in the alternative adjustment

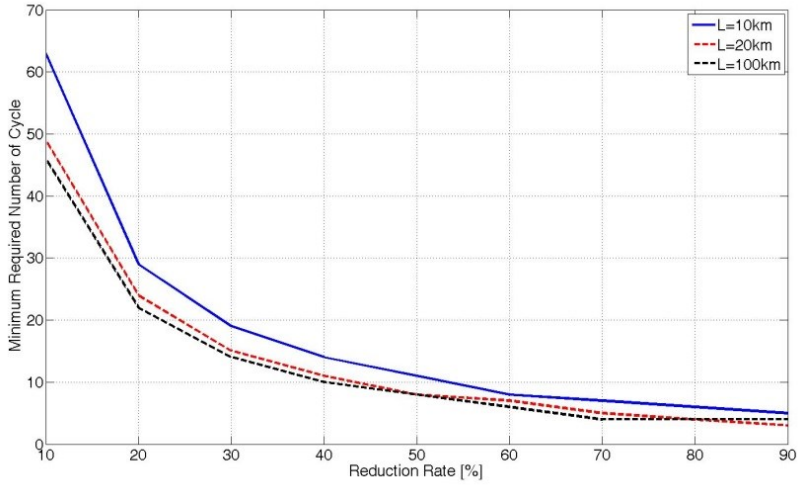

Figure 3-5-5: Graph of minimum required number of cycles for mitigation according to different reduction rates and parallel route length in the alternative adjustment

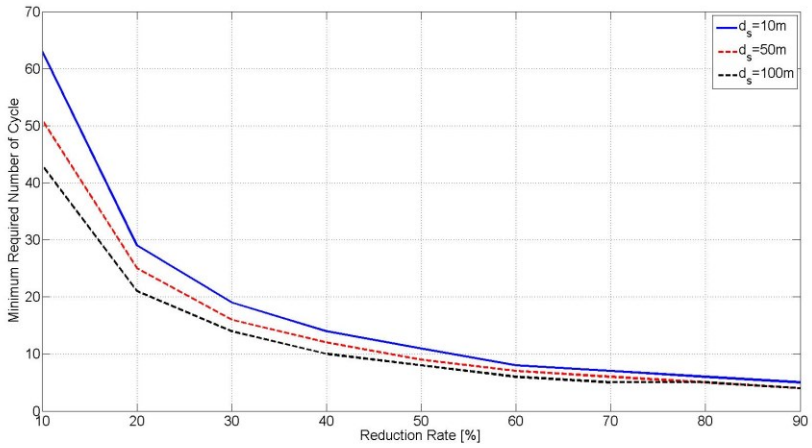

Figure 3-5-6: Graph of minimum required number of cycles for mitigation according to different reduction rates and separation distance d_s in the alternative adjustment

According to the above Figure 3-5-4 ~ 3-5-6, the impact factors on induced voltage or EMF can change the graph of required minimum number of cycles for mitigation in the alternative adjustment but its trend, which is inversely proportional to reduction rate, does not change.

3.6 Sensitivity Study for Evaluation of GPR Interference from Controllable Voltage Source

As discussed in Section 2.3.2, one active mitigation system may have a GPR concern at a grounding point of a controllable voltage source as shown in Figure 2-3-2-2. The GPR caused by the controllable voltage source may cause not only a personnel safety issue but also an interference (disturbance) issue to a reference potential of a voltage detector. In order to avoid severe disturbance on the voltage detector, it is required to secure the separation distance d_{vs} between the grounding point of the controllable voltage source and the reference electrode of the voltage detector.

3.6.1 GPR Calculation

In order to calculate the required d_{vs}, we need to calculate the GPR caused by the grounding current of the controllable voltage source firstly. For GPR calculation, the commonly used vertical electrode with 3m long (L) and 16mm diameter (d) is considered. The grounding resistance R_g can be calculated as follows [11]-IEEE Std-14-2007.

$$R_g = \frac{\rho}{2\pi L}\left[\ln\left(\frac{2L}{d}\right)-1\right] \qquad (3\text{-}6\text{-}1\text{-}1)$$

Since the development of the grounding resistance with vertical electrode is described as that shown in Figure 3-6-1-1 [11].

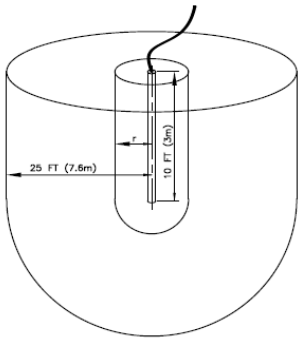

Figure 3-6-1-1: Electrode resistance development, from Reference [11]

Around a grounding electrode, the resistance of the soil is the sum of the series resistances of virtual shells of earth, which are located progressively outward from the rod [11]. The shell nearest the rod has the smallest cross section or circumferential area, so it has the highest resistance [11]. Successive shells outside have larger areas, and thus lower resistances progressively [11]. As the radius from the rod increases, the incremental resistance per unit of radius decreases effectively to nearly zero [11]. Therefore, assuming that the grounding resistance R_g can be completely developed at 300 meters away from the grounding electrode, the resistance increase ratio K_g can be fitted by using data provided in IEEE 142 as

$$K_g(r) = 0.1686 \times \ln\left(1 + \frac{L}{r}\right) \tag{3-6-1-2}$$

The *GPR* as the function of distance *r* can be calculated as follows.

$$GPR(r) = I_g \cdot R_g \cdot K_g(r) = \frac{EMF}{Z_c \gamma} R_g \times 0.1686 \ln(1 + \frac{L}{r}) \tag{3-6-1-3}$$

where,

r : distance from the vertical electrode

I_g : grounding current in RMS value (corresponds to $-I_1$ in Figure 2-3-2-2) can be derived by Equation (2-2-2-1) as the following Equation (3-6-1-4). The detail process to derive Equation (3-6-1-4) can be referred to in Appendix I.

R_g : 31.429 [Ω], resistance of the vertical electrode 3m long (*L*) and 16mm diameter (*d*)

$$I_g = \frac{V_{SA}}{Z_{SA}} = \frac{EMF}{Z_c \gamma} \tag{3-6-1-4}$$

Since grounding current I_g is proportional to the required neutralizing voltage, the *GPR* will be maximized when the active mitigation system applies the maximum neutralizing voltage onto the pipeline's terminal.

As discussed earlier, the criterion for AC corrosion on pipelines is 10V when $\rho > 25\Omega\text{m}$. If the reference potential of the voltage detector is 10V then the final mitigated terminal voltage will be equal to the reference potential of 10V. Therefore, we can consider that the maximum acceptable GPR criterion for the reference potential of the voltage detector is 10V when $\rho > 25\Omega\text{m}$.

In next section, we will discuss how to calculate the require separation distance d_{vs} between a grounding point of a controllable voltage source and a reference electrode of a voltage detector, based on 10V GPR criterion.

3.6.2 *Separation Distance* d_{vs}

Using Equation (3-6-1-3), it is possible to obtain a certain d_{vs}, which is r, to have a certain GPR.

$$d_{vs} = r = \frac{L}{e^{\left(\frac{GPR}{0.1686 \cdot R_g} \cdot \left|\frac{Z_c \cdot \gamma}{EMF}\right|\right)} - 1} \qquad (3\text{-}6\text{-}2\text{-}1)$$

In this thesis, the GPR criterion of 10V is considered.

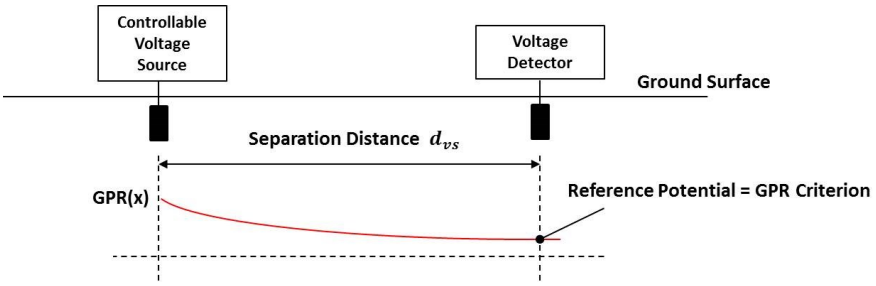

Figure 3-6-2-1: Separation distance d_{vs}

As explained in Section 2.3.2, there is no concern about the disturbance on the reference potential of the voltage detector by the induced voltage on the pipeline. The separation distance between the voltage detector and the pipeline can be normal distance such as 1~2m so the grounding point of the controllable voltage source can be $d_{vs} + (1 \sim 2\text{m})$ from the location of the pipeline's terminal.

Since the grounding current I_g in Equation (3-6-1-3) depends on some impact factors, it is possible to obtain the practical range of the required d_{vs} based on the practical range of currents in overhead AC power lines and following conditions.

Separation distance d_s	20m
Parallel Length L	10km
Soil resistivity ρ	100 Ωm
Internal impedance of controllable voltage source Z_{in_SA}	5+j5 Ω
Grounding resistor of controllable voltage source R_{g_SA}	5 Ω

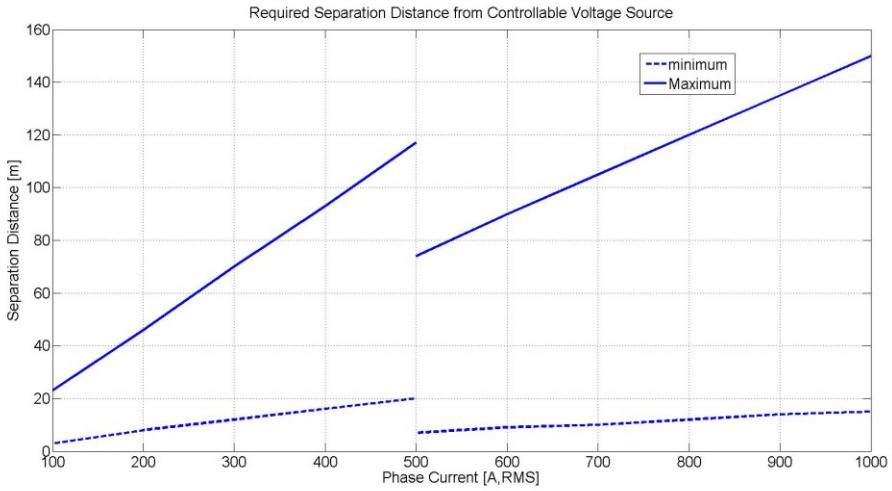

Figure 3-6-2-2: Required separation distance d_{vs} according to phase current

*The term of minimum indicates the result with the minimum conditions of load imbalance and the 3rd and 9th harmonic currents in both the distribution and transmission line cases. The term of maximum means the result with the maximum conditions. As you can see, the required separation distance d_{vs} varies widely according to phase current, load imbalance, and harmonic currents in the overhead AC power lines.

3.6.3 Contour Curves of d_{vs} according to EMF and ρ

As shown in Equation (3-6-1-4), I_g is highly dependent on EMF because Z_c and γ are fixed parameters. Therefore, according to Equation (3-6-2-1), the impact factors on d_{vs} are EMF and ρ.

For the simple way to estimate required d_{vs}, we can consider the contour curves of d_{vs} according to EMF and ρ. Using the probe-wire-based measurement method to be presented in Chapter 4, it is possible to estimate induced EMF on buried pipelines. As long as we know the estimated induced EMF on buried pipelines and ρ, we can also simply estimate required d_{vs} using Equation (3-6-2-1) and the contour curves of d_{vs} according to EMF and ρ without calculation process.

Following Figure 3-6-3-1 ~ 3-6-3-3 show the contour curves of d_{vs} according to EMF and ρ at the fundamental, 3rd , and 9th harmonic frequencies. Using the estimated EMF and ρ, estimated d_{vs} at each harmonic order can be obtained from following contour curves.

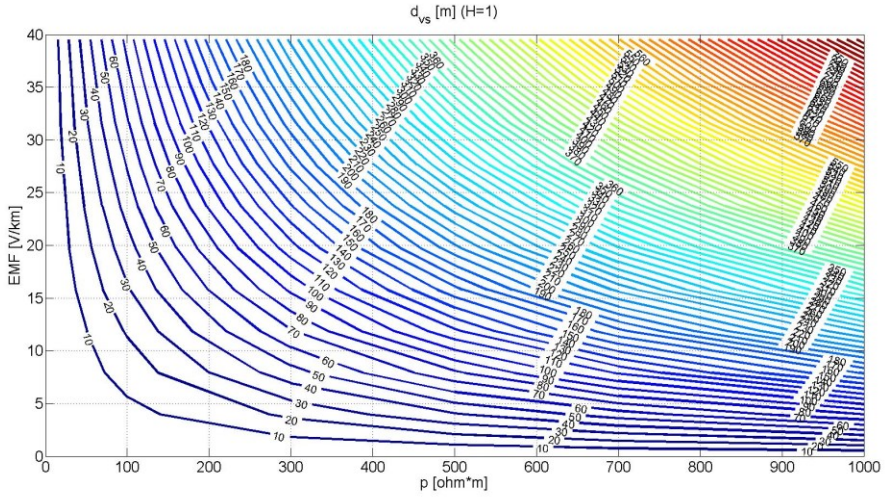

Figure 3-6-3-1: Contour curves of the separation distance d_{vs} according to EMF and ρ at the fundamental frequency

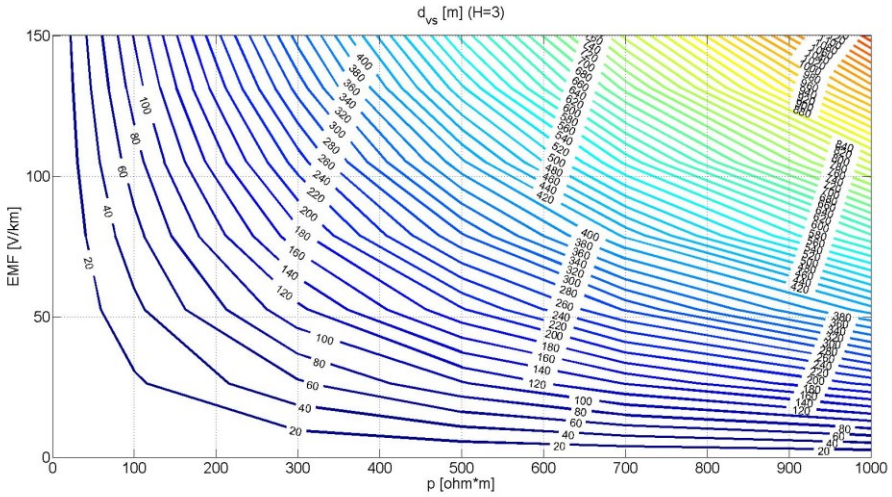

Figure 3-6-3-2: Contour curves of the separation distance d_{vs} according to EMF and ρ at the 3rd harmonic frequency

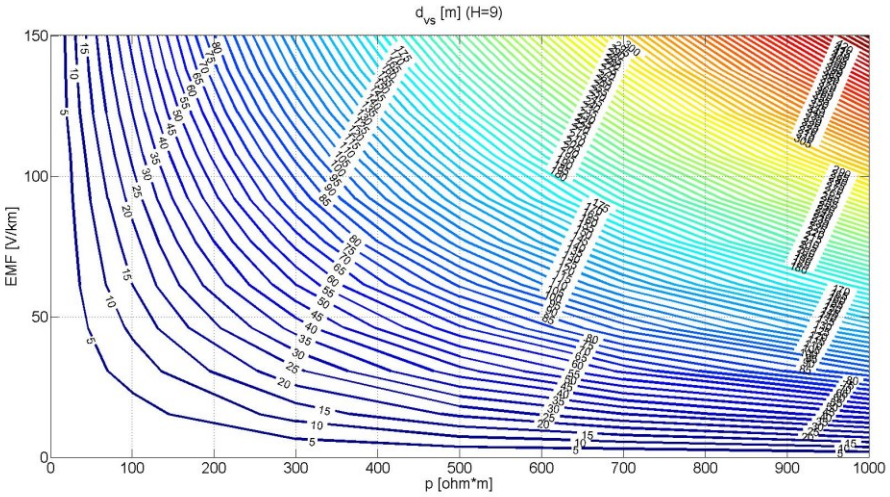

Figure 3-6-3-3: Contour curves of the separation distance d_{vs} according to EMF and ρ at the 9th harmonic frequency

According to the above Figure 3-6-3-1 ~ 3-6-3-3, we can see that d_{vs} increases by the increase of EMF and ρ.

3.6.4 Practical Range of Separation Distance d_{vs}

With consideration of $d_s = 20\text{m}$, $L = 10\text{km}$, $\rho = 100\Omega\text{m}$, $R_{g\_SA} = 5\Omega$, the practical range of d_{vs} is obtained as follows.

Practical Range of d_{vs}	3 ~ 150m

In the case of $d_s = 50\text{m}$, practical range of d_{vs}

Practical Range of d_{vs}	2 ~ 112m

The value of d_{vs} in some cases seems very long. However, in comparison with the minimum anode bed distance from a buried pipeline in the Cathodic Protection method, this distance becomes acceptable. In the CP method for DC corrosion, there are similar requirements for the GPR interference caused by a DC rectifier. According to Reference [12], the minimum anode bed distance from a buried pipe

or an adjacent structure should be 100m, unless field data show that interference is not a problem [12]. Preferred criteria for this minimum distance are 50m for a 30A rated output, 100m for a 50A output, 200m for a 100A output, and 300m for 150A output [12]. Multiple rectifier anode bed installations in the same general area should have anode beds separated by a minimum distance of 300m [12].

3.7 Mitigation Effect according to Application Points for Neutralizing Voltage

So far, we have considered the two terminals of a buried pipeline as the application points for neutralizing voltage. In practice, we may have existing access points to a buried pipeline in between two terminals of it. Since those existing access points are not the positions of two terminals, the equivalent circuit of the active mitigation system with those existing access points is different from the one we have considered before. In Appendix J, it can be referred to how to calculate induced voltage and required neutralizing voltage of the buried pipeline according to different application points for neutralizing voltage.

In this section, mitigation effects according to different application points (not two terminals) for neutralizing voltage are presented. It is based on the 10km long buried pipeline of the case study in Section 2.2.6 and the locations of existing access points are specified as the number of measurement points (#1~#11 with 1km interval).

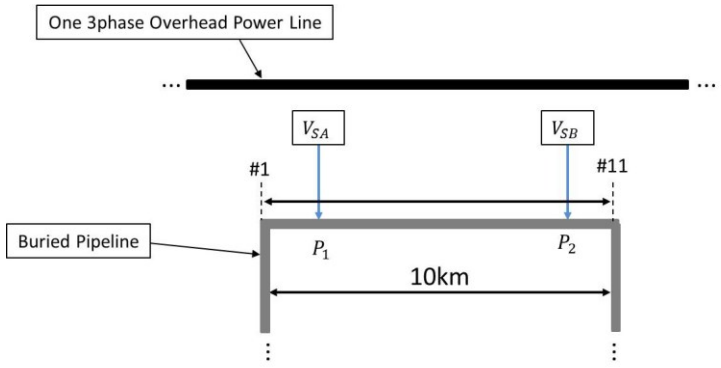

Figure 3-7-1: Existing access points of P_1 and P_2 between two terminals

Following three cases of different access points are considered in this section.

Table 3-7-1: Location of existing access points in sample cases

	Location of Left Access Point P_1 [km]	Location of Right Access Point P_2 [km]
Case 1	#2	#10
Case 2	#3	#9
Case 3	#4	#8

Voltage profile of the buried pipeline after applying proper neutralizing voltage onto the existing access points in each case are as follows. Following Figure 3-7-2 is the fundamental frequency case.

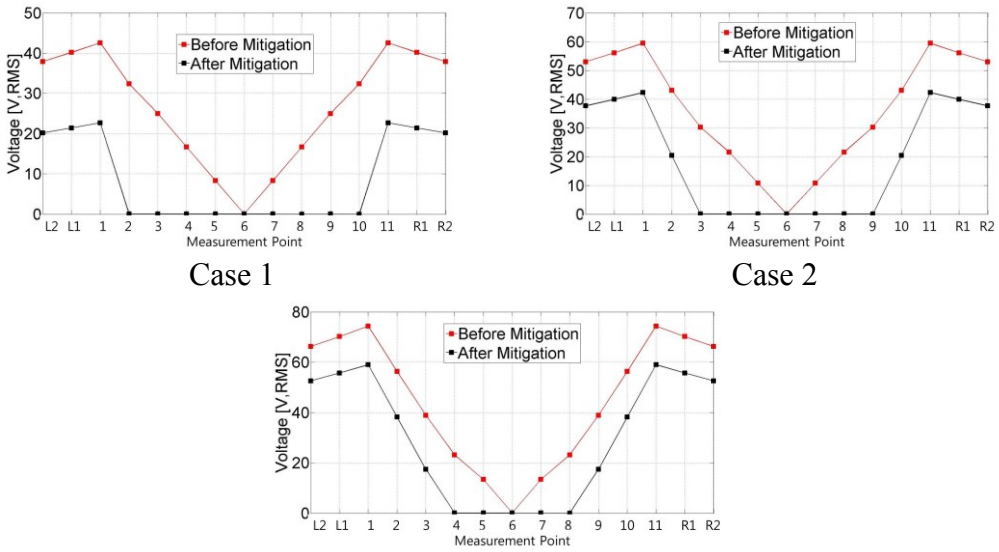

Case 1 Case 2

Case 3

Figure 3-7-2: Mitigation effect according to different application points of neutralizing voltage in Case 1, 2, 3

Measurement point #L1 ~ #L2: points on the left extended part of the pipeline (1km, 2km away from the left terminal respectively)

Measurement point #1 ~ #11: points on the parallel route of the pipeline (11 points divided by 1km segment)

Measurement point #R1 ~ #R2: points on the right extended part of the pipeline (1km, 2km away from the right terminal respectively)

According to Figure 3-7-2, we can find out that the area between two application points for neutralizing voltage can have mitigation effect but other areas in the parallel route have remaining voltage.

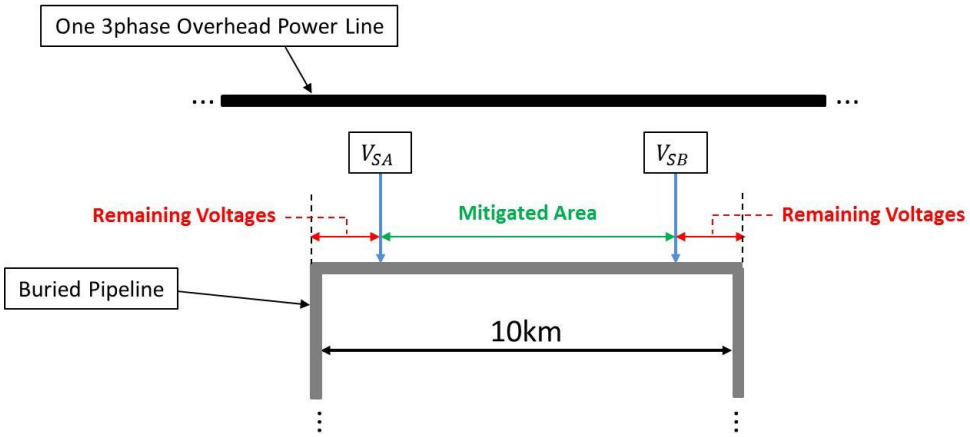

Figure 3-7-3: Mitigated area and remaining voltage

Those remaining voltage increases when the application points for neutralizing voltage are getting far away from each terminal point. In other words, for the acceptable mitigation effect, the application points for neutralizing voltage should be or close to two terminal of the pipeline's parallel route. Consequently, if we have existing access points close to two terminals, we may utilize those existing access points to apply neutralizing voltage without installing terminal rods onto the buried pipeline.

3.8 Summary

We have done sensitivity studies to find out how the major design parameters of the active mitigation systems change according to the impact factors.

Firstly, the following Table 3-8-1 shows the summary result of the sensitivity level of the impact factors.

Table 3-8-1: Summary result of sensitivity level of impact factors

Impact Factors	Sensitivity Level
Phase (Balanced) Current I	★☆☆☆
Load Imbalance Imb	★★★★
Harmonic Currents	★★★★
Separation Distance d_s	★★★★
Equivalent Internal Impedance of Controllable Voltage Source Z_{SA}	★★★★
Length of Parallel Route L	V_A (★★★☆), V_{SA} , S_{SA} (★☆☆☆)
Soil Resistivity ρ	★★☆☆

Secondly, using the contour curves of the normalized major design parameters by residual current $I_{residual}$, it is possible to estimate the major design parameters according to specific values for $I_{residual}$, d_s, Z_{SA}, L, H, ρ without complicated calculation process. The contour curves by EMF can be also used to estimate the major design parameters. EMF can be estimated using the probe-wire-based measurement method to be presented in next Chapter 4.

Thirdly, through sensitivity studies with the practical ranges of the impact factors, we have obtained the practical ranges of the major design parameters as follows.

Table 3-8-2: Practical range of major design parameters in the proposed active mitigation system

Impact Factors	Practical Range
Total Residual Current $I_{residual}$	6 ~ 182 [A, RMS]
Total Induced Terminal Voltage V_A	0.5 ~ 414.9 [V, RMS]
Total Required Neutralizing Voltage V_{SA}	17.5 ~ 1,843.3 [V, RMS]
Total Required Power S_{SA}	0.013 ~ 153.3 [kVA]
Required Separation Distance d_{vs}	3 ~ 150 [m]

Lastly, we have checked out that application points for neutralizing voltage need to be the location of the two terminals (two ends) of a buried pipeline for mitigation. We may use existing access points as the application points for neutralizing voltage but if those existing access points are far away from the location of the two terminals, we will have remaining voltage after mitigation at the areas between one existing access point and one nearest terminal point.

Chapter 4

Probe-Wire-Based Measurement Method for Induced Voltage on Buried Pipelines

The proposed active mitigation device requires the prediction of induced EMF on a pipeline to determine the device rating. Therefore, the maximum EMF should first be obtained. There are two ways to obtain EMFs, namely calculation and measurement. Calculation is not very practical, because the required parameters are not always available and not accurate enough. Field measurements conducted at the peak hour always represent maximum EMF during steady-state operation. Taking some margin into account, the active mitigation device rating can be easily and relative accurately determined.

Direct measuring of the induced voltage on a buried pipeline is not convenient, because the pipeline is buried and covered with a coating material. Therefore, an indirect method to measure or estimate the induced voltage is simpler.

A probe-wire-based measurement method is widely used for measuring telephone interference caused by harmonics in nearby power lines. This method can also be applied to buried pipelines in order to estimate induced EMF along them.

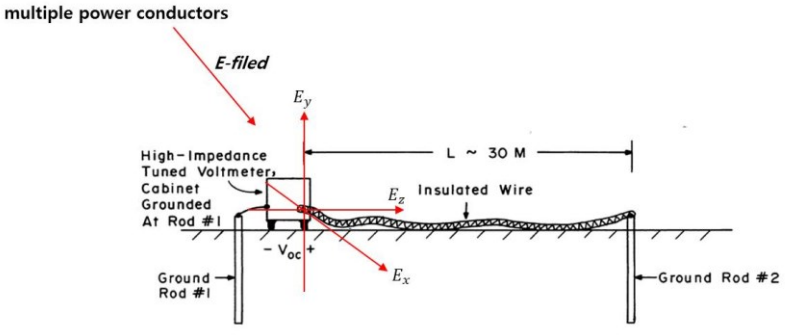

Figure 4-1: Probe-wire-based measurement method, from Reference [13]

If we place a probe wire near the buried pipeline that is parallel to overhead AC power lines, we can expect that quite similar induced EMF will be measured along the probe wire. If it is true, we can estimate induced EMF on the buried pipeline by using the measured EMF along the probe wire, without needing direct access to the buried pipeline. This is the probe-wire-based measurement method for induced voltage on buried pipelines in this thesis. Using the estimated induced EMF on the buried pipeline, it is possible to calculate the induced voltage on it by analytical methods. In this chapter, we will discuss details of the probe-wire-based measurement method for induced voltage on buried pipelines.

4.1 Probe-Wired-Based Measurement Method Issues

As mentioned above, if we place a probe wire near a buried pipeline, the measured voltage (per unit length) along the probe wire will be similar to the induced EMF (per unit length) along the buried pipeline.

$$\begin{matrix}\text{Measured Voltage (V/m)} \\ \text{along a Probe Wire}\end{matrix} \cong \begin{matrix}\text{Induced EMF (V/m)} \\ \text{along a Buried Pipeline}\end{matrix} \qquad (4\text{-}1\text{-}1)$$

In order to estimate induced EMF along the buried pipeline using the probe-wire-based measurement method, the following two issues should be considered:

(1) Capacitive coupling impact from nearby AC power lines on the probe wire

(2) Induced *EMF* difference between the probe wire and the buried pipeline due to their different locations

4.1.1 Capacitive Coupling Impact on Probe-Wire-Based Measurement Method

As mentioned before, induced voltage on buried pipelines in a steady state is only caused by the inductive coupling effect from nearby overhead AC power lines. However, induced voltage on the probe wire on the ground is caused by both the capacitive and the inductive coupling effect from nearby overhead AC power lines.

Induced Voltage on a Probe Wire
=(1) Voltage caused by Inductive Coupling + (2) Voltage caused by Capative Coupling (4-1-1-1)

Induced Voltage on a Buried Pipeline
=(1) Voltage caused by Inductive Coupling (4-1-1-2)

Consequently, in order to estimate induced EMF on buried pipelines using a probe wire, we should deduct the capacitive coupling impact from the measured voltage along the probe wire. The assessment of the capacitive coupling impact on the probe wire is presented in Section 4.2.

4.1.2 EMF gap between a Probe Wire and a Buried Pipeline

According to Faraday's law, EMF on a buried pipeline or a probe wire is that induced on its earth return loop. Due to the difference between the probe wire's and the buried pipeline's location, there is an EMF difference between them. This is called EMF gap (EMF_{gap}) in this thesis. The following Figure 4-1-2-1 helps to understand this explanation.

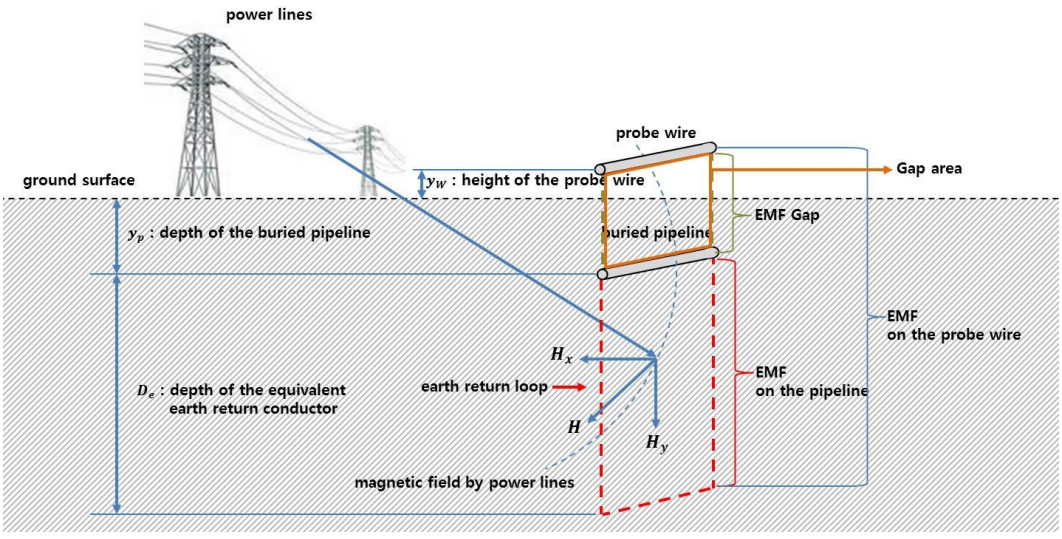

Figure 4-1-2-1: EMF gap between a probe wire and a buried pipeline

In order to estimate induced EMF on the buried pipeline using the probe-wire-based measurement method, we should check whether the EMF gap is

considerable. If the EMF gap is considerable, we need to think about how to compensate it in order to accurately estimate induced EMF on the buried pipeline.

The two issues regarding the capacitive coupling impact and the EMF gap need to be assessed for applicability of the probe-wire-based measurement method. They will be discussed in Section 4.2 and 4.3.

4.2 Assessment of Capacitive Coupling Impact on Probe-Wire-Based Measurement Method

In order to calculate how much capacitive coupling will impact the probe-wire-based measurement method, we need to compare two cases: with and without the capacitive coupling impact. Thus, the first step for the comparison of those two cases is to calculate the measured voltage along the probe wire in each case.

4.2.1 Voltage Measurement V_{OC} with Capacitive Coupling (without Shielding)

The following Figure 4-2-1-1 describes the probe wire's circuit affected by both inductive coupling and capacitive coupling from nearby overhead AC power lines.

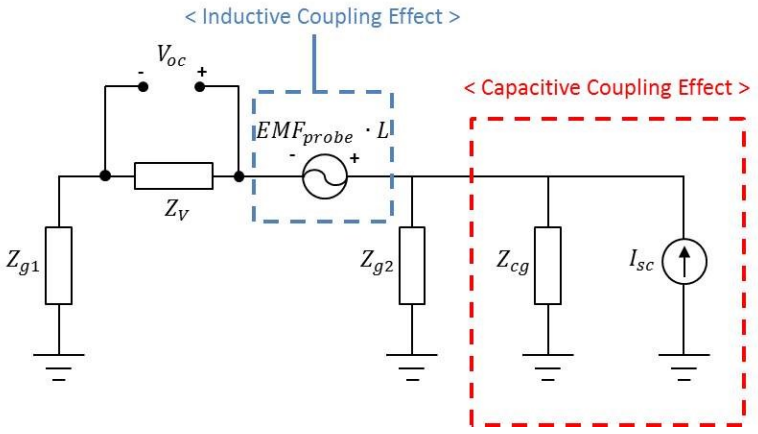

Figure 4-2-1-1: Circuit of the probe wire affected by both inductive and capacitive coupling

where,

EMF_{probe} : induced EMF on the probe wire [V/m]

I_{SC} : current source caused by capacitive coupling [A]

L : length of the probe wire [m]

Z_V : impedance of the voltage meter [Ω]

Z_{g1} : impedance of the ground rod #1 [Ω]

Z_{g2} : impedance of the ground rod #2 [Ω]

Z_{cg} : impedance by the capacitance between the probe wire and the ground [Ω]

V_{OC} : voltage to be measured by the voltage meter [V]

$$I_{SC} = \frac{E_y \cdot y_w}{Z_{cg}} \tag{4-2-1-1}$$

$$Z_{cg} = \frac{1}{2\pi f C_{cg}} \tag{4-2-1-2}$$

$$C_{cg} = \frac{2\pi\varepsilon_0}{\ln\left(\frac{4y_w}{d}\right)} \tag{4-2-1-3}$$

E_y : y-axis component of the electric field caused by the overhead power lines [V/m], The detailed equation to calculate E_y can be referred to in Appendix K.

y_w : y position (height) of the probe wire [m]

C_{cg} : capacitance between the probe wire and the ground surface [F]

d : diameter of the probe wire [m]

The above circuit in Figure 4-2-1-1 contains two voltage and current sources caused by inductive and capacitive coupling from overhead AC power lines.

According to the superposition principle, the measured voltage V_{OC} by the voltage meter will be

$$\begin{aligned} V_{OC} &= (1)V_{OC}\ caused\ by\ EMF_{probe} \cdot L + (2)V_{OC}\ caused\ by\ I_{SC} \\ &= V_{OC1} + V_{OC2} \end{aligned} \tag{4-2-1-4}$$

A. $V_{OC}\ caused\ by\ EMF_{probe}$ **(**V_{OC1}**)**

$V_{OC}\ caused\ by\ EMF_{probe}$ is the contribution by EMF_{probe} to the measured voltage V_{OC} and can be calculated as follows.

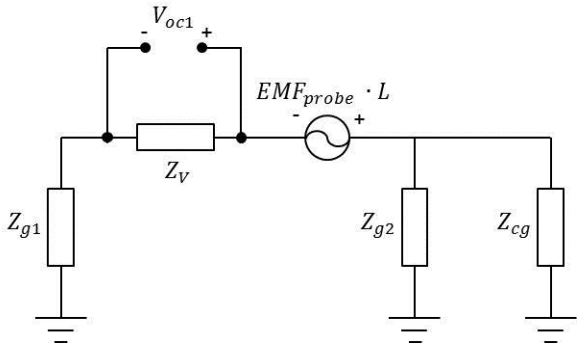

Figure 4-2-1-2: Circuit for $V_{OC}\ caused\ by\ EMF_{probe}$

$$V_{OC}\ caused\ by\ EMF_{probe} = V_{OC1} = -\frac{Z_V}{Z_{g1} + Z_V + \left(Z_{g2}\ //\ Z_{cg}\right)} \cdot EMF_{probe} \cdot L \tag{4-2-1-5}$$

B. $V_{OC}\ caused\ by\ I_{SC}$ **(**V_{OC2}**)**

$V_{OC}\ caused\ by\ I_{SC}$ is the contribution by I_{SC} to the measured voltage V_{OC} and can be calculated as follows.

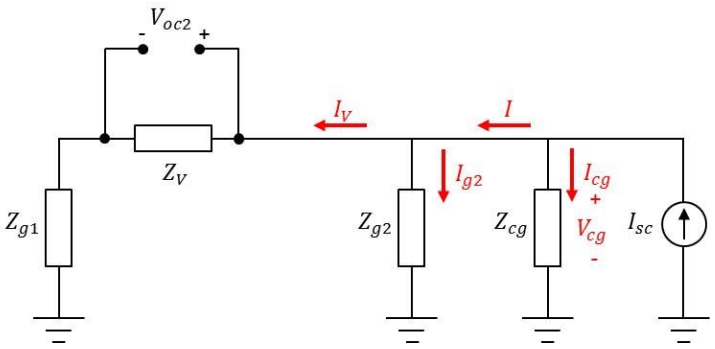

Figure 4-2-1-3: Circuit for V_{OC} *caused by* I_{SC}

$$I_{cg} = \frac{\left(Z_{g1} + Z_V\right) // Z_{g2}}{\left\{\left(Z_{g1} + Z_V\right) // Z_{g2}\right\} + Z_{cg}} \cdot I_{SC} \tag{4-2-1-6}$$

$$V_{cg} = Z_{cg} \cdot I_{cg} \tag{4-2-1-7}$$

$$I = \frac{Z_{cg}}{\left\{\left(Z_{g1} + Z_V\right) // Z_{g2}\right\} + Z_{cg}} \cdot I_{SC} \tag{4-2-1-8}$$

$$I_V = \frac{Z_{g2}}{Z_{g1} + Z_{g2} + Z_V} \cdot I \tag{4-2-1-9}$$

$$V_{OC} \text{ caused by } I_{SC} = V_{OC2} = Z_V \cdot I_V = Z_V \cdot \frac{Z_{g2}}{Z_{g1} + Z_{g2} + Z_V} \cdot \frac{Z_{cg}}{\left\{\left(Z_{g1} + Z_V\right) // Z_{g2}\right\} + Z_{cg}} \cdot I_{SC} \tag{4-2-1-10}$$

C. V_{OC} with Capacitive Coupling (without Shielding)

Based on the above, the voltage measurement V_{OC} with capacitive coupling in Figure 4-2-1-1 is

V_{OC} with Capacitive Coupling (without Shielding) = $V_{OC1} + V_{OC2}$ (4-2-1-11)

where,

$$V_{OC1} = V_{OC} \text{ caused by } EMF_{probe} = -\frac{Z_V}{Z_{g1} + Z_V + \left(Z_{g2} // Z_{cg}\right)} \cdot EMF_{probe} \cdot L$$

$$V_{OC2} = V_{OC}\ caused\ by\ I_{SC} = Z_V \cdot I_V = Z_V \cdot \frac{Z_{g2}}{Z_{g1} + Z_{g2} + Z_V} \cdot \frac{Z_{cg}}{\left\{\left(Z_{g1} + Z_V\right) // Z_{g2}\right\} + Z_{cg}} \cdot I_{SC}$$

As mentioned before, in order to eliminate the capacitive coupling effect from overhead AC power lines, a kind of shielding on the probe wire measurement device needs to be considered [13]. The function of the shielding eliminates Z_{cg} and I_{SC} in Figure 4-2-1-1. However, no shielding is required if the capacitive coupling impact is negligible.

4.2.2 Voltage Measurement V_{OC} without Capacitive Coupling (with Shielding)

The following Figure 4-2-2-1 describes the probe wire's circuit without capacitive coupling from overhead AC power lines (with shielding).

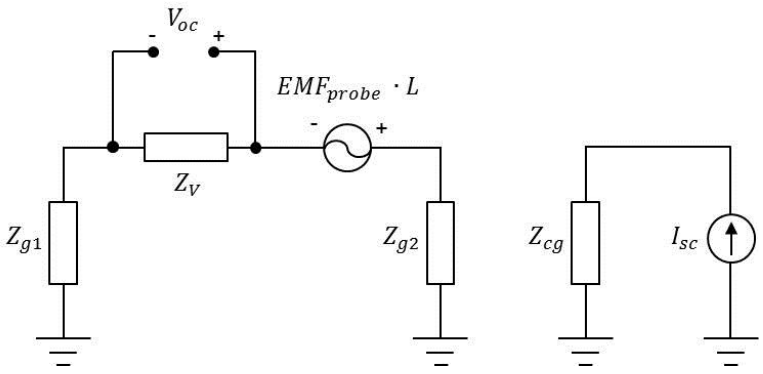

Figure 4-2-2-1: Circuit of the probe wire without capacitive coupling (with shielding)

The measured voltage V_{OC} on the voltage meter in the above case can be calculated as follows.

V_{OC} without the capacitive coupling (with shielding) = V_{OC3} (4-2-2-1)

$$V_{OC3} = -\frac{Z_V}{Z_{g1} + Z_{g2} + Z_V} \cdot EMF_{probe} \cdot L \quad (4\text{-}2\text{-}2\text{-}2)$$

4.2.3 Capacitive Coupling Impact on V_{OC}

The capacitive coupling impact on V_{OC} is the difference between (1) the V_{OC} with capacitive coupling and (2) the V_{OC} without capacitive coupling as follows.

$$\begin{aligned}&\text{Capacitive Coupling Impact on } V_{OC}\\&= (1)\,V_{OC} \text{ with Capacitive Coupling} - (2)\,V_{OC} \text{ without Capacitive Coupling}\\&= (V_{OC1} + V_{OC2}) - V_{OC3}\end{aligned} \tag{4-2-3-1}$$

The difference between V_{OC1} and V_{OC3} is caused by Z_{cg}. Since the value of Z_{cg} is much greater than Z_{g2}, two equations of V_{OC1} and V_{OC3} are almost same. Therefore, V_{OC2} is the only contributor to the difference between V_{OC1} and V_{OC3}.

Considering that the values of Z_{cg} and Z_V are much greater than others, it is possible to obtain the following equation.

$$V_{OC2} \cong Z_{cg} \cdot I_{SC} \tag{4-2-3-2}$$

As long as Z_{g2} can be restricted to a small value, the impact of V_{OC2} is negligible. The capacitance coupling impact will slightly increase if harmonics are considered because of the decrease of Z_{cg}.

The result of the case study in Section 4.4 shows that the capacitive coupling impact on V_{OC} is actually not significant, hence it needs not be considered when we use the probe-wire-based measurement method for buried pipelines. In Section 4.4 a case study will examine the capacitive coupling impact on V_{OC}.

4.3 Assessment of EMF Gap between Probe Wire and Buried Pipeline

In the probe-wire-based measurement method, the EMF gap (difference) between a probe wire and a buried pipeline will be an error of the estimated EMF_{pipe}

(estimated induced EMF along the buried pipeline). For the correction of the EMF gap, we need to think about how to calculate or measure it (EMF_{gap}) in practice. By compensating EMF_{gap} to the probe-wire-based measurement method, it is possible to estimate EMF_{pipe} with a small error.

In Figure 4-1-2-1 we can see the area difference between the probe wire's and the buried pipeline's earth return loops. Using Faraday's law, it is reasonable to consider that EMF_{gap} will be the EMF difference between EMF_{probe} (the probe wire's EMF) and EMF_{pipe} (the pipeline's EMF).

$$EMF_{pipe} \cong EMF_{probe} - EMF_{gap} \tag{4-3-1}$$

where,

$EMF_{gap} = EMF$ at the gap area between the buried pipeline's and the probe wire's earth return loop

In this thesis, it is assumed that induced voltage on the probe wire caused by EMF_{pipe} is negligible. EMF_{gap} can also be calculated by Faraday's law as long as we have the x-axis component of magnetic field intensity along y-axis, $H_x(y)$ in the gap area as follows.

$$EMF_{gap} = -\frac{d\Phi}{dt} = -\frac{d}{dt}\left(\int_0^L \int_{y_w}^{y_p} \mu_0 H_x(y) dy dx \right) \tag{4-3-2}$$

Since buried depth y_p of buried pipelines will be just a few meters in practice, it is possible to consider linear regression with some measured sample data of $H_x(y)$ on the ground. The following Figure 4-3-1 shows linear regression using magnetic sensors.

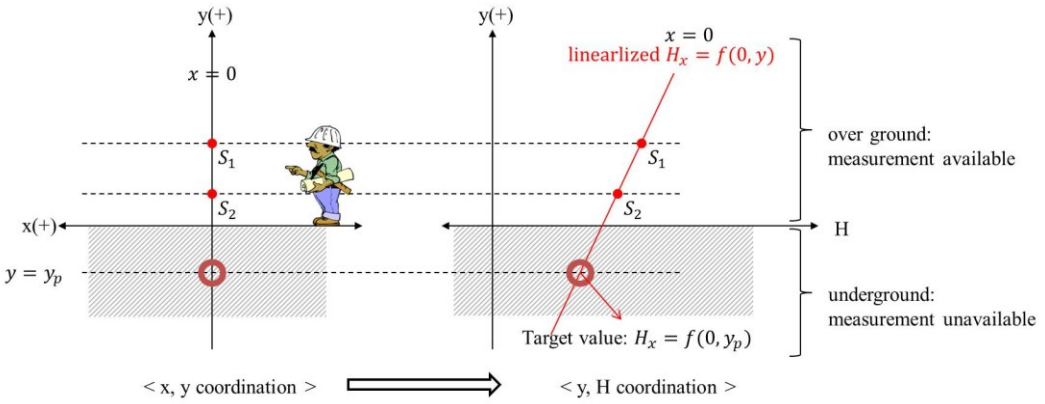

Figure 4-3-1: Estimating H_x by linear regression

Consequently, as long as we can get $H_x(y)$ in the gap area, it is possible to calculate EMF_{gap} using Equation (4-3-2). $H_x(y)$ can be estimated by linear regression as follows. The sample data for linear regression can be measured using magnetic sensors on the ground. In this thesis, only two sensors are considered to measure the sample data of $H_x(y)$.

$$y = a_0 + a_1 \cdot x \tag{4-3-3}$$

$$\begin{bmatrix} n & \sum_{i=1}^{n} x_i \\ \sum_{i=1}^{n} x_i & \sum_{i=1}^{n} x_i^2 \end{bmatrix} \begin{bmatrix} a_0 \\ a_1 \end{bmatrix} = \begin{bmatrix} \sum_{i=1}^{n} y_i \\ \sum_{i=1}^{n} x_i y_i \end{bmatrix} \tag{4-3-4}$$

$$\begin{bmatrix} a_0 \\ a_1 \end{bmatrix} = \begin{bmatrix} n & \sum_{i=1}^{n} x_i \\ \sum_{i=1}^{n} x_i & \sum_{i=1}^{n} x_i^2 \end{bmatrix}^{-1} \begin{bmatrix} \sum_{i=1}^{n} y_i \\ \sum_{i=1}^{n} x_i y_i \end{bmatrix} \tag{4-3-5}$$

where,

x_i, y_i : given data corresponding to sample data of y and $H_x(y)$ respectively

n : number of given data

By the above, it is possible to estimate EMF_{gap} by linear regression using two magnetic sensors. Consequently, it is possible to reduce the error between EMF_{probe} and EMF_{pipe} as follows.

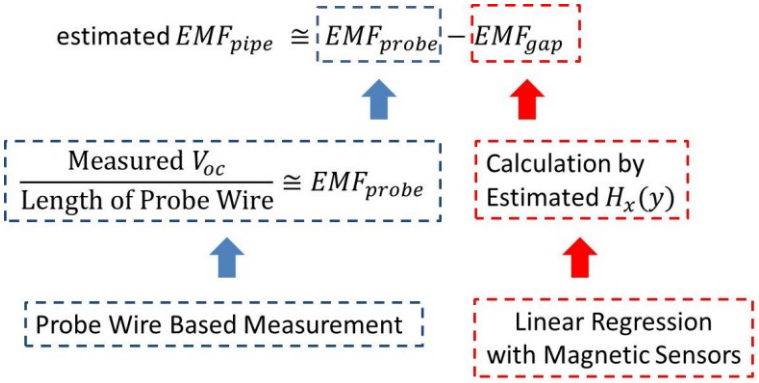

Figure 4-3-2: Estimating EMF_{pipe} by the probe-wired-based measurement method with correction using magnetic sensors

In the next we will take a look at one case study explained by the above.

4.4 Case Study

The following Figure 4-4-1 and Table 4-4-1 and 4-4-2 show one three-phase overhead AC power line circuit and one buried pipeline in the case study.

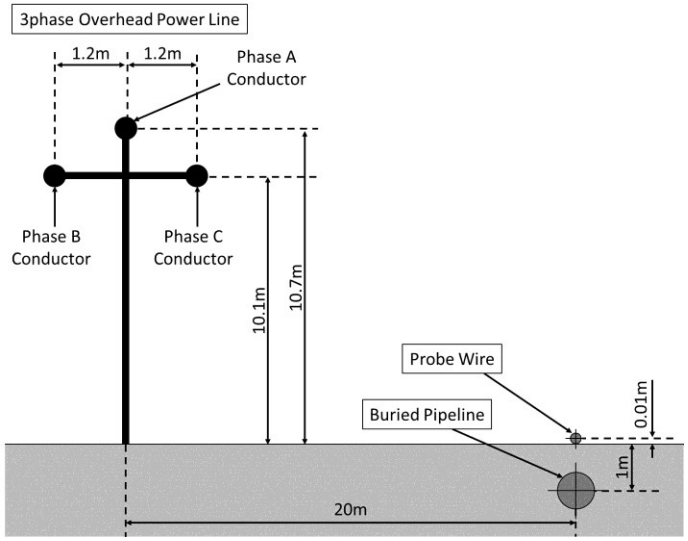

Figure 4-4-1: Side view of case study

Table 4-4-1: Position of phase conductors in case study

Position of Phase Conductor A [m]	(0, 10.7)
Position of Phase Conductor B [m]	(-1.2, 10.1)
Position of Phase Conductor C [m]	(1.2, 10.1)

Table 4-4-2: Parameters in case study

Parameter	Value	Unit
ρ Soil resistivity	100	[Ω]
V Voltage of phase conductor	$\frac{138}{\sqrt{3}}$	[kV,RMS]
I Balanced current of phase conductor	500	[A,RMS]
PF Power factor	0.95	N/A
Imb load imbalance	5	%
Z_V Impedance of voltage meter	10^6	[Ω]
Z_{g1} Impedance of ground rod #1	100	[Ω]
Z_{g2} Impedance of ground rod #2	100	[Ω]
Z_{cg} Impedance at 60Hz between the probe wire and the ground	4.4×10^6	[Ω]

* Other parameters can be found in Appendix G.

Based on the above case study, the capacitive coupling impact and EMF_{gap} in the probe-wire-based measurement method are presented in the following sections.

4.4.1 Capacitive Coupling Impact on Probe-Wire-Based Measurement Method

The following Table 4-4-1-1 shows the comparison between the V_{OC} with capacitive coupling and the V_{OC} without capacitive coupling in the case study.

Table 4-4-1-1: Comparison between the V_{OC} with capacitive coupling and the V_{OC} without capacitive coupling in the case study

	Analytical (1)	Simulation (2)	%Error (1)-(2)
(a) V_{OC} with capacitive coupling	0.312285 [V]	0.312009 [V]	0.088 [%]
(b) V_{OC} without capacitive coupling	0.312284 [V]	0.312008 [V]	0.088 [%]
%Error (a)-(b)	0.0003 [%]	0.0003 [%]	

First of all, the above result shows that analytical calculation of (a) the V_{OC} with capacitive coupling and (b) the V_{OC} without capacitive coupling are almost identical to the simulation results. This means that the analytical equations for (a) and (b) in Section 4.2 are verified by simulations.

Secondly, the above result reveals that the % error between (a) and (b), which corresponds to the capacitive coupling impact on V_{OC}, is very small, 0.0003%. This is because the capacitance between the probe wire and the grounding surface is very small, and the electric field at the ground surface caused by the overhead AC power line in the case study is not considerable. The capacitive coupling impact on the probe wire is negligible. Therefore, we do not have to consider any shielding in the probe-wire-based measurement method. The measured V_{OC} per unit length will be almost identical to the induced EMF on the probe wire (EMF_{probe}, per unit length).

4.4.2 Estimation of EMF_{pipe} by compensating EMF_{gap}

The following Table 4-4-2-1 shows following three kinds of EMF.

(a) **correct** $\boldsymbol{EMF_{pipe}}$: analytically calculated by Carson's equation

(b) **estimated** $\boldsymbol{EMF_{pipe}}$ using the **probe-wire-based measurement method** **(with correction using magnetic Sensors)**

(c) **estimated** $\boldsymbol{EMF_{pipe}}$ using the **probe-wire-based measurement method** (without correction using magnetic sensors)

We should ensure that (b) the estimated EMF_{pipe} with correction using magnetic sensors indicates the estimated EMF on the pipeline based on EMF_{probe} and estimated EMF_{gap} using magnetic sensors as shown in Figure 4-3-3.

Table 4-4-2-1: Comparison of EMFs in the case study

(a) correct EMF_{pipe}	0.01027 [V/m]
(b) estimated EMF_{pipe} (with correction using magnetic sensors)	0.01023 [V/m]
(c) estimated EMF_{pipe} (without correction using magnetic sensors)	0.01041 [V/m]

%Error ((b)-(a))	-0.322 [%]
%Error ((c)-(a))	1.396 [%]

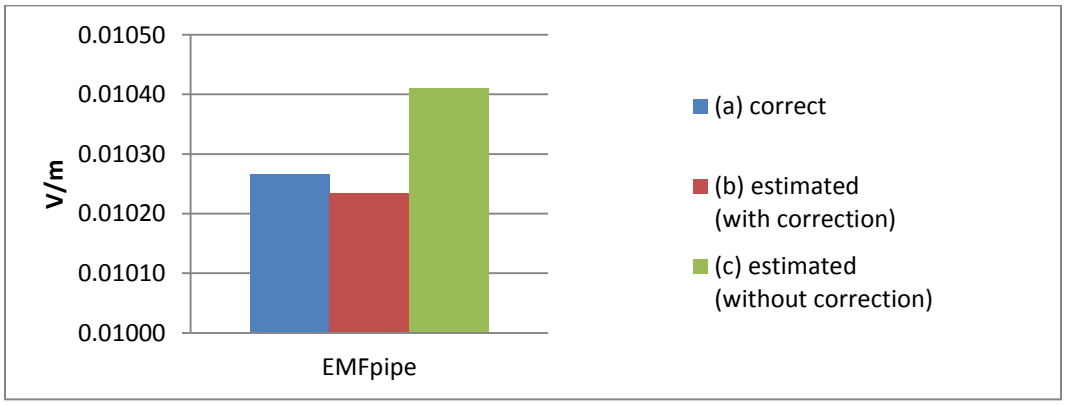

Figure 4-4-2-1: EMF comparison of case study

According to the above result, we can conclude that (b) the estimated EMF_{pipe} with correction using magnetic sensors is close to (a) the correct EMF_{pipe} with a small error of -0.322%. The (b) estimated EMF_{pipe} with correction using magnetic sensors is more accurate compared to (c) the estimated EMF_{pipe} without correction using magnetic sensors.

The case study considered 1m buried depth of the pipeline, and (c) the estimated EMF_{pipe} without correction using magnetic sensors also has the acceptable error of 1.396%. Therefore, if a pipeline is buried at a relatively shallow buried depth such as 1m, then the method of (c) would be acceptable (<5%). However, if a pipeline is buried deeper down, the error of method (c) will be higher (>5%).

The following Figure 4-4-2-2 shows the % error of (b) and (c) by different buried depth of the pipeline in the case study.

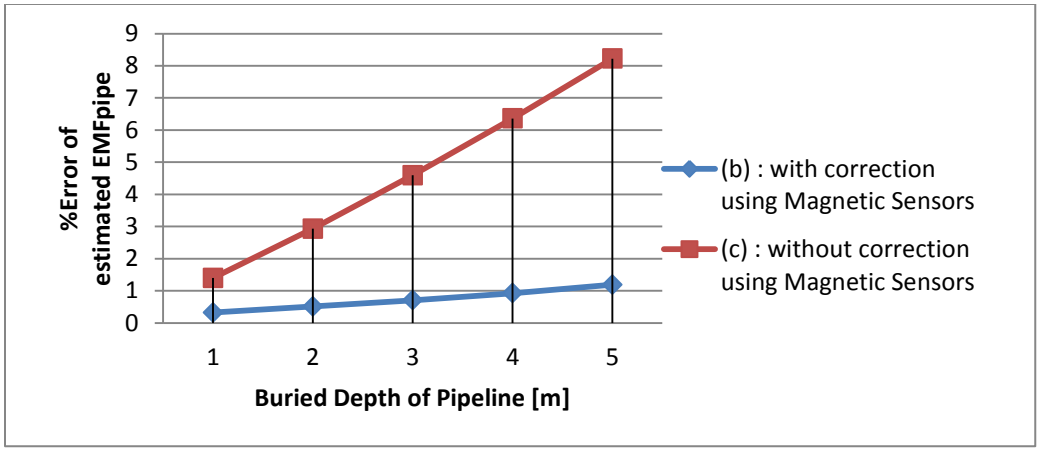

Figure 4-4-2-2: %error of the probe-wire-based measurement method by different buried depth of the pipeline

Figure 4-4-2-2 suggests that the probe-wire-based measurement method is available for buried pipelines, however without shielding and EMF_{gap} compensation. The error is less than 5% as long as the buried depth of the pipeline is within 3m. If the pipeline is buried very deep, magnetic sensors can be employed to correct the error caused by EMF_{gap}.

4.4.3 Case Study with Harmonics

In practice, overhead AC power lines have harmonic components in voltage and currents. As we have already established, the capacitive coupling impact on the probe-wire-based measurement is negligible as long as the probe wire is placed on the ground surface. Therefore, in the probe-wire-based measurement method, it is reasonable to consider only inductive coupling caused by harmonic components in currents of nearby overhead AC power lines.

In order to verify the availability of the probe-wire-based measurement method when considering the harmonic currents of overhead AC power lines, we are going to use the average harmonic sequence data from Section 2-2-6 (Figure 2-2-6-6 and Table 2-2-6-6).

Using the average harmonic sequence data, it is possible to obtain the following harmonic components of induced EMF on the buried pipeline in the case study.

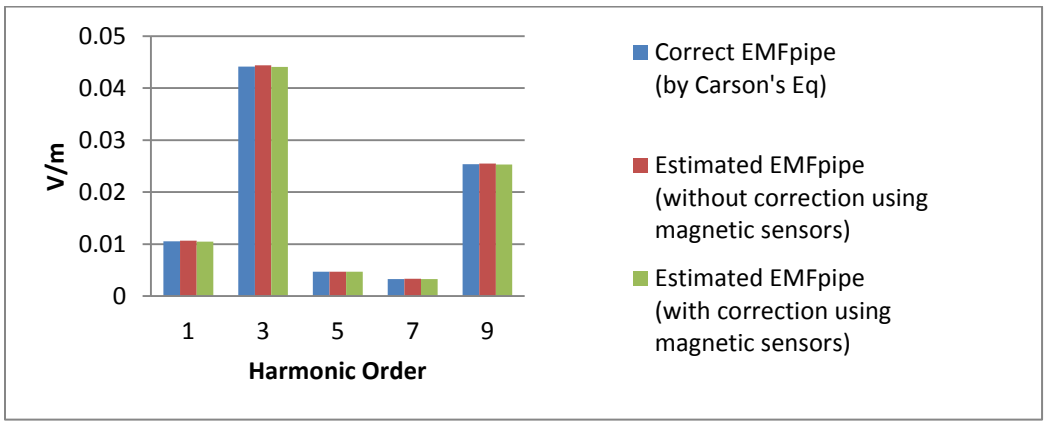

Figure 4-4-3-1: Estimated EMF_{pipe} when considering harmonics

Table 4-4-3-1: Harmonic components of correct EMF_{pipe} and estimated EMF_{pipe} in the case study

	EMF_{pipe} (1)	Estimated EMF_{pipe} (2) (without correction)	%Error (2)-(1)	Estimated EMF_{pipe} (3) (with correction)	%Error (3)-(1)
1st	0.010544	0.010639	0.903	0.010498	-0.438
3rd	0.044151	0.044345	0.439	0.044071	-0.006
5th	0.004682	0.004716	0.722	0.004674	-0.006
7th	0.003311	0.003339	0.839	0.003308	-0.003
9th	0.025351	0.025483	0.519	0.025306	-0.179

*unit : [V/m]

The above result reveals that the probe-wire-based measurement method with and without correction (EMF_{gap} compensation using magnetic sensors) is also available, with small errors, for estimating harmonic components in induced EMF on buried pipelines.

4.5 Field Measurement

In order to calculate overhead AC power lines' harmonic impact, some field measurements have been done, using the probe-wire-based measurement method (without correction using magnetic sensors). As mentioned and shown in Section 1.1.1, the field measurements showed that the 1st, 3rd, and 9th harmonic components are usually dominant (major). More detailed data relating to these field measurements are available in Appendix A.

4.6 Summary

By measuring induced voltage along the probe wire, which is placed near a buried pipeline, it is possible to estimate induced EMF on the buried pipeline. The capacitive coupling impact from overhead AC power lines on a probe wire would be negligible as long as the probe wire is placed on the ground near the buried pipeline. There is a difference (EMF gap) between the pipeline's EMF and the probe wire's EMF. The EMF gap depends on the buried depth of the pipeline and

can be considered as an error on the estimated EMF_{pipe} using the probe-wire-based measurement method. However, the EMF gap can be estimated and compensated to the estimated EMF_{pipe} by linear regression using magnetic sensors. If the buried depth of the pipeline is within 3m, the probe-wire-based measurement method without correction (linear regression) using magnetic sensors is also acceptable with a reasonable error less than 5%. The probe-wire-based measurement method is also available for measuring harmonic components of induced EMF with an acceptable error. This method has been used for field measurements, and reasonable data have been obtained.

Chapter 5

Design Specification for the Proposed Active Mitigation System

As discussed earlier, the design of the proposed active mitigation system depends on the specific conditions of a pipeline's site, so it will be an order based design. In order to determine the design specification for the proposed active mitigation system, a prerequisite study on a concerned pipeline's site is necessary. This study can provide actual information on the impact factors, which were discussed in Chapter 3. Based on that information, we can calculate specific values of the major design parameters of each device in the proposed active mitigation system. In addition, it is possible to estimate the major design parameters of the proposed active mitigation system using contour curves and the estimated EMF, which can be obtained by the probe-wire-based measurement method presented in Chapter 4.

The following flow chart explains the process to determine the design specification of each device in the proposed active mitigation system.

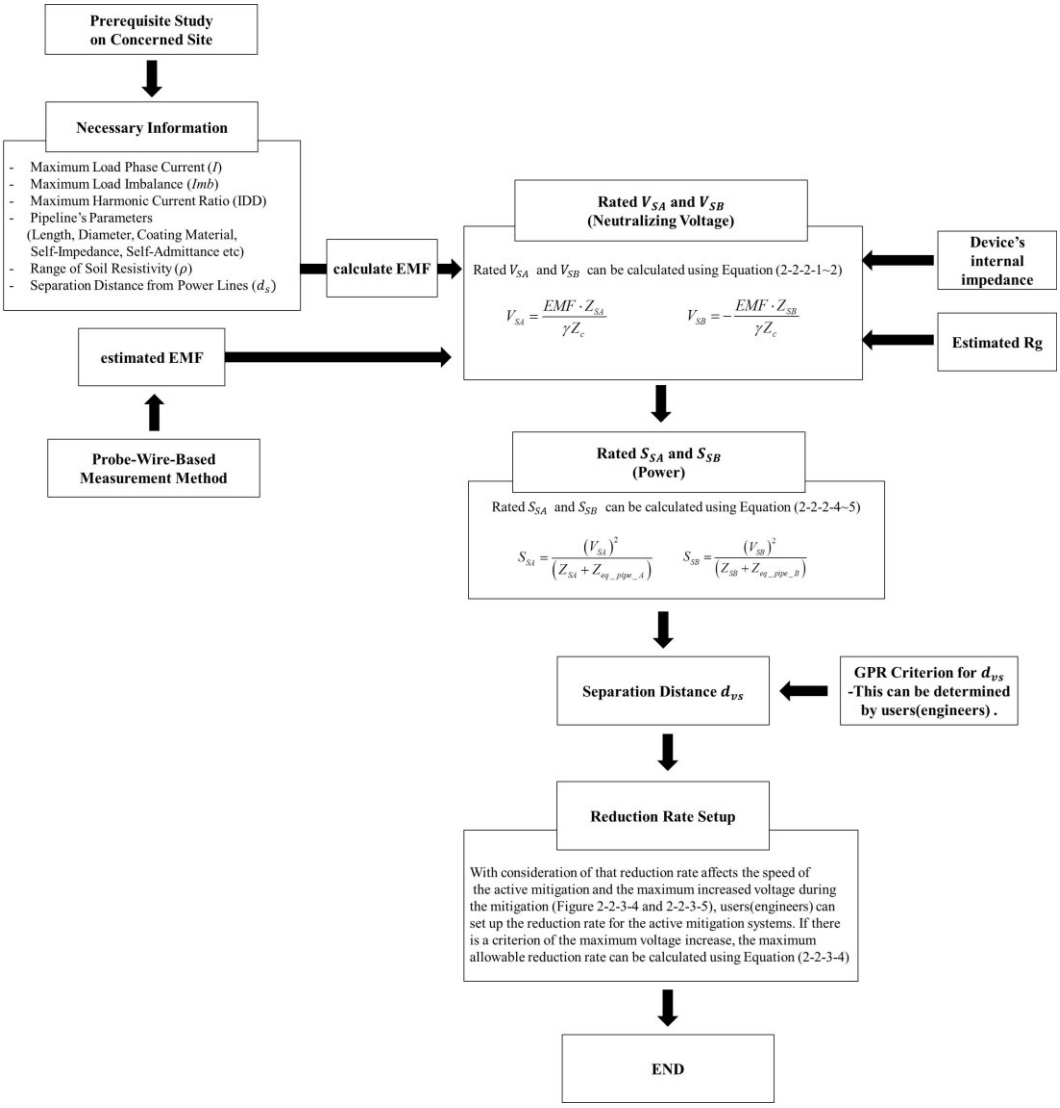

Figure 5-1: Flow chart for the determination of design specification for the proposed active mitigation system

Each device in the proposed active mitigation system will be newly designed. In this chapter we will discuss the individual design specifications of the devices, based on the case study in Section 2.2.6. This chapter can be referred to in order decide how each device should be designed (what functions it should perform) and the specific numerical design parameters required in a specific case (the case study in Section 2.2.6).

The following Table 5-1 again summarizes the major parameters of the case study in Section 2.2.6. Information on the other parameters is available in Appendix G.

Three major harmonic components (1^{st}, 3^{rd}, and 9^{th}) are considered for currents in overhead AC power lines in order to simplify the case. Those harmonic data are based on the average harmonic sequence data from the field measurement in Reference [9].

Table 5-1: Major parameters of the case study of section 2.2.6

Separation distance d_s	20 [m]
Parallel Length L	10 [km]
Soil resistivity ρ	100 [Ωm]
Zero Sequence Current I_0 at H=1	12.68 [A,RMS]
Zero Sequence Current I_0 at H=3	20.45 [A,RMS]
Zero Sequence Current I_0 at H=9	4.68 [A,RMS]
Induced V_A at H=1	32.6 [V,RMS]
Induced V_A at H=3	113.6 [V,RMS]
Induced V_A at H=9	36.7 [V,RMS]

The following Figure 5-2 describes the block diagram of one active mitigation system at one (left) terminal of a buried pipeline.

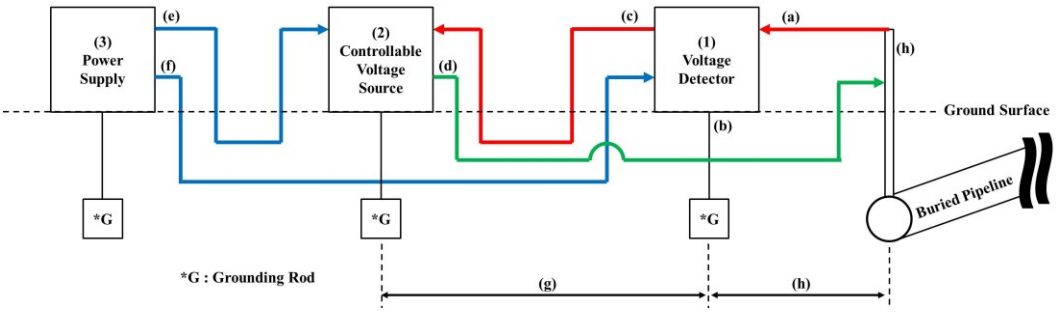

Figure 5-2: Block diagram of the proposed active mitigation system

Since the design specification of the two active mitigation systems for the two terminals is the same, we will discuss only one (left) active mitigation system in this chapter.

5.1 Design Specification of Voltage Detector

As discussed earlier, in the proposed active mitigation system a voltage detector plays a role in obtaining information about a pipeline's terminal voltage. The following block diagram describes the required functions of the voltage detector.

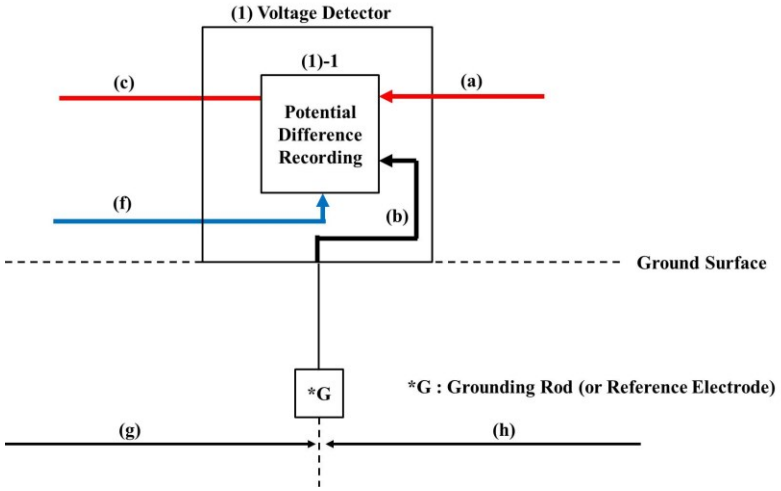

Figure 5-1-1: Block diagram of voltage detector (1)

(a): Potential at one (left) terminal of a buried pipeline

(b): Reference potential at the reference electrode of the voltage detector (1)

(c): Potential difference between (a) and (b) (corresponding to the terminal voltage information)

(f): Sufficient power from the power supply (3)

The potential difference (c) between the potential at one terminal of the pipeline (a) and the reference potential at the reference electrode of the voltage detector (b) is first recorded as the waveform by the voltage detector (1). This potential difference (c) is provided to the controllable voltage source (2). The sampling rate of the voltage detector is 256 per second to ensure accurate detection.

In order to avoid GPR interference on the reference potential (b) of the voltage detector (1), the minimum separation distance d_{vs} (g) from the grounding point of the controllable voltage source must be secured (2).

The voltage detector can be installed at a few meters' (1~2m) distance from the pipeline.

The grounding rod can be a 3m long and 16mm wide (diameter) single rod.

5.2 Design Specification of Controllable Voltage Source

The controllable voltage source (2) in the proposed active mitigation system will be a power electronic-based device. The controllable voltage source (2) should be developed to generate the required voltage waveform using feedback control.

The functions of the controllable voltage source (2) in Figure 5-2 are described in the following block diagram.

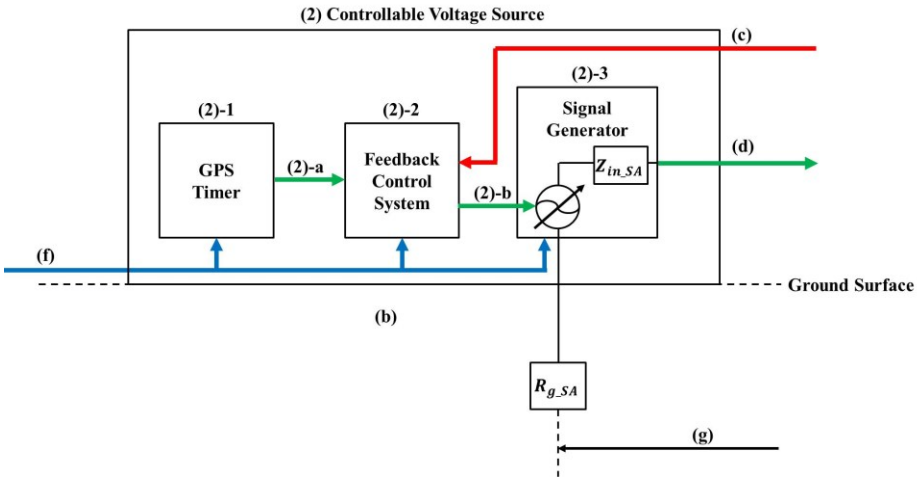

Figure 5-2-1: Block diagram of the controllable voltage source (2)

(c): Potential difference one terminal (a) and the reference potential (b) of the voltage detector (1) (corresponding to the terminal voltage information)

(d): Actual voltage waveform of required neutralizing voltage

(2)-a: Operation signal for the alternative adjustment of neutralizing voltage

(2)-b: Information of magnitude and phase angle of required neutralizing voltage

5.2.1 Required Functions

(2)-1 GPS Timer: The GPS timer sends an automatic signal to trigger its feedback control according to the pre-set time interval T. If the GPS timer for the left device sends signals at $2kT$ (k is integral) instants, the one for the right device sends signals at $(2k+1)T$ instants. The time interval T should be set, e.g. to 1 or 5 minutes, to ensure the implementation of the one-step adjustment that is determined by the feedback control.

(2)-2 Feedback Control System: The function of the feedback control system (2)-2 is to determine the neutralizing voltage waveform based on the terminal voltage information (c) and pre-set voltage reduction rate.

(2)-3 Signal Generator: The signal generator (2)-3 generates the actual voltage waveform of the neutralizing voltage required. This signal generator has an internal impedance of Z_{in_SA} and is grounded by the resistor R_{g_SA}, which indicates the equivalent value of the grounding system. (2). As high GPR may occur at the grounding point of the controllable voltage source (2), the grounding system (2) should be designed to avoid risk to personnel safety caused by high GPR. The design of the grounding system of the controllable voltage source (2) will be further discussed in the next section.

The controllable voltage source (2) needs to be designed with the smallest Z_{in_SA} and R_{g_SA} possible. The recommended values for Z_{in_SA} and R_{g_SA} of the case study in Section 2.2.6 are

Z_{in_SA}	$\leq 5 + j5\ \Omega$
R_{g_SA}	$\leq 5\ \Omega$

In the case study of Section 2.2.6, the rated V_{SA} (maximum magnitude) is as follows.

Rated (maximum) V_{SA}	609.4V
Rated S_{SA}	14.9kVA

5.2.2 Grounding System of Controllable Voltage Source

As discussed earlier, the grounding system of the controllable voltage source (2) should be designed to avoid personnel safety issues caused by high GPR when the active mitigation system is operated.

According to Reference [14]-IEEE Std-80-2000, the average let-go currents for women and men are defined as 10.5mA and 16mA respectively. With consideration of human body resistance R_B of $1000\,\Omega$ and the average let-go current for women of 10.5mA, it is possible to consider the following criterion for the step and touch voltage in a steady-state [11]

$$\text{Criterion for } E_{step} = 16.8V \tag{5-2-2-1}$$

$$\text{Criterion for } E_{touch} = 12.075V \tag{5-2-2-2}$$

In addition, Reference [11]-IEEE Std-142-2007 presents how to design a grounding system in order to meet certain criteria for step and touch voltage. Therefore, the grounding system of the controllable voltage source (2) should be designed according to Reference [11] in order to meet the above criteria (5-2-2-1) and (5-2-2-2) for personnel safety.

For public safety, a safety fence needs to be installed around the grounding grid of the controllable voltage source (2) in order to ban unauthorized access. In the case study of Section 2.2.6, the step voltage within 7m from the grounding point of the controllable voltage source (2) exceeds the above step voltage criterion of 16.8V. After 7m, the step voltage is below the criterion of 16.8V. Therefore, for public safety, a safety fence sized 6m x 6m should be installed around the controllable voltage source (2).

Safety Fence (around the Grounding Point of the Controllable Voltage Source (2))	6m x 6m

5.2.3 Separation Distance d_{vs} for GPR interference caused by Controllable Voltage Source

In the case study of Section 2.2.6, the calculated total grounding current I_g of the controllable voltage source (2) is

Total I_g	36.4 [A,RMS]

This total I_g corresponds to the mesh current I_1 in Figure 2-3-2-2. Based on the total I_g, the minimum separation distance d_{vs} between the voltage detector (1) and the grounding point of the controllable voltage source (2) is

Minimum d_{vs}	47 [m]

5.3 Design Specification of Power Supply

As mentioned earlier, the power supply (3) plays a role in providing sufficient power to the proposed active mitigation system. The major portion of the required power is total delivered power to the buried pipeline through the applied neutralizing voltage. In the case study of Section 2.2.6, the rated (maximum required) power for one (left) active mitigation system is 14.9 kVA. Considering 75% load factor, the power supply can be rated at 20kVA.

Rated $S_{SA.S}$	20kVA

5.4 Summary of Design Specification for Case Study

The following Figure 5-4-1 shows the overall arrangement of the left active mitigation system in the case study of Section 2.2.6.

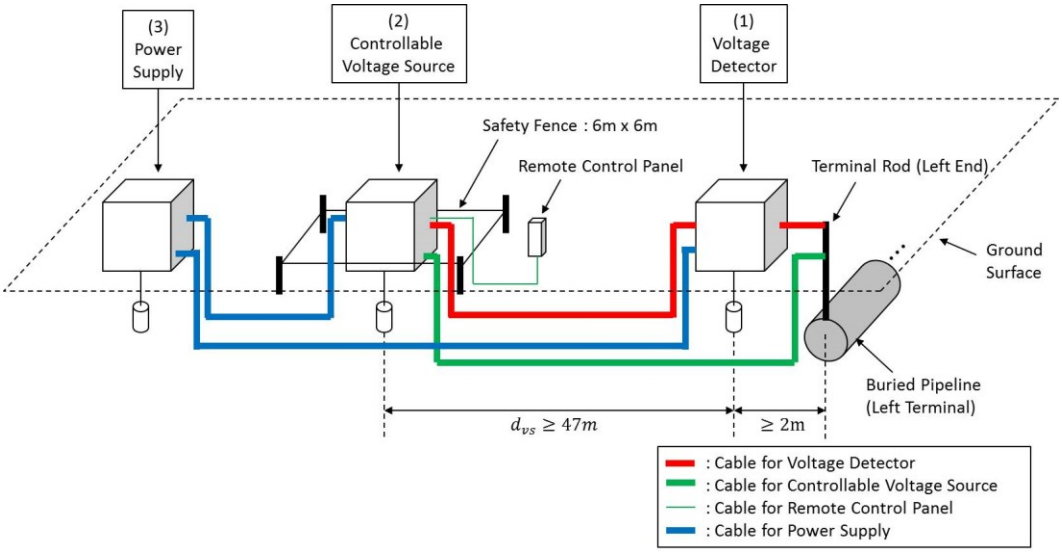

Figure 5-4-1: The overall arrangement of the left active mitigation system in the case study of Section 2.2.6

Each device ((1) ~ (3)) in Figure 5-4-1 should have the required functions specified in the above sections and follow the numerical design specifications.

Table 5-4-1: Summary of Design Specifications of Case Study

(1) Voltage Detector

Minimum d_{vs}	47 m

(2) Controllable Voltage Source

Z_{in_SA}	$\leq 5 + j5\ \Omega$
R_{g_SA}	$\leq 5\ \Omega$
Rated V_{SA}	609.4.1V
Rated S_{SA}	14.9kVA
Total I_g	36.4A
Safety Fence	6m x 6m

(3) Power Supply

Rated $S_{SA.S}$	20kVA

Chapter 6

Conclusion and Future Work

6.1 Contribution of This Thesis

This thesis proposed a new mitigation method for induced voltage on buried pipelines, the so-called active mitigation method. The proposed active mitigation method is to apply two proper neutralizing voltage sources onto two terminals of a buried pipeline. Those two proper neutralizing voltage sources play a role in canceling induced voltage on the buried pipeline. Each active mitigation source comprises a voltage detector, a controllable voltage source, and a power supply. The feedback control system is embedded in the controllable voltage source, to deal with variable induced voltage on the buried pipeline.

This thesis provided analytical equations for the calculation of the voltage and power ratings for the active device and also presented solutions to practical construction issues. Thus, a real pipeline induction mitigation system can easily be built based on the above mentioned development.

Through sensitivity studies, this thesis provided the practical ranges of the major design parameters of the proposed active mitigation system. In addition, this thesis presented sample design specifications for the proposed active mitigation system based on one case study. This will help engineers to design actual devices in the proposed active mitigation system.

This thesis also presented a probe-wire-based method to estimate the EMF that can be utilized for the calculation of the rated voltage and power of the active mitigation device.

6.2 Future Work

Below are some suggestions for further research.

This thesis does not consider CP devices installed on buried pipelines. In practice, we may need to consider already installed CP devices on buried pipelines for DC corrosion prevention. The effect of existing CP devices on the proposed active mitigation system may be a topic for further research.

This thesis assumes that the pipeline is parallel with the power line, and that soil resistivity is uniform. Therefore, only two terminal voltage sources are required along the pipeline. If the pipeline runs through very different soil conditions, more active sources are needed and more complicated coordination is required. This may be a topic further research.

Lastly, this thesis does not deal with hardware design. Consequently, how to achieve the optimized design of the required controller may also be a topic for further research.

References

[1] CIGRE Working Group 36.02 Guide, "Guide on the influence of high voltage AC power systems on metallic pipelines," 1995

[2] W.Xu, J.Yong, B.Xia "Inductive coordination of distribution power line and pipeline," APIC Project 2014A-2

[3] CEOCOR, "A.C. Corrosion on cathodically protected pipelines-guidelines for risk assessment and mitigation measures" 2001

[4] E.W. McAllister, Editor "Pipeline rules of thumb handbook: Quick and accurate solutions to your everyday pipeline problems," 5th Edition, Gulf Professional Publishing

[5] W.Xu, J.Yong, B.Xia "Voltage induction on pipeline caused by power line harmonic current," APIC Project 2015

[6] EPRI Document EL-904, "Mutual design considerations for overhead AC transmission lines and gas transmission pipelines," 1978

[7] "Directives concerning the protection of telecommunication lines against harmful effects from electricity lines," International Telegraph and Telephone Consultative Committee (CCITT), International Telecommunications Union, 1962

[8] Dezhi Tang, Yanxia Du, Minxu Lu, Shaosong Chen, Zitao Jiang, Liang Dong "Study on location of reference electrode for measurement of induced alternating current voltage on pipeline," Int. Trans. Electr. Energ. Syst. 2015; 25; 99-119

[9] W.Xu, J.Yong, "Harmonic characteristics in distribution systems supplying residential loads," APIC Project 2015

[10] W.Xu, Hesam Yazdanpanahi, Fernanda Caseño Lima Trindade "Harmonic distortion levels measured at the Enmax substations – 2012," APIC Project 14

[11] IEEE "IEEE Recommended practice for grounding industrial and commercial power systems," IEEE Std 142-2007

[12] Alireza Bahaori “Cathodic corrosion protection systems : A guide for oil and gas industries,” ISBN: 978-0-12-800274-2

[13] J. Dabkowski, A. Taflove “Mutual design considerations for overhead AC transmission lines and gas transmission pipelines Volume 2 : Prediction and mitigation procedures,” Electric Power Research Institute

[14] IEEE “IEEE Guide for safety in AC substation grounding,” IEEE Std 80-2000

[15] Suad I. Shahl “Electromagnetic interference caused by Iraqi 400kV transmission lines on buried oil pipelines,” Eng & Tech Journal, Vol. 28, No.24, 2010

[16] Rukmangad V. Kondamgire “AC interference effect on NG pipeline and its mitigation techniques,” IOGPC2015-7935, ASME 2015 India Oil and Gas Pipeline Conference

[17] Eskom “Guideline on the electrical co-ordination of pipelines and power lines” 240-66418968

[18] F. P. Dawalibi, W. Vukonich “Recent advance in the mitigation of AC voltages occurring in pipelines located close to electric transmission lines,” IEEE Transaction on Power Delivery, Vol. 9, No. 2, April 1994

[19] Dezhi Tang, Minxu Lu, Yanxia Du, Jiawei Gao, Guangchun Wu “Electrochemical studies on the performance of zinc used for alternating current mitigation,” Corrosion-Houston Tx, March 2015

[20] James Michel “Ampacity characteristics of zinc ribbon,” Paper No. 05621 Corrosion 2005

[21] J. Ma, F. P. Dawalibi, R. D. Southey “Computation and measurement of electrical interference effects in aqueducts due to a nearby parallel transmission line” IEEE 10.1109/ELMAGC. 1997.617176

[22] N. Kioupis, N. Kouloumbi, G. Batis, P. Asteridis “Study of the effect of AC-interference and AC-mitigation on the cathodic protection of a gas pipeline” Conference Paper, May 2003

[23] J.R. Carson, “Wave propagation in overhead wires with ground return,” Bell Syst. Tech. J., vol.5, 99.539-554, 1926

[24] F.Pollaczek, “Uber das feld einer unendlich langen wechselstrom durchlossenen einfachleitung,” E.N.T., vol 3, no. 9, pp.339-359, 1926

[25] Ametani, A.; Miyamoto, Y.; Baba, Y.; Nagaoka, N., “Wave propagation on an overhead multiconductor in a high-frequency region,” *Electromagnetic Compatibility, IEEE Transactions on*, vol.56, no.6, pp.1638,1648, Dec.2014

[26] Electric Power Research Institute “Transmission line reference book 345kV and above,” Second Edition

[27] E.D.Sunde, “Earth conduction effects in transmission systems,” New York: Dover Publications, 1968,pp.14-16 and pp.146-149

[28] H.W.Dommel, “EMTP theory book second edition” May,1992

[29] IEEE “IEEE recommended practice for inductive coordination of electric supply and communication lines,” IEEE Std 776-1992

[30] Grazia Todeschini, David R. Mueller, Greg Young Morris “Telephone interference caused by harmonics distribution systems : Analysis and simulations,” IEEE ISBN 978-1-4799-1303-9

[31] Ernst SCHMAUTZER, René Braunstein, Mario OELZ “Simulation and optimized reduction of induced pipeline voltages caused by High-Voltage lines on inductively interfered pipelines,” CIRED 21th International Conference on Electricity Distribution

[32] NACE “Standard recommended practice : Mitigation of Alternating Current and lightning effects on metallic structures and corrosion control systems,” NACE Standard RP0177-2000

[33] W. Kent Muhlbauer “Pipeline risk management manual : Ideas, techniques, and resources,” ELSEVIER

[34] F.P. Dawalibi, Y. Li, J. Ma “Safety of pipelines in close proximity to electric transmission lines,” 2000 IEEE IAS

[35] Fabio Freschi, Massimo Mitolo, Michele Tartaglia “Effective semianalytical method for simulating grounding grids,” IEEE Transactions VOL. 49, NO.1

[36] Swapnil. G. Shah, Nitin. R. Bhasme P.G “Design of earthing system for HV/EHV AC substation” IJAET ISSN: 22311963

[37] AllenTaflove, Michael Genge, John Dabkowski “Mitigation of buried pipeline voltages due to 60Hz AC inductive coupling : Part I – Design of joint rights-of-way,” IEEE Transaction Vol.PAS-98

[38] E. Sawma, B.Zeitoun, N. Harmouche, S. Georges, M. Hamad, F.H. Slaoui “Electromagnetic induction in pipeline due to overhead high voltage power lines,” 2010 International Conference on Power System Technology

[39] M’Hamed Ouadah, Mourad Zergoug, “Analysis and mitigation of the interference between high voltage power line and buried pipelines,” Conference Internationale des Energies Renouvelables (CIER’13) Sousse, Tunisie-2013

[40] Dejan Markovic, Vic Smith, Sarath Perera “Evaluation of gradient control wire and insulating joints as methods of mitigating induced voltages in gas pipelines,” Australasian Universities Power Engineering Conference 2005

Appendix

Appendix A. Field Measurement using the Probe-Wire-Based Measurement Method

This section presents some field measurement data using the probe-wire-based method presented in Chapter 4.

A-1. Setup of Field Measurement using the Probe-Wire-Based Measurement Method

The following Figure A-1-1 and A-1-2 show the setup of the field measurement. A 30m probe wire runs in parallel to a transmission line with the separation distance of 50m roughly. The voltage meter is used to measure the voltage difference between two terminals of the probe wire which are grounded by two grounding rods. Each measurement is conducted for 15 minutes.

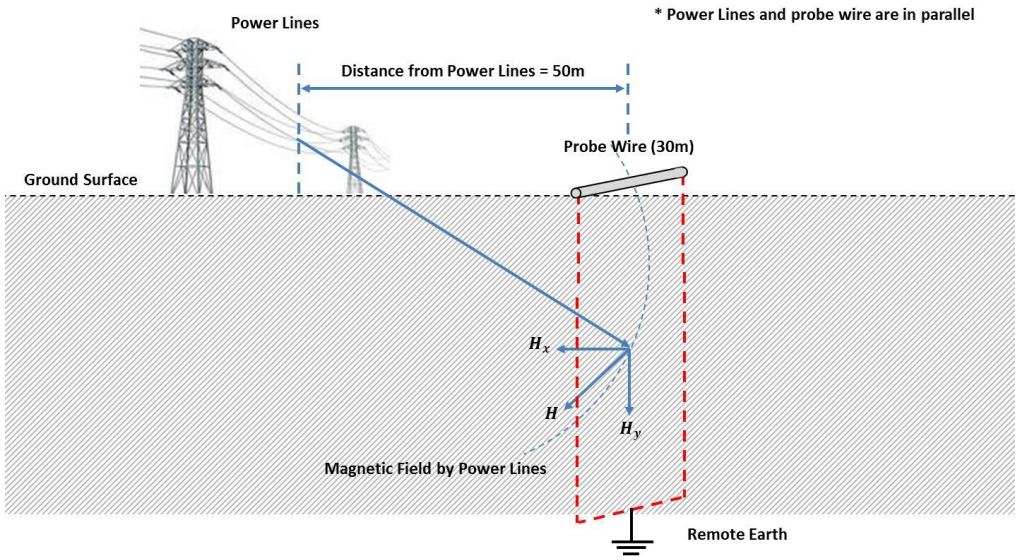

Figure A-1-1: Probe-wire-based measurement method to measure induced voltage caused by near transmission lines.

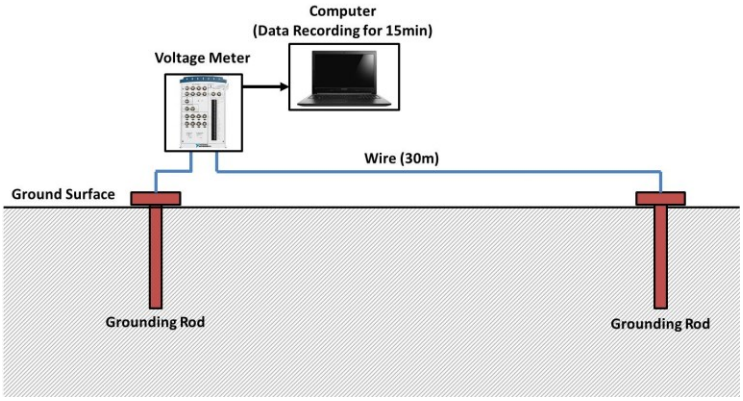

Figure A-1-2: Two grounding locations for induced voltage measurement.

A-2. Field Measurement Summary and Analysis

The following Figure A-2-1 shows 6 cycles induced voltage waveform of one field measurement near 138kV transmission line as an example. Figure A-2-2 and A-2-3 show the average induced harmonic voltage magnitude and percentage of RMS value, respectively. The results show that the 3rd order harmonic voltage is relatively high. For 138 kV #1, #3, #5, #6 measurement cases, the 3rd order harmonic voltage dominates with more than 80% of total RMS value. Especially the 138kV #6 measurement case shows relatively high total induced voltage compared to other measurement data. With consideration of the percentage of RMS of induced harmonic voltage, we can see that statistically the 1st , 3rd , 9th harmonic components would be major components in induced voltage caused by transmission lines.

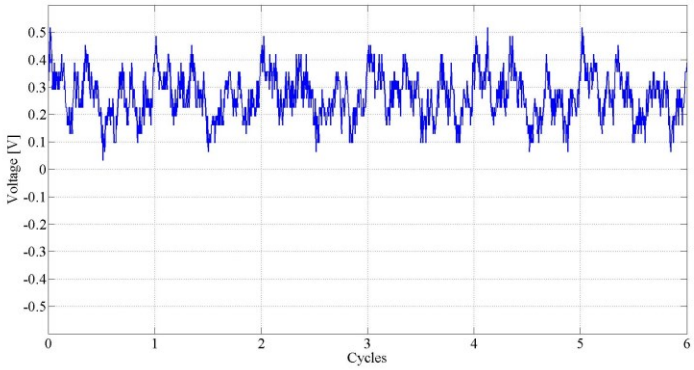

Figure A-2-1: Sample induced voltage waveform of field measurement near 138 kV transmission line.

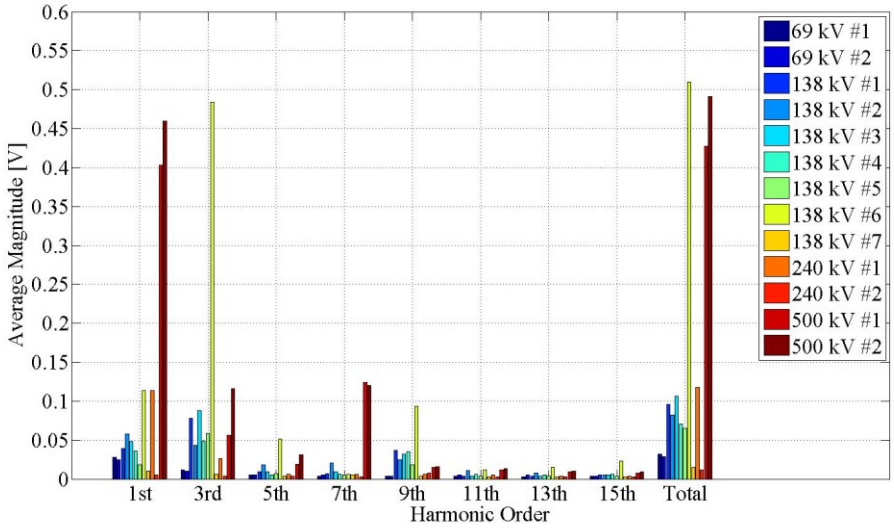

Figure A-2-2: The average induced harmonic voltage magnitudes of each field measurement.

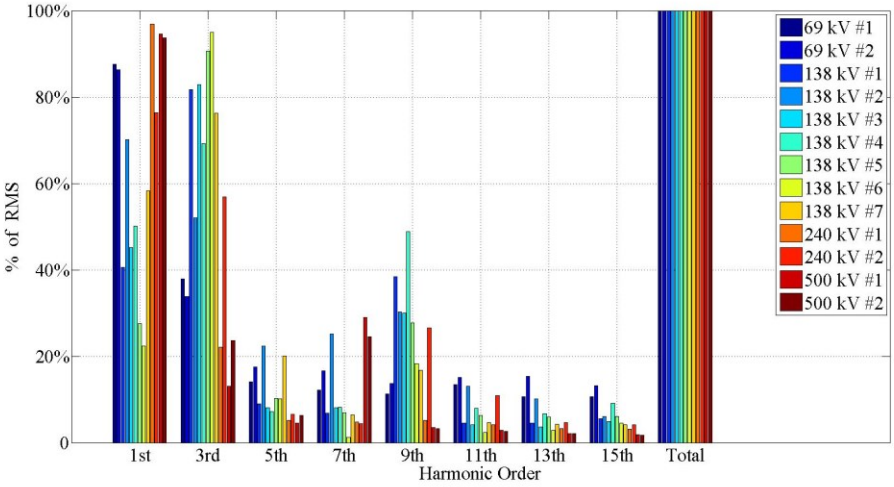

Figure A-2-3: The normalized induced harmonic voltage of each field measurement.

The following Table A-2-1 shows the detail data of each field measurement case.

Table A-2-1 Summary of induced fundamental and harmonic voltage on the probe wire of each field measurement.

1 – 69kV Case #1									
H	1st	3rd	5th	7th	9th	11th	13th	15th	RMS
Mag [V]	0.0283	0.0123	0.0046	0.004	0.0037	0.0043	0.0034	0.0035	0.0323
% of RMS	87.6	38.1	14.2	12.4	11.5	13.3	10.5	10.8	100

2 – 69kV Case #2									
H	1st	3rd	5th	7th	9th	11th	13th	15th	RMS
Mag [V]	0.0254	0.0099	0.0052	0.0049	0.004	0.0045	0.0045	0.0039	0.0294
% of RMS	86.4	33.7	17.7	16.7	13.6	15.3	15.3	13.3	100

3 – 138kV Case #1									
H	1st	3rd	5th	7th	9th	11th	13th	15th	RMS
Mag [V]	0.0388	0.0781	0.0086	0.0065	0.0367	0.0043	0.0043	0.0053	0.0955
% of RMS	40.6	81.8	9.0	6.8	38.4	4.5	4.5	5.5	100

4 – 138kV Case #2									
H	1st	3rd	5th	7th	9th	11th	13th	15th	RMS
Mag [V]	0.0577	0.0429	0.0184	0.0208	0.0249	0.0108	0.0083	0.005	0.0823
% of RMS	70.1	52.1	22.4	25.3	30.3	13.1	10.1	6.1	100

5 – 138kV Case #3									
H	1st	3rd	5th	7th	9th	11th	13th	15th	RMS
Mag [V]	0.0481	0.0883	0.0086	0.0087	0.0319	0.0045	0.0038	0.0052	0.1065
% of RMS	45.2	82.9	8.1	8.1	30.0	4.2	3.6	4.9	100

6 – 138kV Case #4									
H	1st	3rd	5th	7th	9th	11th	13th	15th	RMS
Mag [V]	0.0357	0.0493	0.0051	0.0058	0.0349	0.0056	0.0048	0.0065	0.0713
% of RMS	50.1	69.2	7.2	8.2	48.9	7.9	6.7	9.1	100

7 – 138kV Case #5									
H	1st	3rd	5th	7th	9th	11th	13th	15th	RMS
Mag [V]	0.0178	0.0586	0.0066	0.0045	0.0179	0.0041	0.0038	0.0038	0.0646
% of RMS	27.6	90.6	10.3	7.0	27.7	6.3	5.9	6.0	100

8 – 138kV Case #6									
H	1st	3rd	5th	7th	9th	11th	13th	15th	RMS
Mag [V]	0.1140	0.4844	0.0515	0.0061	0.0935	0.0125	0.0150	0.0231	0.5099
% of RMS	22.4	95.0	10.1	1.2	18.3	2.4	2.9	4.5	100

9 – 138kV Case #7									
H	1st	3rd	5th	7th	9th	11th	13th	15th	RMS
Mag [V]	0.0514	0.0674	0.0178	0.0056	0.0148	0.0041	0.0038	0.0037	0.0883
% of RMS	58.3	76.3	20.1	6.4	16.7	4.7	4.3	4.2	100

10 – 240kV Case #1									
H	1st	3rd	5th	7th	9th	11th	13th	15th	RMS
Mag [V]	0.114	0.026	0.006	0.0056	0.006	0.0049	0.0039	0.0036	0.1177
% of RMS	96.9	22.1	5.1	4.8	5.1	4.2	3.3	3.1	100

11 – 240kV Case #2									
H	1st	3rd	5th	7th	9th	11th	13th	15th	RMS
Mag [V]	0.1008	0.0751	0.0087	0.0058	0.0351	0.0143	0.0060	0.0055	0.1319
% of RMS	76.4	56.9	6.6	4.4	26.6	10.9	4.6	4.2	100

12 – 500kV Case #1									
H	1st	3rd	5th	7th	9th	11th	13th	15th	RMS
Mag [V]	0.4032	0.0559	0.0193	0.1239	0.0151	0.0124	0.0092	0.0078	0.4265
% of RMS	94.5	13.1	4.5	29.1	3.5	2.9	2.2	1.8	100

13 – 500kV Case #2									
H	1st	3rd	5th	7th	9th	11th	13th	15th	RMS
Mag [V]	0.4598	0.1159	0.0311	0.1201	0.0158	0.0127	0.0104	0.0086	0.4907
% of RMS	93.7	23.6	6.3	24.5	3.2	2.6	2.1	1.8	100

Appendix B. Gradient-Control-Wire Method

The most widely used mitigation method for AC induced voltage on pipelines is Gradient-Control-Wire method [15]. Gradient control wires consist of one or two zinc wires buried in parallel with buried pipeline with regular electrical connections to the pipeline [16]. They comprise discrete sections of up to (but not exceeding) 400m in length [17]. The ends of successive sections shall not be in direct contact [17].

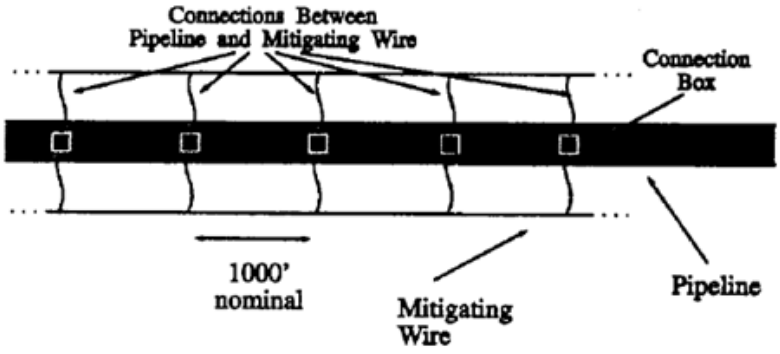

Figure B-1: Typical gradient control wire installation: plan view [18]

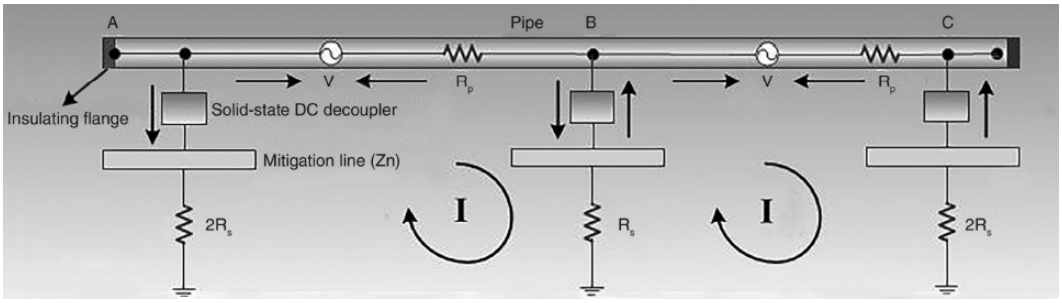

Figure B-2: Description of the service behavior of zinc ribbon used as mitigation wire [19]

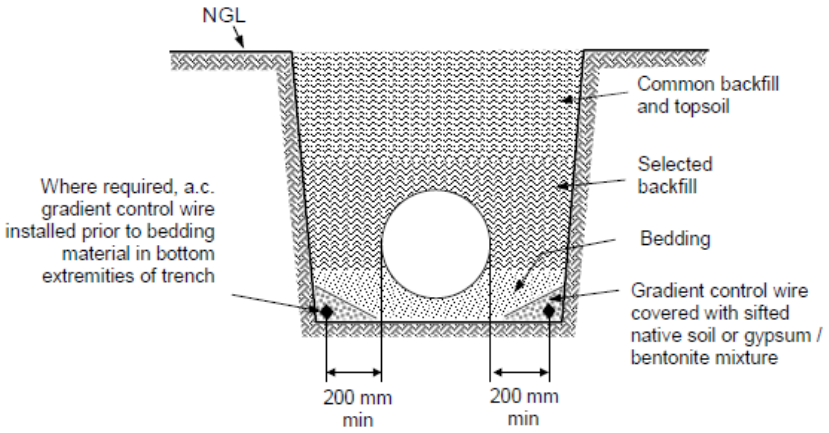

Figure B-3: Installation of gradient control wire in trench [17]

The effects of gradient control wires can be summarized as follows.

1- **Grounding Effect**: Gradient control wires provide grounding to protecting structure in relation to inductive interference. Since the grounding resistance of zinc ribbons, which are regularly connected to the pipeline, is lower than the high leakage resistance of coating material of the pipeline, induced current of the pipeline can flow and be distributed into the soil [19]. Therefore, induced voltage on the pipeline can be reduced due to the additional grounding effect by the zinc ribbons. It is important to consider the soil structure of the earth for the design of a gradient control wire system [20].
2- **GPR effect**: They also raise potential of local earth and reducing touch and coating stress voltage [16]. Since GPR caused by gradient control wires brings the reduced potential difference between the pipeline and the soil, touch and step voltage can be reduced.
3- **Cathodic Protection**: Gradient control wires can be made from zinc, magnesium, or copper [16]. If gradient control wires are made of Zinc, they behave like extensive sacrificial anode and can provide cathodic protection for considerable lengths of the pipeline to which they are connected [18].

Most of the work on AC mitigation is concentrated on the optimization of the location and the length of zinc ribbon, the direction of connections, and the selection of a DC decoupler [19]. Designing safe and cost-efficient gradient control wire systems requires computer modeling of these conductor systems in the soil structures obtained from detailed measurements at these locations [18]. Finite Element Method based software such as CDEGS and ANSIS software package are typically used for the analysis.

The following Figure B-4 shows one sample case using the gradient-control-wire method based on the analysis by CDEGS [21]. Three pipelines are influenced by nearby 500kV overhead power lines and 6 gradient control wires (2 wires per one pipeline) were installed along the parallel route of about 2.316km.

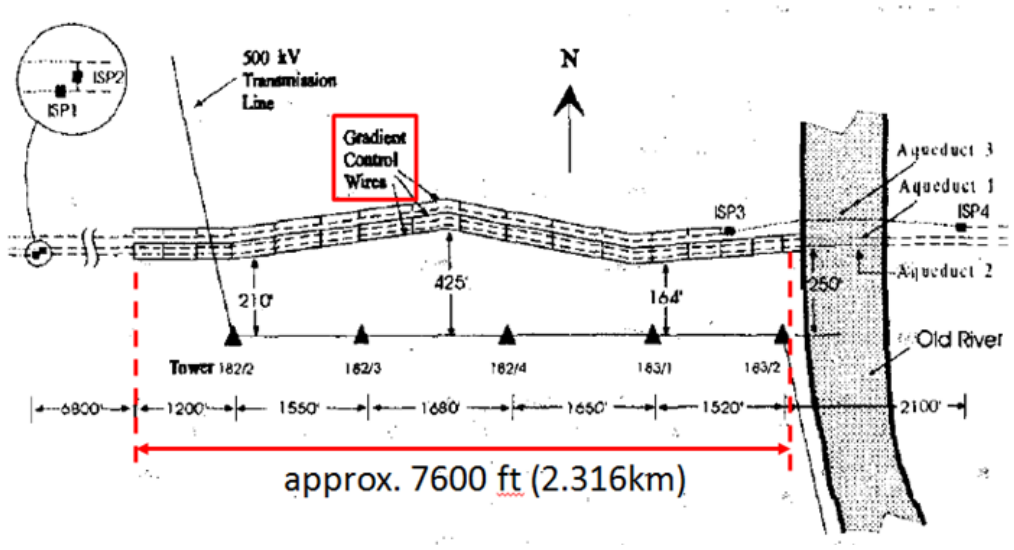

Figure B-4: Plan view of the transmission line and aqueduct configuration [21]

Maximum induced voltage at a steady-state condition is 73V and the maximum voltage with mitigation is 16V as follows [21].

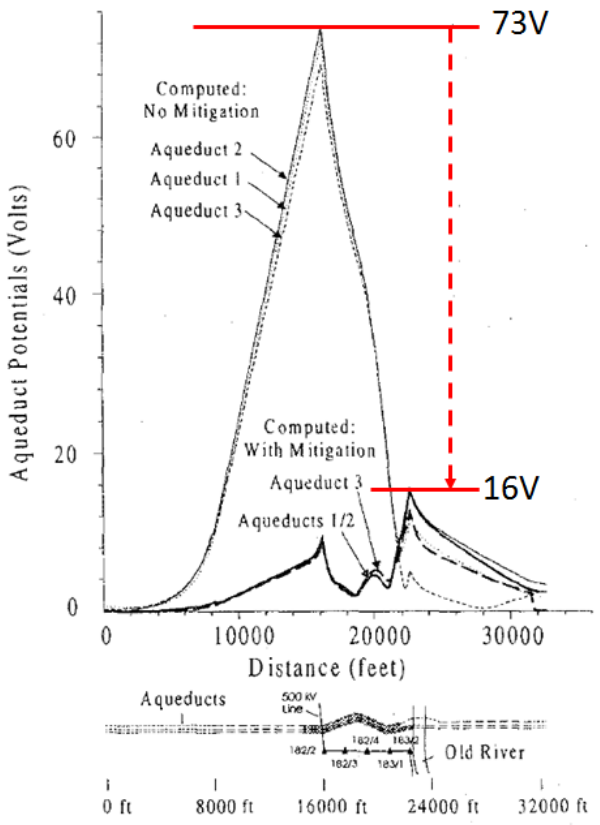

Figure B-5: Computed aqueduct potentials due to inductive interference during steady state conditions [21]

For simple analysis without commercial software, one discrete zinc ribbon is considered as one lumped grounding resistance connected to the pipeline in this section. The lumped grounding resistance of one discrete zinc ribbon is determined by its length, diameter, buried depth, and soil resistivity. The dissipation resistance R_g of the gradient control wire is given by the following equation [22].

$$R_g = \frac{\rho}{2\pi l} \ln\left(\frac{l^2}{sd}\right) \tag{B-1}$$

where,

ρ : soil resistivity [Ωm]

l : length of the ribbon [m]

s : burial depth [m]

d : average thickness or diameter [m]

In Equation (B-1), the self-resistance of the wires is ignored and this limits its application to lengths to approximately 500m [17].

Installation of gradient control wires depends on specific site conditions and its cost effect so there is no absolute design for installation of gradient control wires. Depending on specific pipelines' conditions, gradient control wires may be installed only at the severest locations such as two terminals of buried pipeline or installed along long route.

In order to figure out rough mitigation effect using gradient control wires and compare it with the proposed active mitigation method, three simple cases for the gradient-control-wire method are assumed based on the case study in Section 2.2.6. The following Figure B-6 and Table B-1 compare the proposed active mitigation method and the gradient-control-wire method.

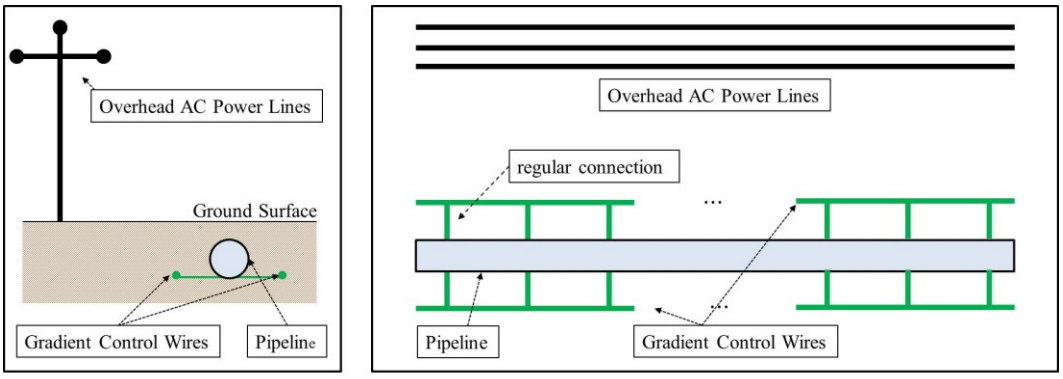

Scheme of gradient-control-wire method

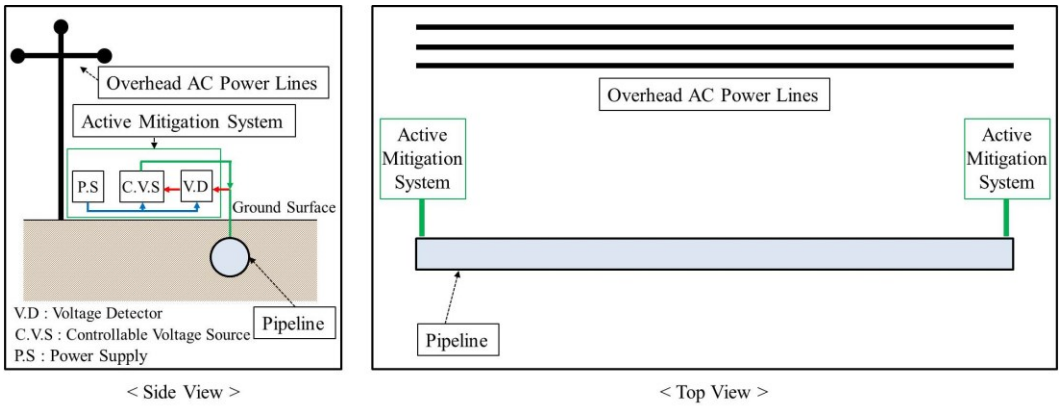

Scheme of proposed active mitigation method

Figure B-6: Scheme comparison between proposed active mitigation method and gradient-control wire method

Table B-1: Mitigation effect comparison between the proposed active mitigation method and gradient-control-wire method

	Before mitigation [V, RMS]	After mitigation [V, RMS]	Installation Location
Proposed active mitigation method	52.8	≤ 10	Two terminals
Gradient-control-wire method	52.8	12.1 (Case 1) 10.8 (Case 2) 10.6 (Case 3)	1km long (Case 1) 2km long(Case 2) 5km long(Case 3)

* Case 1: double zinc ribbon, 500m installation from each terminal of the pipeline (Total installation length: 1km)

* Case 2: double zinc ribbon, 1km installation from each terminal of the pipeline (Total installation length: 2km)

* Case 3: double zinc ribbon, installation along the whole pipeline (Total installation length: 5km)

Parameters' information about the above comparison are as follows.

Pipeline

Length of parallel route L	5 [km]
Maximum induced voltage	52.8 [V, RMS]

*Other parameters are based on the case study in Section 2.2.6.

Gradient control wires (zinc ribbon)

Length of one discrete zinc ribbon	250 [m]
Burial depth	2 [m]
Diameter	0.0127 [m]
Soil resistivity	100 [Ωm]
Grounding resistance of one discrete zinc ribbon	0.9368 [Ω]
Installation Case 1	Two discrete double zinc ribbons from two terminals (500m installation from each terminal)
Installation Case 2	Four discrete double zinc ribbons from two terminals (1km installation from each terminal)
Installation Case 3	Full installation along the pipeline with double zinc ribbon (5km installation)

Appendix C. Calculation of EMF

C-1. EMF at the Fundamental Frequency

Induced EMF on a buried pipeline by one nearby power line can be expressed as follows.

$$EMF = Z_m \cdot I \tag{C-1-1}$$

where,

Z_m : mutual impedance between the buried pipeline and the nearby power line.

I : current in the nearby power line.

If a buried pipeline is in parallel to one overhead three-phase AC power line, the total induced EMF on the buried pipeline will be

$$Total\ EMF = Z_{mA} \cdot I_A + Z_{mB} \cdot I_B + Z_{mC} \cdot I_C \tag{C-1-2}$$

The widely used methods to calculate the mutual impedance Z_m between two earth-return conductors in parallel are following two equations by Pollaczek and Carson [23][24].

$$Z_{m\_Pollaczek} = \frac{\rho m^2}{2\pi} \int_{-\infty}^{\infty} \frac{\exp(-h|\alpha| + h_p\sqrt{\alpha^2 + m^2}}{|\alpha| + \sqrt{\alpha^2 + m^2}} \exp(j\alpha x) d\alpha \tag{C-1-3}$$

where,

$$m = \sqrt{\frac{j\omega\mu_0}{\rho}}$$

$$Z_{m\_Carson} = \frac{\mu_0\omega}{\pi} \int_{-\infty}^{\infty} \left(\sqrt{\alpha^2 + j} - \alpha\right) e^{\left(-(h-h_p)\sqrt{\frac{\mu_0\omega}{\rho}}\alpha\right)} \cos\left(\sqrt{\frac{\mu_0\omega}{\rho}}\alpha\right) d\alpha \tag{C-1-4}$$

where,

$\mu_0 = 4\pi \times 10^{-7}$[H/m]

$\omega = 2\pi f$

ρ = soil resistivity [Ωm]

h = height of overhead conductor [m]

h_p = depth of buried conductor [m]

x = horizontal distance between overhead conductor and buried conductor

According to Reference [7], the above Carson's equation can be simplified by replacing $y\sqrt{\alpha^2 + m^2}$ with $y|\alpha|$ so Carson and Pollaczek's equations are basically same [25].

The above equations of Z_m are precise but they are too complex to use. For a simpler and easier calculation, several industrial guides recommend the following Carson-Clem equation which is the approximation form of the equations of Carson and Pollaczek [1][6][7].

$$Z_m = \frac{\pi \mu_0 f}{4} + j\mu_0 f \left[\ln\left(\frac{2}{gd\sqrt{\frac{\omega\mu_0}{\rho}}} \right) + \frac{1}{2} \right] \qquad \text{(C-1-5)}$$

where,

d =geometrical distance between conductors [m]

According to Carson-Clem equation, the mutual impedance Z_m between one buried pipeline and one power line is a function of

- the distance d between one buried pipeline and one power line

- soil resistivity ρ

- frequency f

C-2. EMF at Harmonic Frequencies

Carson-Clem equation is valid only if the geometrical distance between one buried pipeline and one nearby overhead power line satisfies the following condition (C-2-1).

$$d < 90\sqrt{\frac{\rho}{f}} \tag{C-2-1}$$

According to the above equation, the value of d at harmonic frequencies is very small so Carson-Clem equation is not valid for the usual case of which geometrical distance d exceeds the above condition (C-2-1). Consequently, it is required to find out the other simplified form of Carson's equation which has a reasonable error at harmonic frequencies.

According to Reference [23], the above Carson's equation (C-1-4) can be expressed as the following Carson's series form.

$$Z_{m\_Carson} = \frac{\mu_0\omega}{\pi}\int_{-\infty}^{\infty}\left(\sqrt{\alpha^2+j}-\alpha\right)e^{\left(-(h-h_p)\sqrt{\frac{\mu_0\omega}{\rho}}\alpha\right)}\cos\left(\sqrt{\frac{\mu_0\omega}{\rho}}\alpha\right)d\alpha = \frac{\mu_0\omega}{\pi}(P+jQ) \tag{C-2-2}$$

$$P = \frac{\pi}{8} - r\frac{\cos\theta}{3\sqrt{2}} + r^2\frac{\left[0.6728+\log\left(\frac{2}{r}\right)\right]\cos(2\theta)+\theta\sin(2\theta)}{16} + r^3\frac{\cos(3\theta)}{45\sqrt{2}} - r^4\frac{\pi\cos(4\theta)}{1536}\cdots \tag{C-2-3}$$

$$Q = \frac{1}{4}+\frac{1}{2}\log\left(\frac{2}{1.7811r}\right)+r\frac{\cos\theta}{3\sqrt{2}} - r^2\frac{\pi\cos(2\theta)}{64} + r^3\frac{\cos(3\theta)}{45\sqrt{2}} - \frac{\left[1.0895+\log\left(\frac{2}{r}\right)\right]\cos(4\theta)+\sin(4\theta)}{384}\cdots \tag{C-2-4}$$

$$r = \sqrt{\frac{\mu_0 \omega}{\rho}} \times \sqrt{\left(h - h_p\right)^2 + x^2} \tag{C-2-5}$$

$$\theta = \frac{x}{h - h_p} \tag{C-2-6}$$

For the simplified equation of Z_m at harmonic frequencies, we can consider selecting enough terms that satisfy the geometrical distance condition (C-2-1) with an acceptable error from the above Carson's series. Following things show the limited but typical range of frequency, soil resistivity, and the separation distance between one buried pipeline and one nearby power line [5].

- Frequency: 60 ~ 540 Hz
- Soil resistivity: 30 ~ 200 Ω
- Separation distance: 0 ~ 100 m

Based on those typical ranges, error studies have been conducted then the enough terms, which causes an acceptance error less than 5% compared to Carson's equation, were selected as follows [5].

$$Z_{m\_Carson} = \frac{\mu_0 \omega}{\pi}\left(P + jQ\right)$$

$$P \cong \frac{\pi}{8} - r\frac{\cos\theta}{3\sqrt{2}} + r^2 \frac{\left[0.6728 + \log\left(\frac{2}{r}\right)\right]\cos\left(2\theta\right) + \theta\sin\left(2\theta\right)}{16} \tag{C-2-7}$$

$$Q \cong \frac{1}{4} + \frac{1}{2}\log\left(\frac{2}{1.7811r}\right) + r\frac{\cos\theta}{3\sqrt{2}} - r^2\frac{\pi\cos\left(2\theta\right)}{64}$$

Using these simplified equations, we can calculate induced *EMF* with the acceptable error less than 5% at harmonic frequencies.

Appendix D. Calculation of Pipeline's Parameters

Self-impedance and self-admittance of a buried pipeline can be calculated based on Sunde's equation [23]. Especially for the fundamental frequency, following equations are recommended to calculate self-impedance z and self-admittance y of buried pipelines by several industrial guides [1][6].

$$z = z_i + j\frac{\omega\mu_0}{\pi\alpha' m'^2}\left[\gamma K_1\left(\alpha'\gamma\right) - \sqrt{m'^2+\gamma^2}\,K_1\left(\alpha'\sqrt{m'^2+\gamma^2}\right)\right]$$

$$\cong z_i + j\frac{\omega\mu_0}{2\pi}\ln\frac{1.85}{\alpha'\sqrt{m'^2+\gamma^2}} \tag{D-1}$$

$$= z_i + j\frac{\omega\mu_0}{2\pi}\ln\frac{1.85}{\alpha'\sqrt{\gamma^2 + j\omega\mu_0\left(\frac{1}{\rho}+j\omega\varepsilon\right)}}$$

$$z_i = R_i + jX_i = \frac{\sqrt{\omega\mu_r\mu_0\rho_p}}{\sqrt{2}\pi D}\left[\frac{\sinh\left(t_n\right)+\sin\left(t_n\right)}{\cosh\left(t_n\right)-\cos\left(t_n\right)} + j\frac{\sinh\left(t_n\right)+\sin\left(t_n\right)}{\cosh\left(t_n\right)-\cos\left(t_n\right)}\right] \tag{D-2}$$

$$y\left(\gamma\right) = \frac{1}{\pi\left(\frac{1}{\rho}+j\omega\varepsilon\right)}K_0\left(\alpha'\gamma\right) \cong \left(y_i^{-1} + \frac{\ln\left(\frac{1.12}{\alpha'\gamma}\right)}{\pi\left(\frac{1}{\rho}+j\omega\varepsilon\right)}\right)^{-1} \tag{D-3}$$

$$y^{-1} = y_i^{-1} + \frac{\ln\left(\frac{1.12}{\alpha'\gamma}\right)}{\pi\left(\frac{1}{\rho}+j\omega\varepsilon\right)} \tag{D-4}$$

$$y = \frac{\pi D}{r_c} + j\omega\frac{\varepsilon_0\varepsilon_r\pi D}{\delta_c} \tag{D-5}$$

where,

$$m'^2 = j\omega\mu_0\left(\frac{1}{\rho} + j\omega\varepsilon\right)$$

K_0 and K_1 are Bessel functions

z_i and y_i are internal impedance and admittance respectively

μ_r = relative permeability of pipeline, 300

ρ_p = resistivity of pipeline [Ωm]

$\varepsilon_0 = 8.85\times10^{-12}$[F/m]

ε_r = relative electrical permittivity of pipeline coating, 5

ε = electrical permittivity of soil [F/m], 3

r_c = specific coating resistance [Ωm] (polyethylene coating=1×10^5, bituminous coating=1×10^3)

D = diameter of pipeline [m], 0.6

a = radius of pipeline [m], 0.3

h_p = depth of buried conductor [m], 1

$a' = \sqrt{a^2 + 4h_p^2}$

δ_c = thickness of pipeline coating [m], 0.004

g = Euler's constant, 1.7811

t_n = pipeline wall thickness [m], $t_n = 0.0157\dfrac{\sqrt{2\omega\mu_r\mu_0\rho_p}}{\rho_p}D^{0.421}$

γ =propagation constant of pipeline [m^{-1}], $\gamma = \sqrt{zy}$

The final approximated forms of self-impedance z and self-admittance y are valid only if $\alpha'\gamma$ and $\alpha'\sqrt{m'^2+\gamma^2}$ are less than 0.01 [5]. This limited condition depends on both soil resistivity ρ and frequency f. With consideration of the typical range of soil resistivity ρ (30~100 Ωm), the limited condition is satisfied at the fundamental and harmonic frequencies.

Appendix E. Verification of Equation for V(x) caused by V_{SA}

In Section 2.2.1, the analytical equation of $V(x)\,caused\,by\,V_{SA}$ has been derived as follows.

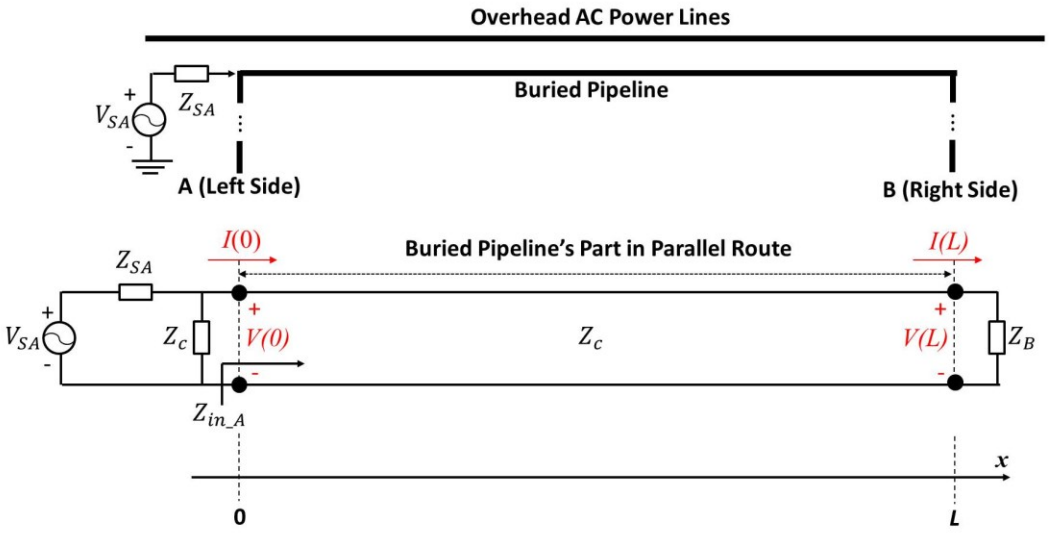

Figure E-1: Circuit of buried pipeline with V_{SA} at left terminal

$$V(x)\,caused\,by\,V_{SA} = \left[\left(\frac{\left(Z_{in\_A}//Z_c\right)}{Z_{SA}+\left(Z_{in\_A}//Z_c\right)}\right)\left(\frac{1}{1+\nu_2 e^{-2\gamma L}}\right)V_{SA}\right]e^{-\gamma x}\left(1+\nu_2 e^{-2\gamma(L-x)}\right) \qquad \text{(E-1)}$$

where,

$$Z_{in\_A} = Z_c\frac{Z_B + Z_C\tanh(\gamma L)}{Z_C + Z_B\tanh(\gamma L)}, \quad \nu_2 = \frac{Z_B - Z_C}{Z_B + Z_C}$$

Z_{SA} : equivalent internal impedance of active mitigation systems at the left terminal.

Z_B : equivalent impedance at the right terminal ($Z_B = Z_{SB}//Z_c$)

Z_{SB} : equivalent internal impedance of active mitigation systems at the right terminal

This section presents the simulation result to verify the above Equation (E-1) using the following circuit.

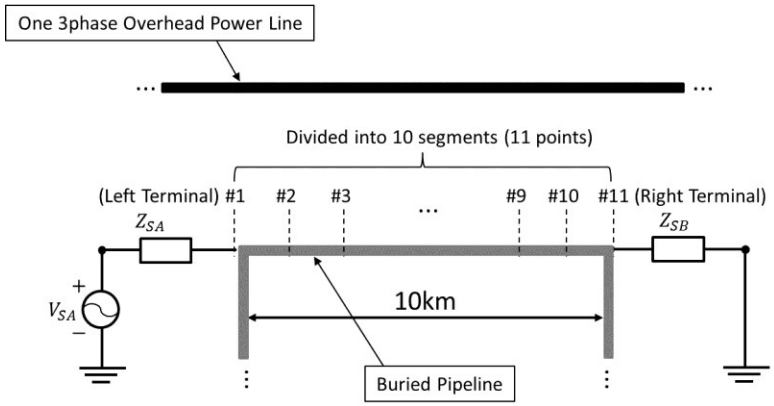

Figure E-2: Applied V_{SA} and the pipeline divided into 10 Segments

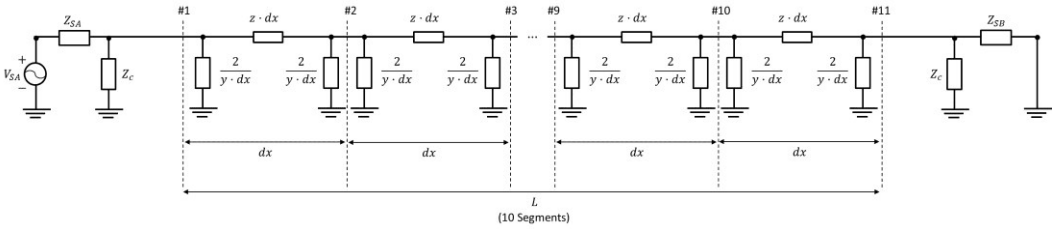

Figure E-3: Applied V_{SA} and the pipeline divided into 10 Segments (2)

Parameters for the above circuit analysis are the same with the case study of Section 2.2.6. The applied V_{SA} has three major harmonic components as follows.

V_{SA} at H=1 (at the fundamental Frequency)	156.755 + j127.627
V_{SA} at H=3 (at the 3rd Harmonic Frequency)	312.968 + j458.748
V_{SA} at H=9 (at the 9th Harmonic Frequency)	89.184 + j302.333

The following data shows the results using Equation (E-1) and the circuit simulation of Figure E-3.

Table E-1: Voltage profile caused by V_{SA} according to harmonic order

V_{SA} at H=1	Analytical [V], (1)	Simulation [V], (2)	%Error, (2)-(1)
Voltage at #1	44.630	44.632	0.005
Voltage at #2	41.631	41.630	-0.002
Voltage at #3	38.742	38.738	-0.009
Voltage at #4	35.958	35.953	-0.015
Voltage at #5	33.281	33.274	-0.023
Voltage at #6	30.712	30.703	-0.030
Voltage at #7	28.256	28.245	-0.038
Voltage at #8	25.919	25.907	-0.047
Voltage at #9	23.714	23.700	-0.057
Voltage at #10	21.655	21.640	-0.069
Voltage at #11	19.762	19.746	-0.083

V_{SA} at H=3	Analytical [V], (1)	Simulation [V], (2)	%Error, (2)-(1)
Voltage at #1	113.949	114.020	0.063
Voltage at #2	107.000	107.048	0.045
Voltage at #3	100.233	100.266	0.033
Voltage at #4	93.507	93.529	0.023
Voltage at #5	86.712	86.725	0.015
Voltage at #6	79.781	79.786	0.006
Voltage at #7	72.691	72.686	-0.008
Voltage at #8	65.471	65.451	-0.030
Voltage at #9	58.201	58.163	-0.065
Voltage at #10	51.031	50.970	-0.121
Voltage at #11	44.188	44.098	-0.204

V_{SA} at H=9	Analytical [V], (1)	Simulation [V], (2)	%Error, (2)-(1)
Voltage at #1	29.362	29.596	0.796
Voltage at #2	26.525	26.672	0.555
Voltage at #3	23.729	23.794	0.274
Voltage at #4	21.104	21.097	-0.030
Voltage at #5	18.872	18.820	-0.279
Voltage at #6	17.193	17.126	-0.388
Voltage at #7	15.993	15.930	-0.394
Voltage at #8	14.965	14.894	-0.477
Voltage at #9	13.759	13.646	-0.825
Voltage at #10	12.188	12.001	-1.535
Voltage at #11	10.344	10.081	-2.543

The above data shows that the simulation result is the almost same with the result using Equation (E-1). Consequently, we can say that Equation (E-1) has been verified by simulation.

Appendix F. Simplified Equation for Neutralizing Voltage

This appendix shows how to obtain the simplified form of the required neutralizing voltage. It begins with the following matrix equation.

$$\begin{bmatrix} V_{SA} \\ V_{SB} \end{bmatrix} = \begin{bmatrix} N_{11} & N_{12} \\ N_{21} & N_{22} \end{bmatrix}^{-1} \begin{bmatrix} \frac{Z_C}{\gamma} A \\ -\frac{Z_C}{\gamma} B \end{bmatrix} \tag{F-1}$$

where,

$$A = \frac{EMF}{2Z_c} \frac{(1+\nu_1)\nu_2 - (1+\nu_2)e^{\gamma L}}{e^{2\gamma L} - \nu_1\nu_2}, \; B = \frac{EMF}{2Z_c} \frac{(1+\nu_2)\nu_1 - (1+\nu_1)e^{\gamma L}}{e^{2\gamma L} - \nu_1\nu_2} e^{\gamma L}$$

$$N_{11} = \left(\frac{\left(Z_{in\_A} // Z_c\right)}{Z_{SA} + \left(Z_{in\_A} // Z_c\right)} \right) \left(\frac{1}{1+\nu_2 e^{-2\gamma L}} \right) \nu_2 e^{-2\gamma L} = \frac{Z_c(1+\nu_2 e^{-2\gamma L})}{2Z_{SA} + Z_c\left(1+\nu_2 e^{-2\gamma L}\right)} \left(\frac{1}{1+\nu_2 e^{-2\gamma L}} \right) \nu_2 e^{-2\gamma L}$$

$$N_{12} = \left(\frac{\left(Z_{in\_B} // Z_c\right)}{Z_{SB} + \left(Z_{in\_B} // Z_c\right)} \right) \left(\frac{1}{1+\nu_1 e^{-2\gamma L}} \right) e^{-\gamma L} = \frac{Z_c(1+\nu_1 e^{-2\gamma L})}{2Z_{SB} + Z_c\left(1+\nu_1 e^{-2\gamma L}\right)} \left(\frac{1}{1+\nu_1 e^{-2\gamma L}} \right) e^{-\gamma L}$$

$$N_{21} = \left(\frac{\left(Z_{in\_A} // Z_c\right)}{Z_{SA} + \left(Z_{in\_A} // Z_c\right)} \right) \left(\frac{1}{1+\nu_2 e^{-2\gamma L}} \right) = \frac{Z_c(1+\nu_2 e^{-2\gamma L})}{2Z_{SA} + Z_c\left(1+\nu_2 e^{-2\gamma L}\right)} \left(\frac{1}{1+\nu_2 e^{-2\gamma L}} \right)$$

$$N_{22} = \left(\frac{\left(Z_{in\_B} // Z_c\right)}{Z_{SB} + \left(Z_{in\_B} // Z_c\right)} \right) \left(\frac{1}{1+\nu_1 e^{-2\gamma L}} \right) \nu_1 e^{-\gamma L} = \frac{Z_c(1+\nu_1 e^{-2\gamma L})}{2Z_{SB} + Z_c\left(1+\nu_1 e^{-2\gamma L}\right)} \left(\frac{1}{1+\nu_1 e^{-2\gamma L}} \right) \nu_1 e^{-\gamma L}$$

The above components of [N] matrix are based on the following equations.

$$Z_A = \frac{1+\nu_1}{1-\nu_1} Z_c, \; Z_B = \frac{1+\nu_2}{1-\nu_2} Z_c$$

$$Z_{in\_A} = Z_c \frac{Z_B + Z_c \tanh(\gamma L)}{Z_c + Z_B \tanh(\gamma L)} = Z_c \frac{1+\nu_2 e^{-2\gamma L}}{1-\nu_2 e^{-2\gamma L}}$$

$$Z_{in\_B} = Z_c \frac{Z_A + Z_c \tanh(\gamma L)}{Z_c + Z_A \tanh(\gamma L)} = Z_c \frac{1+\nu_1 e^{-2\gamma L}}{1-\nu_1 e^{-2\gamma L}}$$

From Equation (F-1), we can consider one single equation for V_{SA} as follows.

$$V_{SA} = \frac{1}{N_{11}N_{22} - N_{12}N_{21}} \left(N_{22} \cdot \frac{Z_c}{\gamma} A + N_{12} \cdot \frac{Z_c}{\gamma} B \right) \tag{F-2}$$

where,

$$\frac{1}{N_{11}N_{22} - N_{12}N_{21}} = \frac{\left[2Z_{SA} + Z_c\left(1+\nu_2 e^{-2\gamma L}\right)\right]\left[2Z_{SB} + Z_c\left(1+\nu_1 e^{-2\gamma L}\right)\right]}{{Z_c}^2 \cdot e^{-\gamma L} \cdot \left(\nu_1\nu_2 e^{-2\gamma L} - 1\right)}$$

$$N_{22} \cdot \frac{Z_c}{\gamma} A = \frac{Z_c(1+\nu_1 e^{-2\gamma L})}{2Z_{SB} + Z_c\left(1+\nu_1 e^{-2\gamma L}\right)} \left(\frac{1}{1+\nu_1 e^{-2\gamma L}} \right) \nu_1 e^{-\gamma L} \cdot \frac{EMF}{2\gamma} \frac{(1+\nu_1)\nu_2 - (1+\nu_2)e^{\gamma L}}{e^{2\gamma L} - \nu_1\nu_2}$$

$$N_{12} \cdot \frac{Z_c}{\gamma} B = \frac{Z_c(1+\nu_1 e^{-2\gamma L})}{2Z_{SB} + Z_c\left(1+\nu_1 e^{-2\gamma L}\right)} \left(\frac{1}{1+\nu_1 e^{-2\gamma L}} \right) \cdot \frac{EMF}{2\gamma} \frac{(1+\nu_2)\nu_1 - (1+\nu_1)e^{\gamma L}}{e^{2\gamma L} - \nu_1\nu_2}$$

The complicated Equation (F-2) can be finally organized as the following process.

$$\frac{1}{N_{11}N_{22} - N_{12}N_{21}} \left(N_{22} \cdot \frac{Z_c}{\gamma} A + N_{12} \cdot \frac{Z_c}{\gamma} B \right) =$$

$$= \frac{EMF \cdot \left[2Z_{SA} + Z_c\left(1+\nu_2 e^{-2\gamma L}\right)\right]}{2\gamma \cdot Z_c \cdot e^{-\gamma L}\left(e^{2\gamma L} - \nu_1\nu_2\right)\left(\nu_1\nu_2 e^{-2\gamma L} - 1\right)} \left\{ \left[(1+\nu_1)\nu_2 - (1+\nu_2)e^{\gamma L} \right] \nu_1 e^{-\gamma L} + \left[(1+\nu_2)\nu_1 - (1+\nu_1)e^{\gamma L} \right] \right\}$$

$$= \frac{EMF}{2\gamma \cdot \nu_1 \cdot e^{-\gamma L}\left(e^{2\gamma L} - \nu_1\nu_2\right)} \left\{ \left[(1+\nu_1)\nu_2 - (1+\nu_2)e^{\gamma L} \right] \nu_1 e^{-\gamma L} + \left[(1+\nu_2)\nu_1 - (1+\nu_1)e^{\gamma L} \right] \right\}$$

$$= \frac{EMF}{2\gamma \cdot \nu_1 \cdot e^{-\gamma L}\left(e^{2\gamma L} - \nu_1\nu_2\right)} \left\{ \left[\nu_1\nu_2 e^{-\gamma L} + \nu_1^2\nu_2 e^{-\gamma L} \right] + \left[-(1+\nu_1)e^{\gamma L} \right] \right\}$$

$$= \frac{-EMF \cdot (1+\nu_1)}{2\gamma \cdot \nu_1 \cdot \left(\nu_1\nu_2 e^{-\gamma L} - e^{\gamma L}\right)} \left\{ \nu_1\nu_2 e^{-\gamma L} - e^{\gamma L} \right\}$$

$$= \frac{-EMF \cdot (1+\nu_1)}{2\gamma \cdot \nu_1}$$

$$= \frac{EMF \cdot Z_{SA}}{\gamma \cdot Z_c}$$

$$V_{SA} = \frac{EMF \cdot Z_{SA}}{\gamma \cdot Z_c} \tag{F-3}$$

Similarly, we can obtain the following equation for V_{SB}.

$$V_{SB} = -\frac{EMF \cdot Z_{SB}}{\gamma \cdot Z_c} \tag{F-4}$$

As you can see, the required neutralizing voltage V_{SA} and V_{SB} are basically independent from the pipeline's length L and constant by assuming the even-distributed soil resistivity.

Appendix G. Parameters for Case Study

Table G-1: Parameters of case study in section 2.2.6

Parameter	Value	Unit
P_{ca} Position of the phase conductor A	(0, 10.7)	[m]
P_{cb} Position of the phase conductor B	(-1.2, 10.1)	[m]
P_{cc} Position of the phase conductor C	(1.2, 10.1)	[m]
I_c current of the phase conductor	500	[A,RMS]
Load Imbalance	5	[%]
$P_p(x_p, y_p)$ Position of the buried pipeline	(20,-1)	[m]
L Length of the pipeline in the parallel effective zone	10	[km]
ρ Soil Resistivity	100	[Ω]
z at H=1 Series Impedance at H=1	0.1467 + j0.5433	[Ω / km]
z at H=3 Series Impedance at H=3	0.3293 + j1.3949	[Ω / km]
z at H=9 Series Impedance at H=9	0.7966 + j3.6197	[Ω / km]
y at H=1 Shunt Admittance at H=1	0.0126 + j0.0052	[S/km]
y at H=3 Shunt Admittance at H=3	0.0126 + j0.0157	[S/km]

y at H=9 Shunt Admittance at H=9	0.0126 + j0.0472	[S/km]
γ at H=1 Propagation Constant at H=1	0.0577 + j0.0658	[1/km]
γ at H=3 Propagation Constant at H=3	0.0743 + j0.1527	[1/km]
γ at H=9 Propagation Constant at H=9	0.1005 + j0.4134	[1/km]
Z_c at H=1 Characteristic Impedance at H=1	5.7724 + j2.8306	[Ω]
Z_c at H=3 Characteristic Impedance at H=3	8.2319 + j1.8505	[Ω]
Z_c at H=9 Characteristic Impedance at H=9	8.7099 + j0.1900	[Ω]
EMF Induced EMF on the Pipeline	-23.4103 –j7.0318	[V/km]
Parameter K_{11}	0.221 + j0.011	
Parameter K_{12}	0.076 – j0.061	
Parameter K_{21}	0.076 – j0.061	
Parameter K_{22}	0.221 + j0.011	
Calculated V_{SA} Required Neutralizing Voltage For Left Terminal	-413.6 + j254.5	[V]
Z_{SA} Internal Impedance of the Left AMS	10 + j5	[Ω]
Calculated V_{SB} Required Neutralizing Voltage For Left Terminal	413.6 – j254.5	[V]

Z_{SB} Internal Impedance of the Left AMS	10 + j5	[Ω]

Table G-2: Parameters of case study with average harmonic sequence data in section 2.2.6

Parameter	Value	Unit
I_0 at H=1 Zero Sequence Current at H=1	12.68	[A, RMS]
I_0 at H=3 Zero Sequence Current at H=3	20.45	[A, RMS]
I_0 at H=9 Zero Sequence Current at H=9	4.68	[A, RMS]
I_g at H=1 (for Left AMS) Grounding Current at H=1	18.1	[A, RMS]
I_g at H=3 (for Left AMS) Grounding Current at H=3	30.8	[A, RMS]
I_g at H=9 (for Left AMS) Grounding Current at H=9	6.8	[A, RMS]
Total I_g (for Left AMS) Total Grounding Current	36.4	[A, RMS]
Total S Required Total Power (for Left AMS)	14.868	[kVA]
EMF at H=1	0.4477 + j10.1655	[V/km]
EMF at H=3	10.6024 + j42.8576	[V/km]
EMF at H=9	7.1209 + j24.3225	[V/km]
V_A *caused by EMF* at H=1	32.6	[V, RMS]

V_A *caused by EMF* at H=3	113.6	[V, RMS]
V_A *caused by EMF* at H=9	36.7	[V, RMS]
Required V_{SA} at H=1	202.1	[V, RMS]
Required V_{SA} at H=3	555.3	[V, RMS]
Required V_{SA} at H=9	315.2	[V, RMS]
Parameter K_{11} at H=1	0.221 + j0.011	
Parameter K_{12} at H=1	0.076 – j0.061	
Parameter K_{21} at H=1	0.076 – j0.061	
Parameter K_{22} at H=1	0.221 + j0.011	
Parameter K_{11} at H=3	0.165 - j0.122	
Parameter K_{12} at H=3	-0.034 – j0.072	
Parameter K_{21} at H=3	-0.034 – j0.072	
Parameter K_{22} at H=3	0.165 - j0.122	
Parameter K_{11} at H=9	0.030 + j0.088	
Parameter K_{12} at H=9	0.018 + j0.028	

Parameter K_{21} at H=9	0.018 + j0.028	
Parameter K_{22} at H=9	0.030 + j0.088	

Table G-3: Parameters of case study in section 4.4

Parameter	Value	Unit
Z_V Impedance of the voltage meter	10^6	[Ω]
Z_{g1} Impedance of the ground rod #1	100	[Ω]
Z_{g2} Impedance of the ground rod #2	100	[Ω]
* C_g Capacitance between the probe wire and the ground	601.94	[pF]
y_w y position (height) of the probe wire	0.01	[m]
d Diameter of the probe wire	0.01	[m]
* I_{SC} Current caused by the capacitive coupling between the probe wire and overhead power lines	20.07	[μA ,RMS]
* EMF_{probe} EMF on the probe wire by overhead power lines	5.5	[mV(RMS)/m]
L length of the probe wire	15	[m]
y_p y position of the pipeline	-1	[m]
ρ Soil resistivity	100	[Ωm]

V_c Phase voltage	$\frac{138}{\sqrt{3}}$	[kV,RMS]
I_c Phase current	500	[A,RMS]
Imb Load Imbalance	5	[%]
PF_1 power factor	0.95	N/A

Appendix H. Earth Potential around Buried Pipeline

According to Reference [8], the earth potential near the buried pipeline having induced voltage is not zero and it depends on several factors: (1) the unbalanced current of nearby overhead AC power lines, (2) soil resistivity, (3) the coating resistivity of the pipeline, (4) the distance between the pipeline and overhead AC power lines. The following Figure H-1 shows some cases of earth potential near one buried pipeline by different unbalanced currents in nearby overhead AC power lines.

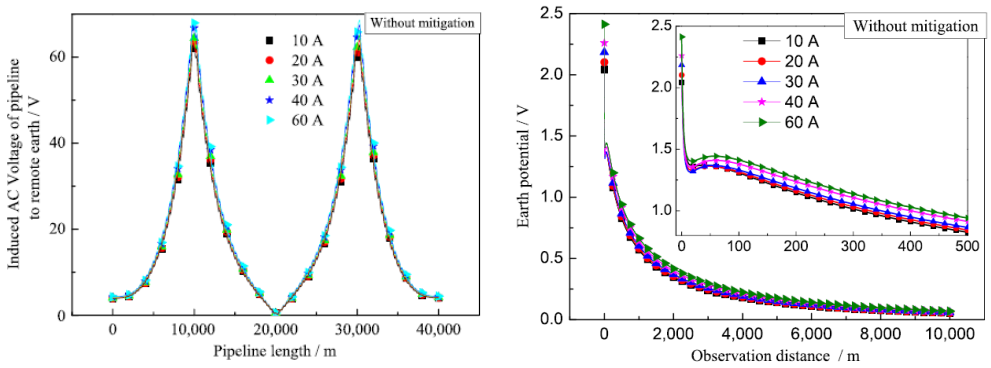

Figure H-1: Induced voltage and earth potential of a pipeline, from Reference [8]

The above results have been obtained by professional simulation software CDEGS [8]. The buried pipeline in the above has no mitigation wire and is away from the nearby overhead AC power lines by 30 meters.

As shown in the above, the terminal voltage ranges from 62V to 67V and the earth potential at the position of the pipeline's terminal is just a few volts (2.04~2.41V). It depends on imbalanced currents in the nearby overhead AC power lines. If we apply the proposed active mitigation method to the above buried pipeline, the induced terminal voltage decreases then the earth potential around the terminal also decreases. Therefore, the final earth potential rise caused by the pipeline would be negligible because the induced voltage on the pipeline is mitigated by active mitigation systems.

Appendix I. Grounding Current

The following Figure I-1 shows the equivalent circuit of a buried pipeline with two active mitigation systems at two terminals.

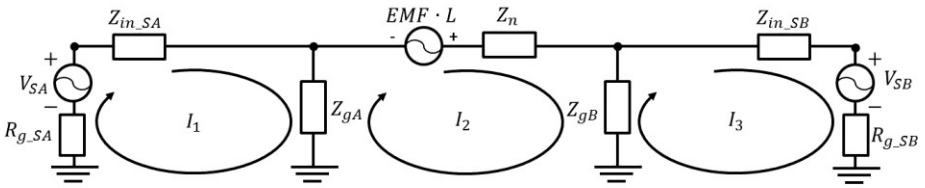

Figure I-1: Equivalent circuit of a buried pipeline with active mitigation systems

In the 1st loop of the above circuit, it is possible to derive the following mesh equation.

$$(Z_{in\_SA} + R_{g\_SA}) \cdot I_1 + Z_{gA} \cdot (I_1 - I_2) = V_{SA} \tag{I-1}$$

If V_{SA} and V_{SB} are the proper neutralizing voltage sources for perfect mitigation then $Z_{gA} \cdot (I_1 - I_2) = 0$. Therefore, Equation (I-1) will be

$$(Z_{in\_SA} + R_{g\_SA}) \cdot I_1 = V_{SA} \tag{I-2}$$

From Equation (I-2), we can obtain the following equation for the grounding current I_g of the left active mitigation system.

$$I_g = -I_1 = -\frac{V_{SA}}{Z_{in\_SA} + R_{g\_SA}} \tag{I-3}$$

The simplified equation of V_{SA} is

$$V_{SA} = \frac{EMF \cdot Z_{SA}}{\gamma Z_c} \tag{I-4}$$

The detail process to derive Equation (I-4) can be referred to in Appendix F.
Using Equation (I-4) and $Z_{SA} = Z_{in\_SA} + R_{g\_SA}$, Equation (I-3) can be organized as follows.

$$I_g = -\frac{EMF}{\gamma Z_c} \tag{I-5}$$

If the pipeline is not in the perfect mitigation state, the grounding current I_g of the left active mitigation system can be calculated by voltage division rule in the above circuit.

$$I_g = \frac{Total\,V_{Rg\_SA}}{R_{g\_SA}} \tag{I-6}$$

where,

$$Total\,V_{Rg\_SA} = (1)V_{Rg\_SA}\ caused\ by\ V_{SA} + (2)V_{Rg\_SA}\ caused\ by\ EMF + (3)V_{Rg\_SA}\ caused\ by\ V_{SB} \tag{I-7}$$

$$V_{Rg\_SA}\ caused\ by\ V_{SA} = -\frac{R_{g\_SA}}{Z_{in\_SA} + R_{g\_SA} + Z_{eq\_pipe\_A}} V_{SA} \tag{I-8}$$

$$V_{Rg\_SA}\ caused\ by\ EMF = -\left(\frac{Z_A}{Z_n + Z_A + Z_{eq\_B}} EMF \cdot L \right) \frac{R_{g\_SA}}{Z_{in\_SA} + R_{g\_SA}} \tag{I-9}$$

$$V_{Rg\_SA}\ caused\ by\ V_{SB} = \left(\frac{Z_{eq\_pipe\_B}}{Z_{in\_SB} + R_{g\_SB} + Z_{eq\_pipe\_B}} V_{SB} \right) \left(\frac{Z_A}{Z_n + Z_A} \right) \left(\frac{R_{g\_SA}}{Z_{in\_SA} + R_{g\_SA}} \right) \tag{I-10}$$

$$Z_{eq\_pipe\_A} = Z_{gA} // \left\{ Z_n + Z_{gB} // \left(Z_{in\_SB} + R_{g\_SB} \right) \right\} \tag{I-11}$$

$$Z_{eq\_pipe\_B} = Z_{gB} // \left\{ Z_n + Z_{gA} // \left(Z_{in\_SA} + R_{g\_SA} \right) \right\} \tag{I-12}$$

$$Z_A = Z_{gA} // \left(Z_{in\_SA} + R_{g\_SA} \right) \tag{I-13}$$

$$Z_B = Z_{gB} // \left(Z_{in\_SB} + R_{g\_SB} \right) \tag{I-14}$$

Appendix J. Analytical Equations for Calculating Induced Voltage of Buried Pipeline according to Different Application Points for Neutralizing Voltage

This section presents the analytical equations to calculate voltage in a buried pipeline when neutralizing voltage is applied to different application points. The following Figure J-1 describes the case when we apply two neutralizing voltage sources to certain existing access points to the pipeline instead of two terminals of it.

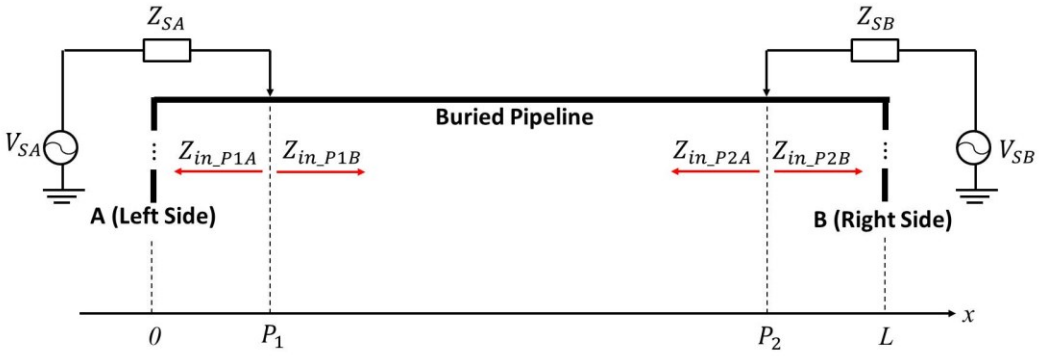

Figure J-1: Circuit of the buried pipeline with V_{SA}, V_{SB} applied to existing access points of P_1 and P_2

According to the above circuit, we have four boundary conditions at x=0, P_1, P_2, and L. Therefore, it is possible to classify three different areas and four different input equivalent impedance values as follows.

Area 1: $0 \le x \le P_1$, Area 2: $P_1 < x \le P_2$, Area 3: $P_2 < x \le L$

$$Z_{in\_P1A} = Z_c,\ Z_{in\_P1B} = Z_c \frac{Z_{eq\_P2} + Z_C \tanh\left(\gamma\left(P_2 - P_1\right)\right)}{Z_C + Z_{eq\_P2} \tanh\left(\gamma\left(P_2 - P_1\right)\right)}$$

$$Z_{in\_P2A} = Z_c \frac{Z_{eq\_P1} + Z_C \tanh\left(\gamma\left(P_2 - P_1\right)\right)}{Z_C + Z_{eq\_P2} \tanh\left(\gamma\left(P_2 - P_1\right)\right)},\ Z_{in\_P2B} = Z_c$$

$$Z_{eq\_P1} = (Z_{SP1} // Z_c),\ Z_{eq\_P2} = (Z_{SP2} // Z_c)$$

$$\nu_1 = \frac{Z_{eq\_P1} - Z_C}{Z_{eq\_P1} + Z_C},\ \nu_2 = \frac{Z_{eq\_P2} - Z_C}{Z_{eq\_P2} + Z_C}$$

If we separate induced EMFs according to three different area as specified in the above, we can consider totally five different sources such as EMF_1 in area 1, EMF_2 in area 2, EMF_3 in area 3, V_{SA}, and V_{SB}. Based on those different voltage sources, we can consider analytical equation for the voltage caused by each source in each area as follows.

J-1. $V(x)$ **caused by** V_{SA}

- $0 \le x \le P_1$

$$V(x)\,caused\,by\,V_{SA} = \left[\left(\frac{\left(Z_{in\_P1A} // Z_{in\_P1B}\right)}{Z_{SP1} + \left(Z_{in\_P1A} // Z_{in\_P1B}\right)}\right)V_{SA}\right]\left(1 + \nu_2 e^{-2\gamma(P_2 - P_1)}\right)e^{-\gamma(-x + P_1)} \qquad \text{(J-1-1)}$$

- $P_1 < x \le P_2$

$$V(x)\,caused\,by\,V_{SA} = \left[\left(\frac{\left(Z_{in\_P1A} // Z_{in\_P1B}\right)}{Z_{SP1} + \left(Z_{in\_P1A} // Z_{in\_P1B}\right)}\right)V_{SA}\right]e^{-\gamma(x - P_1)}\left(1 + \nu_2 e^{-2\gamma(P_2 - x)}\right) \qquad \text{(J-1-2)}$$

- $P_2 < x \le L$

$$V(x)\,caused\,by\,V_{SA} = \left[\left(\frac{\left(Z_{in\_P1A} // Z_{in\_P1B}\right)}{Z_{SP1} + \left(Z_{in\_P1A} // Z_{in\_P1B}\right)}\right)V_{SA}\right]e^{-\gamma(P_2 - P_1)}\left(1 + \nu_2\right)e^{-\gamma(x - P_2)} \qquad \text{(J-1-3)}$$

J-2. $V(x)$ **caused by** V_{SB}

- $0 \le x \le P_1$

$$V(x)\,caused\,by\,V_{SB} = \left[\left(\frac{\left(Z_{in\_P2A} // Z_{in\_P2B}\right)}{Z_{SP2} + \left(Z_{in\_P2A} // Z_{in\_P2B}\right)}\right)V_{SB}\right]e^{-\gamma(P_2 - P_1)}\left(1 + \nu_1\right)e^{-\gamma(-x + P_1)} \qquad \text{(J-2-1)}$$

- $P_1 < x \le P_2$

$$V(x)\,caused\,by\,V_{SB} = \left[\left(\frac{\left(Z_{in\_P2A}\,//\,Z_{in\_P2B}\right)}{Z_{SP2}+\left(Z_{in\_P2A}\,//\,Z_{in\_P2B}\right)}\right)V_{SB}\right]e^{-\gamma(P_2-x)}\left(1+\nu_1 e^{-2\gamma(x-P_1)}\right) \quad \text{(J-2-2)}$$

- $P_2 < x \le L$

$$V(x)\,caused\,by\,V_{SB} = \left[\left(\frac{\left(Z_{in\_P2A}\,//\,Z_{in\_P2B}\right)}{Z_{SP2}+\left(Z_{in\_P2A}\,//\,Z_{in\_P2B}\right)}\right)V_{SB}\right]\left(1+\nu_1 e^{-2\gamma(P_2-P_1)}\right)e^{-\gamma(x-P_2)} \quad \text{(J-2-3)}$$

J-3. $V(x)$ **caused by** EMF_1

- $0 \le x \le P_1$

$$V(x)\,caused\,by\,EMF_1 = -\frac{Z_c}{\gamma}\left(Ae^{\gamma x} - P1e^{-\gamma x}\right) \quad \text{(J-3-1)}$$

where,

$$Z_{eq\_A} = Z_c,\ Z_{eq\_P1B} = \left(Z_{SP1}\,//\,Z_{in\_P1B}\right),\ A = \frac{EMF}{2Z_c}\frac{\left(1+\nu_A\right)\nu_{P1} - (1+\nu_{P1})e^{rP_1}}{e^{2\gamma P_1} - \nu_A\nu_{P1}}$$

$$P1 = \frac{EMF}{2Z_c}\frac{\left(1+\nu_{P1}\right)\nu_A - (1+\nu_A)e^{rP_1}}{e^{2\gamma P_1} - \nu_A\nu_{P1}}e^{rP_1},\ \nu_A = 0,\ \nu_{P1} = \frac{Z_{eq\_P1B} - Z_c}{Z_{eq\_P1B} + Z_c}$$

- $P_1 < x \le P_2$

$$V(x)\,caused\,by\,EMF_1 = \left[V(P_1)\right]e^{-\gamma(x-P_1)} \quad \text{(J-3-2)}$$

where,

$$V(P_1) = -\frac{Z_c}{\gamma}\left(Ae^{\gamma P_1} - P1e^{-\gamma P_1}\right)$$

- $P_2 < x \le L$

$$V(x)\,caused\,by\,EMF_1 = \left[V(P_1)\right]e^{-\gamma(P_2-P_1)}\left(1+\nu_2\right)e^{-\gamma(x-P_2)} \quad \text{(J-3-3)}$$

J-4. $V(x)$ **caused by** EMF_2

- $0 \le x \le P_1$

$$V(x)\,caused\ by\ EMF_2 = \left[V(P_1)\right]e^{-\gamma(-x+P_1)} \tag{J-4-1}$$

- $P_1 < x \le P_2$

$$V(x)\,caused\ by\ EMF_2 = -\frac{Z_c}{\gamma}\left(P1e^{\gamma(x-P_1)} - P2e^{-\gamma(x-P_1)}\right) \tag{J-4-2}$$

where,

$$P1 = \frac{EMF}{2Z_c}\frac{\left(1+\nu_{P1}\right)\nu_{P2} - (1+\nu_{P2})e^{r(P_2-P_1)}}{e^{2\gamma(P_2-P_1)} - \nu_{P1}\nu_{P2}},$$

$$P2 = \frac{EMF}{2Z_c}\frac{\left(1+\nu_{P2}\right)\nu_{P1} - (1+\nu_{P1})e^{r(P_2-P_1)}}{e^{2\gamma(P_2-P_1)} - \nu_{P1}\nu_{P2}}e^{r(P_2-P_1)}$$

$$\nu_{P1} = \frac{Z_{eq\_P1A} - Z_c}{Z_{eq\_P1A} + Z_c},\ \nu_{P2} = \frac{Z_{eq\_P2B} - Z_c}{Z_{eq\_P2B} + Z_c}$$

- $P_2 < x \le L$

$$V(x)\,caused\ by\ EMF_2 = \left[V(P_2)\right]e^{-\gamma(x-P_2)} \tag{J-4-3}$$

J-5. $V(x)$ **caused by** EMF_3

- $0 \le x \le P_1$

$$V(x)\,caused\ by\ EMF_3 = \left[V(P_2)\right]e^{-\gamma(-P_1+P_2)}e^{-\gamma(-x+P_1)} \tag{J-5-1}$$

- $P_1 < x \le P_2$

$$V(x)\,caused\ by\ EMF_3 = \left[V(P_2)\right]e^{-\gamma(-x+P_2)} \tag{J-5-2}$$

- $P_2 < x \le L$

$$V(x)\,caused\ by\ EMF_3 = -\frac{Z_c}{\gamma}\left(P2e^{\gamma(x-P_2)} - Be^{-\gamma(x-P_2)}\right) \tag{J-5-3}$$

where,

$$P2 = \frac{EMF}{2Z_c}\frac{(1+\nu_{P2})\nu_B - (1+\nu_B)e^{r(L-P_2)}}{e^{2\gamma(L-P_2)} - \nu_{P2}\nu_B},$$

$$B = \frac{EMF}{2Z_c}\frac{(1+\nu_B)\nu_{P2} - (1+\nu_{P2})e^{r(L-P_2)}}{e^{2\gamma(L-P_2)} - \nu_{P2}\nu_B}e^{r(L-P_2)}$$

$$\nu_{P2} = \frac{Z_{eq\_P2A} - Z_c}{Z_{eq\_P2A} + Z_c},\ \nu_B = 0$$

By superposition principle, it is possible to calculate total voltage as follows.

$$\begin{aligned} Total\,V(x) = {} & V(x)\,caused\ by\ EMF_1 + V(x)\,caused\ by\ EMF_2 + V(x)\,caused\ by\ EMF_3 \\ & + V(x)\,caused\ by\ V_{SA} + V(x)\,caused\ by\ V_{SB} \end{aligned}$$

Appendix K. Electric Field Intensity caused by Overhead Power Lines

This section presents how to calculate the electric field intensity caused by overhead AC power lines. According to Reference [26], it is assumed that there is no free charge in the air and the earth is a perfect conductor. This is different from the way to calculate the magnetic field intensity H. The reason is that, in the case of the calculation of electric field intensity E, the time required for charges to redistribute on the earth surface under the action of a change in applied field is extremely small compared to the period of the power frequency [26]. For this reason, the electric field intensity E can be calculated as follows.

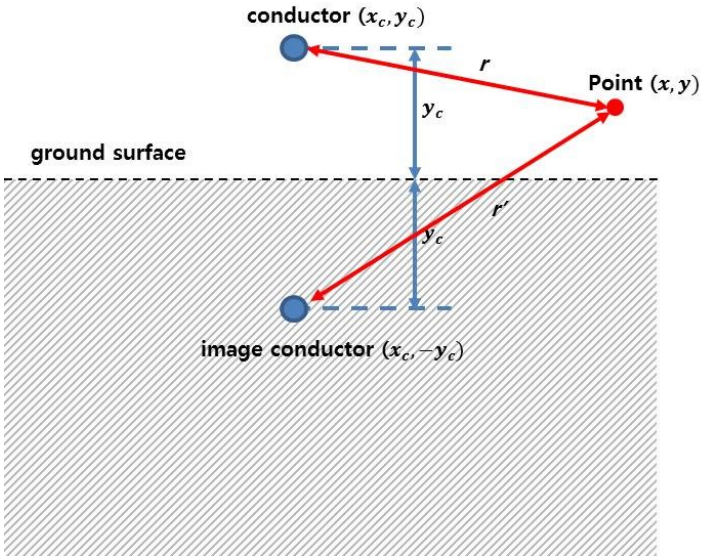

Figure K-1: Image method for the calculation of electric field intensity E

$$\vec{E} = E_r \cdot \vec{u}_r + E_{r'} \cdot \vec{u}_{r'} \tag{K-1}$$

$$E_r = \frac{Q}{2\pi\varepsilon_0 r} \cdot \vec{u}_r \tag{K-2}$$

$$r = \sqrt{(x_c - x)^2 + (y_c - y)^2} \tag{K-3}$$

$$\vec{u}_r = \frac{(x_c - x)}{r} \cdot \vec{u}_x + \frac{(y_c - y)}{r} \cdot \vec{u}_y \tag{K-4}$$

$$E_{r\prime} = \frac{-Q}{2\pi\varepsilon_0 r'} \cdot \vec{u}_{r\prime} \tag{K-5}$$

$$\mathrm{r}' = \sqrt{(x_c - x)^2 + (y_c + y)^2} \tag{K-6}$$

$$\vec{u}_{r\prime} = \frac{(x_c - x)}{r'} \cdot \vec{u}_x + \frac{(y_c + y)}{r'} \cdot \vec{u}_y \tag{K-7}$$

$$[Q] = [P]^{-1}[V] \tag{K-8}$$

$$P_{aa} = \frac{1}{2\pi\varepsilon_0} \ln\left(\frac{4y_a}{d_a}\right) \tag{K-9}$$

$$d_{eq} = D\sqrt[n]{\frac{nd}{D}} \tag{K-10}$$

$$P_{ab} = \frac{1}{2\pi\varepsilon_0} \ln\left[\frac{(x_a - x_b)^2 + (y_a + y_b)^2}{(x_a - x_b)^2 + (y_a - y_b)^2}\right]^{1/2} \tag{K-11}$$

where

$[Q]$ = matrix of the charges of the power lines

$[P]$ = matrix of the Maxwell potential coefficient of the power lines

$[V]$ = matrix of the voltage of the power lines

D = bundle diameter

n = number of subconductors

d = diameter of subconductors

Appendix L. Simulation Circuits by Matlab/Simulink

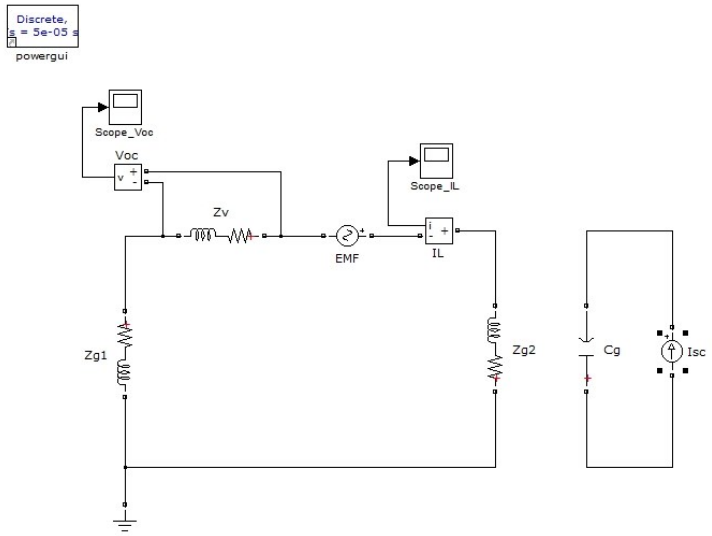

Figure L-1: Circuit for the case without capacitive coupling(with Shielding) in Section 3.4.1 ($V_{OC} = V_{OC1}$)

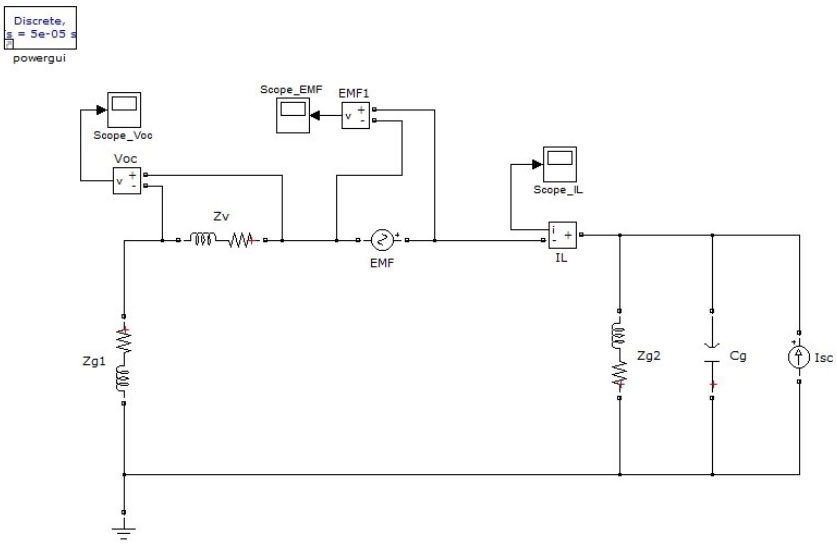

Figure L-2: Circuit for the case with capacitive coupling(without Shielding) in Section 3.4.1 ($V_{OC} = V_{OC2} + V_{OC3}$)

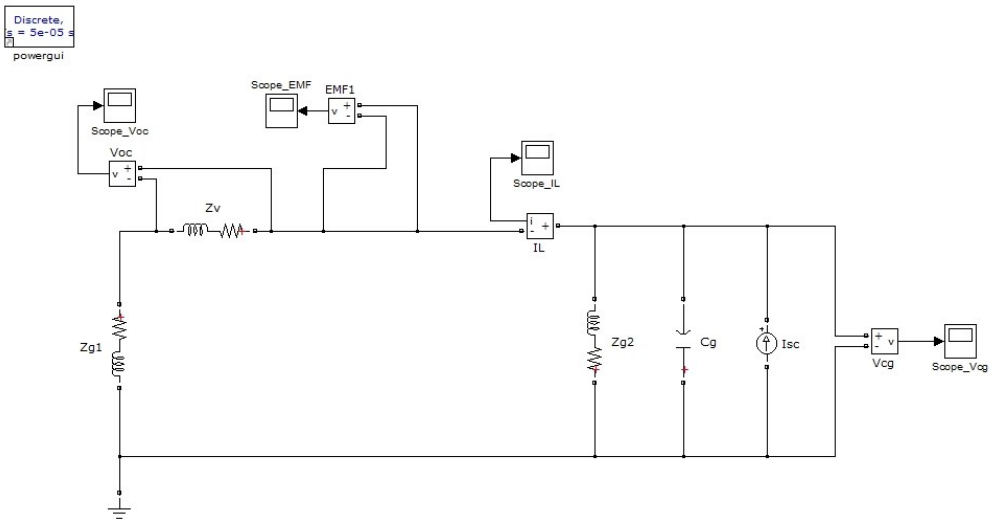

Figure L-3: Circuit for the measurement of V_{cg} in Section 3.4.1

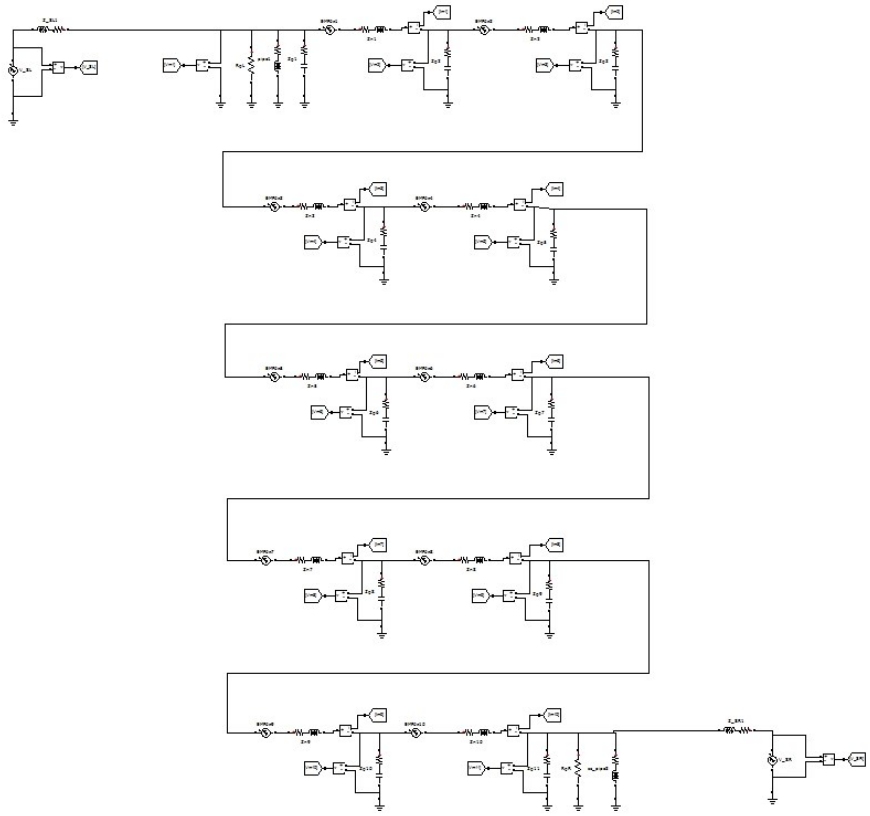

Figure L-4: Circuit of the buried pipeline with 10-segment pi-model in Section 2.2.6